COMMUNITY PROJECT FUNDING FY23

Project Title: Advanced Hydrologic Monitoring, Assessment, and Flood Forecasting for Eastern Iowa

Project Award Number: NOAA-NWS-NWS-CIPO-2023-20

Since 1988, Iowa has experienced over 1,000 flood-related, county-level Presidential Disaster Declarations requiring billions of dollars in recovery funds. The enhanced monitoring, data visualization, online communications systems, and map-based flood forecast system implemented in this project will lessen the impacts of future floods by protecting property and lives and reducing recovery costs from future floods.

Figure 1: Hydrostation in a crop field near West Union, IA

To better understand and monitor hydrologic conditions, this project expanded the Iowa Flood Center's network of hydrologic stations to install one hydrologic station in each county in congressional Districts 1 and 2 that does not currently have a station (31 counties). The second project activity included the completion of a hydrologic assessment. Watershed groups across Iowa need technical resources to prioritize areas most frequently impacted by floods. Through this funding, the project team, conducted a hydrologic assessment for two newly formed watershed management authorities (WMAs), the Maquoketa River and Lower Cedar River watersheds. This modeling helps communicate areas vulnerable to flooding. The WMA Boards will use this information for decision-making to prioritize funding within their watershed.

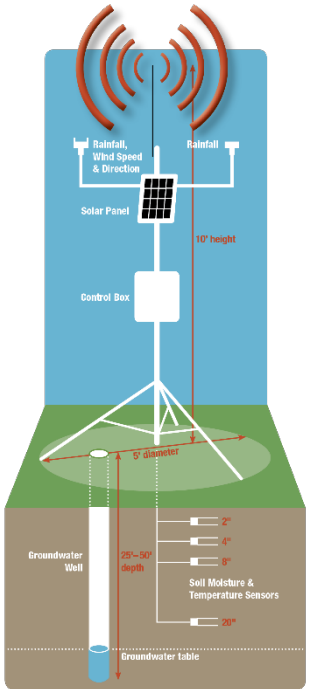

Figure 2: Graphic of Iowa Flood Center hydrologic station components.

Hydrologic Monitoring

Each hydrologic station measures rainfall, wind speed and direction, soil moisture and temperature, and water levels in a shallow groundwater well. The network informs our forecast models and provides critical publicly available data to local landowners, researchers, and agencies. The hydrologic stations connect directly with one of NOAA's primary focus areas – Unscrewed Research – by providing critical data to help researchers monitor and understand our global environment. The central U.S. does not have a robust and/or uniform array of hydrologic sensors to

help researchers and local stakeholders monitor local hydrologic conditions at the onset of flooding in real time. These hydrologic stations are low cost, low maintenance, robust, and collect and transmit reliable data every few minutes (as programmed).

Data collected by these sensors is immediately useful to local agencies and community members, who have access to the data through existing online visualization systems developed and maintained by the Iowa Flood Center at the University of Iowa. Data are visualized on the **Iowa Flood Information System.**

Data from the robust network of hydrologic stations help researchers monitor the short and long-term impact of climate change on water resources above and below ground.

The hydrologic stations were installed in the following 31 Eastern Iowa counties in 2024 in Congressional Districts 1 and 2 that do not currently have a station. See Appendix A for contact information for each county. These counties are: Benton, Blackhawk, Butler, Cedar, Cerro Gordo, Chickasaw, Clayton, Clinton, Delaware, Des Moines, Dubuque, Floyd, Hardin, Henry, Howard, Jackson, Jasper, Jefferson, Jones, Lee, Linn, Louisa, Mahaska Marion, Mitchell, Muscatine, Scott, Van Buren, Warren, Washington, and Worth.

Outreach

In May 2023, team members from IIHR and the Iowa Geological Survey (IGS) hosted an educational field day for Muscatine FFA students at the Muscatine Agricultural Learning Center. During the event, students engaged with an IGS soil scientist and drill rig operator, gaining insights into their careers and observing a hands-on soil and drill rig demonstration. Additionally, the students examined the soil profile revealed during the installation of a shallow groundwater well and learned about the hydrostation, including how to access and interpret the data it collects.

In addition to the field day event, we have established several demonstration sites at public spaces managed by County Conservation Boards. These sites serve to educate the public on the importance of data collection, featuring monitoring stations equipped with informational signage that directs visitors to an online platform for real-time data access. Furthermore, site hosts will integrate this data into their natural resource education programs for K-12 students attending scheduled events in the area.

Figure 3: IGS Soil Scientist holds up a soil profile.

Figure 4: IGS Soil Scientist and Drill Rig Operator demonstrate the well drilling.

Map of Hydrologic Station Deployment

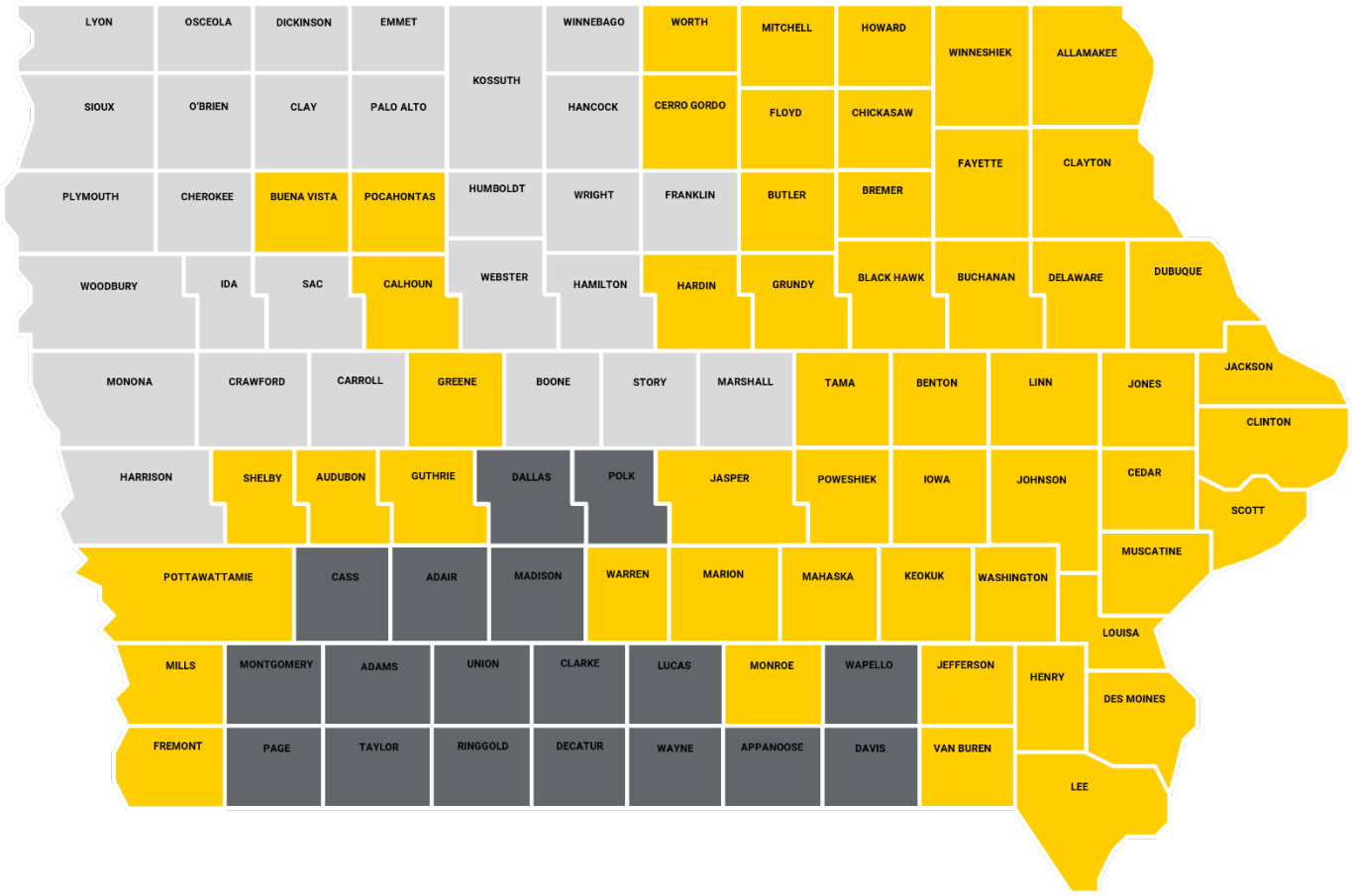

Figure 3: All gold-colored counties have an operating hydrostation. Through this funding, eastern Iowa counties in Congressional Districts 1 and 2 received 31 new hydrostations. Dark gray counties in Congressional District 3 will potentially receive funding for FY25.

Hydrologic Assessment and Flood Forecasting

The Lower Cedar River Watershed and Maquoketa River Watershed have already completed the first, and sometimes most difficult, step of creating a Watershed Management Authority in their watershed. A WMA is a mechanism for cities, counties, soil and water conservation districts (SWCDs), and other stakeholders to cooperatively engage in watershed planning and management. The WMA is formed by a Chapter 28E Agreement by two or more eligible political subdivisions within a specific eight-digit hydrologic unit code watershed. A board of directors governs the WMA. Forming a WMA can be challenging because it requires a variety of different entities, sometimes with conflicting or competing priorities and interests, to agree to work together to establish common goals for their watershed. The stakeholders in the Lower Cedar River and Maquoketa River watersheds have agreed to work together because they acknowledge the need to improve their water resources and to reduce flooding.

The hydrologic assessment communicates areas vulnerable to flooding. Iowa Flood Center researchers will develop a hydrologic model of the Maquoketa River Watershed and Lower Cedar Watershed using United States Army Corps of Engineers (USACE) Hydrologic Engineering Center Hydrologic Modeling System (HEC-HMS) software (HEC 2023). HEC-HMS is a modeling framework from which a suite of physically based methods can be used to simulate components of the hydrologic cycle, including precipitation, storage, evapotranspiration, infiltration, and runoff generation. The model was used to investigate the effects of best management practices, such as prairie restoration, cover crops, and distributed storage (ponds and wetlands), on flooding in the two watersheds under both current and future climate conditions. The results supplement the Maquoketa River Watershed Plan (IISC 2021a, 2021b) and Lower Cedar Watershed Management Plan and help to guide watershed planning and management decisions.

The Maquoketa River Watershed project will include the entire watershed in Eastern Iowa, including parts of the following counties: Buchanan, Clayton, Clinton, Delaware, Dubuque, Fayette, Jackson, and Jones.

The Lower Cedar River, also entirely within Eastern Iowa, includes parts of the following counties: Cedar, Jones, Johnson, Linn, Louisa, Muscatine, Scott.

Outreach

Throughout the hydrologic modeling process, the Iowa Flood Center project team actively participated in quarterly Watershed Management Authority (WMA) Board meetings from 2022 to 2024. During these meetings, team members provided updates on the hydrostation expansion and the ongoing hydrologic assessment. Final reports were delivered at the Maquoketa River WMA meeting in October 2024 and the Lower Cedar WMA Board meeting in November 2024. The WMA Board members intend to utilize the model's findings to pursue funding for conservation implementation in the priority areas identified.

Figure 4: Iowa Flood Center Program Manager, Kate Giannini, presents to the Maquoketa River WMA Board.

References

Iowa Flood Information System: **https://ifis.iowafloodcenter.org/ifis/**

Hydrologic Engineering Center. 2023. HEC-HMS User's Manual version 4.10. Retrieved February 23, 2023, from ***https://www.hec.usace.army.mil/confluence/hmsdocs/hmsum/4.10***.

Iowa Initiative for Sustainable Communities. 2021a. Maquoketa River Watershed Management Plan. The University of Iowa School of Planning and Public Affairs.

Iowa Initiative for Sustainable Communities. 2021b. Maquoketa River Watershed Management Plan Phase II: Subwatershed Implementation. The University of Iowa School of Planning and Public Affairs.

Lower Cedar Watershed Management Plan

Appendix A:

County	Location	Address	Contact Name:	Contact Email:	GPS Coordinates
Benton	Rodgers Park	2113 57th Trail, Vinton, IA 52349	Shelby Williams	swilliams@bentoncountyparks.com	42.19259, -92.08821
Blackhawk	Lanehaven Farms	11335 Gibson Rd. Hudson, IA 50643	Blake Hollis	bghollis@lanehaven.com	42.34972, -92.49487
Butler	Butler County EM Headquarters	610 Oak St. Allison, IA 50602	Chris Showalter	cshowalter@butlercounty.iowa.gov	42.75159, -92.78731
Cedar	Private Landowner: See coordinates		John Rummelhart JR	jrummelhart@mchsi.com	41.8057, -91.28883
Cerro Gordo	Cerro Gordo Sherriff Department	17262 Lark Ave. Mason City, IA 50401	Eric Whipple	ewhipple@cgcounty.org	43.14493, -93.2831
Chickasaw	Split Rock County Park	3090 Pembroke Ave. Fredericksburg, IA 50630	Chad Humpal and Jeff Bernatz	c.humpal@chickasawcounty.iowa.gov; j.bernatz@chickasawcounty.iowa.gov	42.91403, -92.23861
Clayton	Turkey River Cabin Concerts	24199 295th St. Elkader, IA	Gary Siegwarth	garysiegwarth@gmail.com	42.80192, -91.32386
Clinton	Clinton County Conservation Board	2308 255th St. Grand Mound, IA 52751	Phil Visser	pvisser@clintoncounty-ia.gov	41.80752, -90.64493
Delaware	Manchester Municipal Airport	1561 Early Stagecoach Rd, Manchester, IA 52057	Tim Vick (city administrator)	tvick@manchester-ia.org	42.48478, -91.49746
Des Moines	Mediapolis Community School District	725 N Northfield St. Mediapolis, IA 52637	Roger Thornburg	thornburgr@mepoedu.org	41.015, -91.15802
Dubuque	Dubuque Regional Airport	10965 Aviatio Dr. Dubuque, IA 52003	Dan Klaas	dklaas@cityofdubuque.org	42.40372, -90.70105
Floyd	Cedar Valley Transportation Center	600 18th St. Charles City	Jason Webster and Cory Spieker	jwebster@floydcoia.org	43.04553, -92.66787

Hardin	Arthur Hiker Wildlife Area	Zearing, IA	Thomas Craighton; Wes Wiese	tcraighton@hardincountyia.gov; Wes Wiese	42.20933, -93.27489
Henry	Private Landowner: See coordinates		Thom Miller	thommillerfarms@gmail.com	41.15537, -91.48667
Howard	Souhrada Wildlife Area	8998-8356 US hwy 63 Lime Springs, IA	Jeff Korsmo	jkorsmo@howardcounty.iowa.gov	43.39253, -92.29766
Jackson	Hurtsville Interpretive Center	18670 63rd St., Maquoketa, IA 52060	Nathan Jones	njones@jacksoncounty.iowa.gov	42.09046, -90.68421
Jasper	Neal Smith Wildlife Refuge	9981 Pacific St. Prairie City, IA 50228	Scott Gilje	scott_gilje@fws.gov	41.55611, -93.28514
Jefferson	Private Landower-Jason Steele	See coordinates	Jason Steele	jason.steele@usda.gov	41.02558, -91.76579
Jones	Private Landowner: TJ Davis	See coordinates	TJ Davis	tjdavis.tde@gmail.com	42.15116, -91.31404
Lee	Private Landowner: Bill Brookhiser	See coordinates	Bill Brookhiser	whchestnut92@hotmail.com	40.71309, -91.2436
Linn	Morgan Creek	7617 Worcester Rd, Cedar Rapids, IA	Shaun Reilly	shaun.reilly@linncountyiowa.gov	41.98923, -91.7702
Louisa	Louisa County Langwood Education Center	14019 H Ave, Wapello, IA 52653	Jacob Ewart	jewart@louisacountyia.gov	41.26313, -91.15241
Mahaska	Environmental Learning Center	2342 IA 92, Oskaloosa, IA 52577	Chris Clingan	clingan@mahaskacountyia.gov	41.2958, -92.61328
Marion	Landowner: Brad Deprenger		Brad Deprenger	deprefarms@gmail.com	41.46517, -93.02123
Mitchell	County Conservation Board - Mitchell County Home Park		Mike Miner	mminer@mitchellcoia.us	43.31721, -92.7902
Muscatine	Muscatine County Environment	3300 Cedar St., Muscatine, IA 52761	Sam Paul and Bruce Read (Kent Feeds)	sam.paul@mcsdonline.org; Bruce.read@kentww.com	41.42228, -91.08296

	al Learning Center				
Scott	City of Durant	Feldhan Park Durant, Iowa	Dawn Smith	dsmith@cityofdurantiowa.com	41.59904, -90.89355
Van Buren	Landowner: Tom McMahon		Tom McMahon	tom.mcmahon@lisco.com	40.85681, -91.95413
Warren	Landowner: Tim Goode		Tim Goode	trgoode@iastate.edu	41.172093, -93.385787
Washington	Marr Park-Conservation Education Center	2943 Highway 92, Ainsworth, IA 52201	Zach Rozmus	zachwccb@gmail.com	41.28869, -91.57183
Worth	Northwood County Shed Site	600 16th St. N, Northwood, IA 50459	AJ Stone	aj.stone@worthcounty.org	43.44621, -93.20976

HYDROLOGIC MODELING AND EVALUATION OF DISTRIBUTED FLOOD MANAGEMENT PRACTICES IN THE LOWER CEDAR RIVER WATERSHED

by

Daniel Gilles, Nathan Young, Kate Giannini, and Logan Mahoney

Submitted to

Lower Cedar River Watershed Management Authority

Limited Distribution Report No. 543

IOWA

IIHR—Hydroscience and Engineering

IIHR – Hydroscience and Engineering
College of Engineering
The University of Iowa
Iowa City, Iowa 52242-1585

January 2025

TABLE OF CONTENTS

1. Watershed Description 1
1.1 Hydrology 1
1.2 Instrumentation/Data Records 4
1.3 Geology and Soils 5
1.4 Topography 10
1.5 Land Cover 13
1.6 Best Management Practices 14
1.7 Soils 16
1.8 Baseflow and Runoff Historic Trends 20
1.9 Monthly Water Cycle 23
1.10 Floods of Record 24
1.11 Flood Frequency Estimates 26
2. Model Development 27
2.1 Subbasin Delineation 28
2.2 Soil Moisture Accounting Loss Model 30
2.2.1 Canopy Storage 30
2.2.2 Surface Storage 31
2.2.3 Soil Profile Storage 31
2.2.4 Groundwater storage 31
2.2.5 Evapotranspiration 31
2.3 Runoff Transform 32
2.4 Channel Routing 33
2.5 Baseflow 33
2.6 Model Inputs and Parameters 33
2.6.1 Elevations 33
2.6.2 Soil Properties 34
2.6.3 Surface Storage 34
2.6.4 Runoff Hydrographs 34
2.6.5 Channel Routing 35
2.6.6 Baseflow 35
3. Model Forcing 36

3.1 Precipitation 36
3.2 Temperature 37
4. Model Calibration 37
5. Model Validation 43
5.1 May–Sep 2024 Validation Period 43
6. Watershed Management Alternatives 46
6.1 High Runoff Potential Areas 46
6.2 Mitigating the Effects of High Runoff with Increased Infiltration 51
6.2.1 Conversion of Row Crop Agriculture to Tall-Grass Prairie 51
6.2.2 Improved Agricultural Conditions from Planting Cover Crops 57
6.3 Mitigating the Effects of High Runoff with Distributed Storage 60
6.3.1 Siting of Ponds in the Lower Cedar River Watershed 61
6.4 Comparison of Watershed Scenarios for Historic Storm Events 67
6.4.1 May – June 2008, Storm Event 67
6.4.2 June – July 2014, Storm Event 73
6.4.3 August 2016, Storm Event 78
6.4.4 June 2024, Transposed Storm Event 83
6.5 Impact of Practices Implemented Throughout the Cedar River Watershed 89
7. Summary and Conclusions 93
7.1 Cedar River Water Cycle and Watershed Conditions 93
7.2 Lower Cedar River Hydrologic Model 94
7.3 Watershed Scenarios for the Lower Cedar River Watershed 95
7.3.1 Increased Infiltration in the Watershed 96
7.3.2 Increased Storage on the Landscape 96
7.3.3 Increased Infiltration and Increased Storage 97
7.3.4 Concluding Remarks 97
References 99

LIST OF FIGURES

Figure 1-1. The Cedar River Watershed (6,726 mi^2) drains into the Lower Cedar River Watershed (1,098 mi^2)..... 2

Figure 1-2. The Lower Cedar River Watershed crosses several political boundaries, falling within 7 counties in total..... 3

Figure 1-3. Average annual precipitation from PRISM 30-year precipitation normal (1981-2024). (PRISM Climate Group, Oregon State University, 2024)..... 4

Figure 1-4. Eight digit Hydrologic Unit Code (HUC10) subwatersheds are within the Lower River Watershed. USGS discharge sensors and IFC stage sensors are shown, along with dam locations and maximum storage. Rain gages locationed near the watershed are also shown..... 5

Figure 1-5. The majority of the Lower Cedar River Watershed lies within three Iowa Landform Regions – the Iowan Surface and Southern Iowa Drift Plain, and Iowa-Cedar Lowland..... 6

Figure 1-6. Typical Iowan Surface cross-section (Prior & Hutchinson, 2024)..... 7

Figure 1-7. Areas of karst material and sinkhole locations in the watershed..... 8

Figure 1-8. Typical Southern Iowa Drift Plain cross-section (Prior & Hutchinson, 2024)..... 9

Figure 1-9. Depth to bedrock in the Lower Cedar River Watershed..... 10

Figure 1-10. Iowa statewide LiDAR topography collected 2019-2020..... 11

Figure 1-11. Topography slope classifications..... 12

Figure 1-12. Soils that require artificial drainage to maximize yields (Iowa DNR, 2024)..... 13

Figure 1-13. 2023 National Land Cover Database classifications (U.S. Geological Survey, 2023)..... 14

Figure 1-14. Best Management Practices in the watershed during 2007-2010. From the Iowa Best Management Practices (BMP) Mapping Project..... 16

Figure 1-15. SSURGO soil taxonomic classes (Soil Survey Staff, NRCS, USDA, 2024)..... 17

Figure 1-16. Distribution of Hydrologic Soil Groups. Hydrologic Soil Groups reflect the degree of runoff potential a particular soil has, with Type A representing the lowest runoff potential and Type D representing the highest runoff potential..... 19

Figure 1-17. Annual volumes of precipitation, streamflow, baseflow, and runoff in inches of depth for watershed area upstream of Conesville, Iowa..... 20

Figure 1-18. Annual totals for: (a) precipitation; (b) streamflow; (c) baseflow; and (d) runoff at Conesville, IA..... 21

Figure 1-19. Cumulative annual totals for: (a) precipitation; (b) streamflow; (c) baseflow; and (d) runoff at Conesville, Iowa. Flow trendlines show a change in slope around 1980..... 22

Figure 1-20. Double-mass curves using cumulative annual precipitation with cumulative annual (a) streamflow, (b) baseflow, and (c) runoff, and (d) all data at Conesville, Iowa..... 23

Figure 1-21. Average monthly water cycle for the Cedar River Watershed at Conesville, Iowa. The plots show the average monthly precipitation, streamflow, baseflow, and runoff in inches, based on the period 1950–2024..... 24

Figure 1-22. (a) Annual maximum peak discharge, (b) flood occurrences by month, and (c) calendar day of flood occurrence for the Cedar River at Conesville, Iowa..... 25

Figure 2-1. Hydrologic processes that occur in a watershed. Modeling considered the precipitation, infiltration, evapotranspiration, percolation, base flow and overland components of the water cycle. 27

Figure 2-2. HMS model development of the Lower Cedar River Watershed. The watershed was divided into 670 subbasins for modeling. 29

Figure 2-3. HEC-HMS model subbasin area histogram and boxplot 30

Figure 2-4. Soil Moisture Accounting (SMA) model 32

Figure 2-5. Subbasin runoff hydrograph conceptual model. Rainfall is partitioned into a runoff depth according to the Soil Moisture Accounting model, which is then converted to discharge using the Clark unit hydrograph method. 35

Figure 3-1. AORC gridded radar precipitation and temperature observations were used to force the model simulations. 36

Figure 4-1. Observed and simulated flow hydrographs at USGS gaging station on Indian Creek at Marion for the calibration period. 39

Figure 4-2. Selected peak flow events during the 2012-2016 calibration period. 40

Figure 4-3. Monthly flow volume in depth (inches) for Indian Creek at Marion, May 2012 – Aug 2016, normalized by upstream drainage area 41

Figure 4-4. Observed and simulated flow hydrographs at USGS gaging station on the Cedar River at Conesville for the calibration period. 42

Figure 4-5. Monthly flow volume in depth (inches) for Cedar River at Conesville, May 2012 – Aug 2016, normalized by upstream drainage area 43

Figure 5-1. Simulated flow hydrographs with observed flow at USGS gaging stations for the 2024 validation period. 44

Figure 5-2. Monthly flow volume in depth (inches) at Marion (top) and Conesville (bottom) for May-Sep 2024, normalized by upstream drainage area 45

Figure 6-1. SCS design storm hyetograph, showing the timing of the rainfall and example infiltration for a given subbasin area. 47

Figure 6-2. Modeled runoff coefficient using the SCS design storm at each HEC-HMS subbasin. 48

Figure 6-3. Modeled runoff coefficient using the SCS design storm aggregated at each HUC 12 watershed. 48

Figure 6-4. SCS curve number grid. 49

Figure 6-5. SCS curve number map by HEC-HMS subbasin. 50

Figure 6-6. SCS curve number map by HUC 12 watershed. 50

Figure 6-7. Historical vegetation prior to European settlement (Government Land Office plat maps, 1832-1859). 53

Figure 6-8. Model index locations selected for comparisons of hypothetical flood mitigation scenarios to current conditions 55

Figure 6-9. Simulated hydrographs at index locations for native vegetation scenario and SCS design storm. 56

Figure 6-10. Average peak flow reductions for native vegetation scenarios and design storm. 57
Figure 6-11. Simulated hydrographs at index locations for cover crop/ improved soil health scenario and SCS design storm. 59
Figure 6-12. Average peak flow reductions for cover crop/ improved soil health scenario and SCS design storm. 60
Figure 6-13. Schematic of a pond constructed to provide flood storage 61
Figure 6-14. Distributed storage scenarios - 50 ponds (top), 100 ponds (middle), 250 ponds (bottom), placed at the outlet of headwater subbasins. 62
Figure 6-15. Aggregation of pond storage-discharge curves and drainage areas within a subbasin. 63
Figure 6-16. Individual detention pond inflow, outflow and storage behavior for the SCS Design Storm. 64
Figure 6-17. Simulated hydrographs at index locations for detention pond scenarios and SCS design storm. 65
Figure 6-18. Average peak flow reductions for detention pond scenarios and SCS design storm. 66
Figure 6-19. May 25 – June 15, 2008, cumulative rainfall used for simulating watershed scenarios 68
Figure 6-20. Simulated hydrographs at index locations for native vegetation scenario and May 25 – June 15, 2008, storm event. 69
Figure 6-21. Simulated hydrographs at index locations for cover crops / soil health improvement scenario and May 25 – June 15, 2008, storm event. 70
Figure 6-22. Simulated hydrographs at index locations for detention pond scenarios and May 25 – June 15, 2008, storm event. 71
Figure 6-23. Average peak flow reductions for April – September 2008, native vegetation (top), cover crop/ improved soil health (middle), and distributed storage (bottom) 72
Figure 6-24. June 29 – July 5, 2014, cumulative rainfall used for simulating watershed scenarios. 73
Figure 6-25. Simulated hydrographs at index locations for native vegetation scenario and June 29 – July 5, 2014, storm event. 74
Figure 6-26. Simulated hydrographs at index locations for cover crops / soil health improvement scenario and June 29 – July 5, 2014, storm event. 75
Figure 6-27. Simulated hydrographs at index locations for detention pond scenarios and June 29 – July 5, 2014, storm event. 76
Figure 6-28. Average peak flow reductions for April - September 2014, native vegetation (top), cover crop/ improved soil health (middle), and distributed storage (bottom) 77
Figure 6-29. August 10-17, 2016, cumulative rainfall used for simulating watershed scenarios. 78
Figure 6-30. Simulated hydrographs at index locations for native vegetation scenario and June 15 – August 20, 2016 period. 79
Figure 6-31. Simulated hydrographs at index locations for cover crops / soil health improvement scenario and June 15 – August 20, 2016 period. 80
Figure 6-32. Simulated hydrographs at index locations for detention pond scenarios and June 15 – August 20, 2016 period. 81

Figure 6-33. Average peak flow reductions for April – September 2016, native vegetation (top), cover crop/ improved soil health (middle), and distributed storage (bottom)..... 82

Figure 6-34. Cumulative rainfall from the June 19 – June 23, 2024 Flood event was transposed to the Lower Cedar River Watershed..... 83

Figure 6-35. Transposed June 19 – June 23, 2024 cumulative rainfall from northwest Iowa used for simulating watershed scenarios..... 84

Figure 6-36. Simulated hydrographs at index locations for native vegetation scenario and June 19 – June 23, 2024 transposed storm event..... 85

Figure 6-37. Simulated hydrographs at index locations for cover crops / soil health improvement scenario and June 19 – June 23, 2024 transposed storm event. 86

Figure 6-38. Simulated hydrographs at index locations for detention pond scenarios and June 19 – June 23, 2024 transposed storm event..... 87

Figure 6-39. Average peak flow reductions for the June 19 – June 23, 2024 transposed storm event, and native vegetation (top), cover crop/ improved soil health (middle), and distributed storage (bottom). 88

Figure 6-40. Summary of peak discharge reductions across all model index locations and historical events for each scenario. 89

Figure 6-41. HEC-HMS subbasin delineation of the Cedar River Watershed (Mahoney, 2024). 91

Figure 6-42. Average peak flow reduction percentages for the 100% conversion scenario to native prairie or cover crops at locations on the Cedar River (Austin, Charles City, Cedar Rapids, Conesville) and two tributaries (Beaver Creek, Little Cedar River) (Mahoney, 2024). 92

Figure 6-43. Average results for all 3 scenarios of distributed storage ponds at locations on the Cedar River (Austin, Charles City, Cedar Rapids, Conesville) and two tributaries (Beaver Creek, Little Cedar River) (Mahoney, 2024). 92

1. WATERSHED DESCRIPTION

This chapter provides an overview of current Lower Cedar River Watershed conditions, including hydrology, geology, topography, land use, and hydrologic/meteorologic instrumentation, and historic water cycle, as well as a summary of previous floods of record.

1.1 Hydrology

The Lower Cedar River Watershed as defined by the boundary of eight-digit Hydrologic Unit Code (HUC 8) 07080206 is located in eastern Iowa and encompasses approximately 1,098 square miles (mi^2). The upper portion of the Cedar River Watershed has a watershed area of 6,726 square miles that drains into the Lower Cedar River Watershed, shown in Figure 1-1. The Lower Cedar River Watershed is approximately 14% of the total Cedar River Watershed. The Cedar River continues through the Lower Cedar Watershed before meeting the Iowa River, at Columbus Junction, Iowa. The Lower Cedar River Watershed boundary falls within 7 counties in total, as shown in Figure 1-2, which include Linn, Jones, Johnson, Cedar, Scott, Muscatine, and Wapello counties. A summary of the county areas and percentages of total watershed area is shown in Table 1-1.

Table 1-1. County areas within the Lower Cedar River Watershed.

County	Area (mi^2)	Percentage
Cedar	437	40%
Muscatine	288	26%
Linn	264	24%
Johnson	73	7%
Scott	28	3%
Louisa	6	1%
Jones	3	0%

Average annual precipitation in Iowa ranges from 30–40 inches, with the lowest precipitation in the northwest corner of the state and the highest in the southeast corner (PRISM Climate Group, Oregon State University, 2024). The average annual precipitation within the Lower Cedar River Watershed is shown in Figure 1-3. About 70% of the annual precipitation falls as rain during the months of April–September. During this period, thunderstorms capable of producing torrential rains are possible, with the peak frequency of such storms occurring in June. However, most flooding events in the Lower River Watershed are primarily driven by spring

snowmelt along with heavy precipitation events, as discussed in later sections. This watershed along with the rest of the state has experienced increased variability in annual precipitation since 1975, along with a general increase in the amount of spring rainfall (Berendzen, et al., 2011)

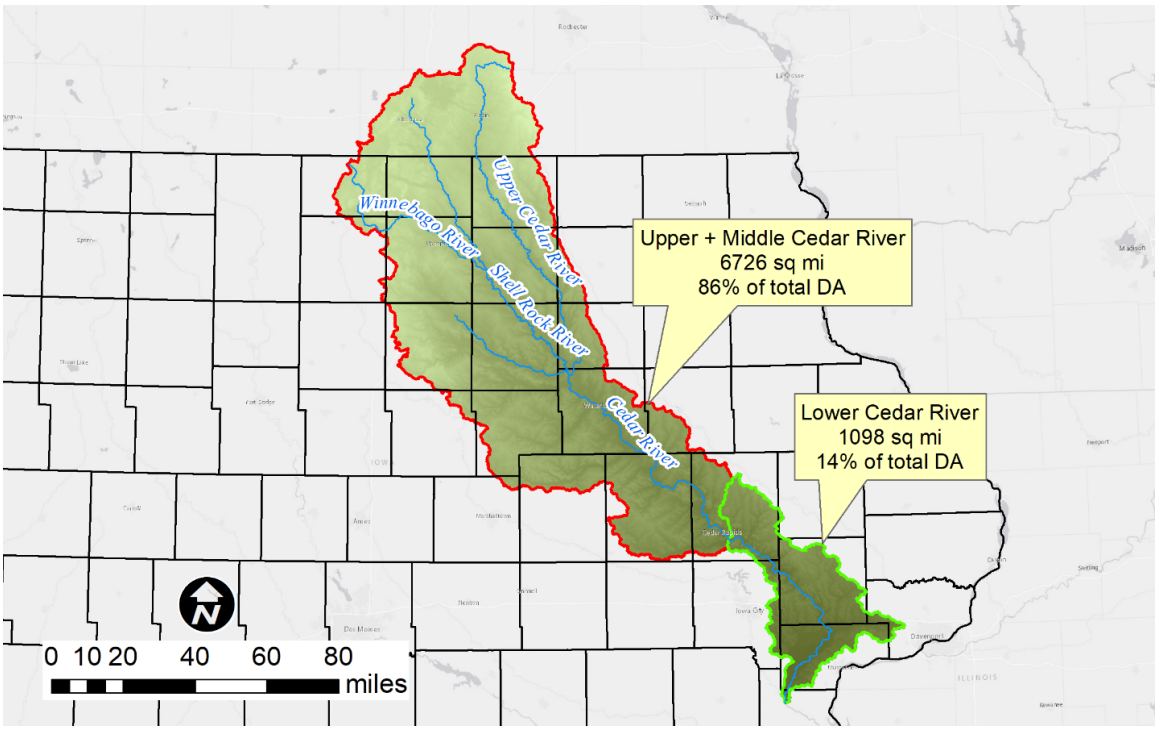

Figure 1-1. The Cedar River Watershed (6,726 mi^2) drains into the Lower Cedar River Watershed (1,098 mi^2).

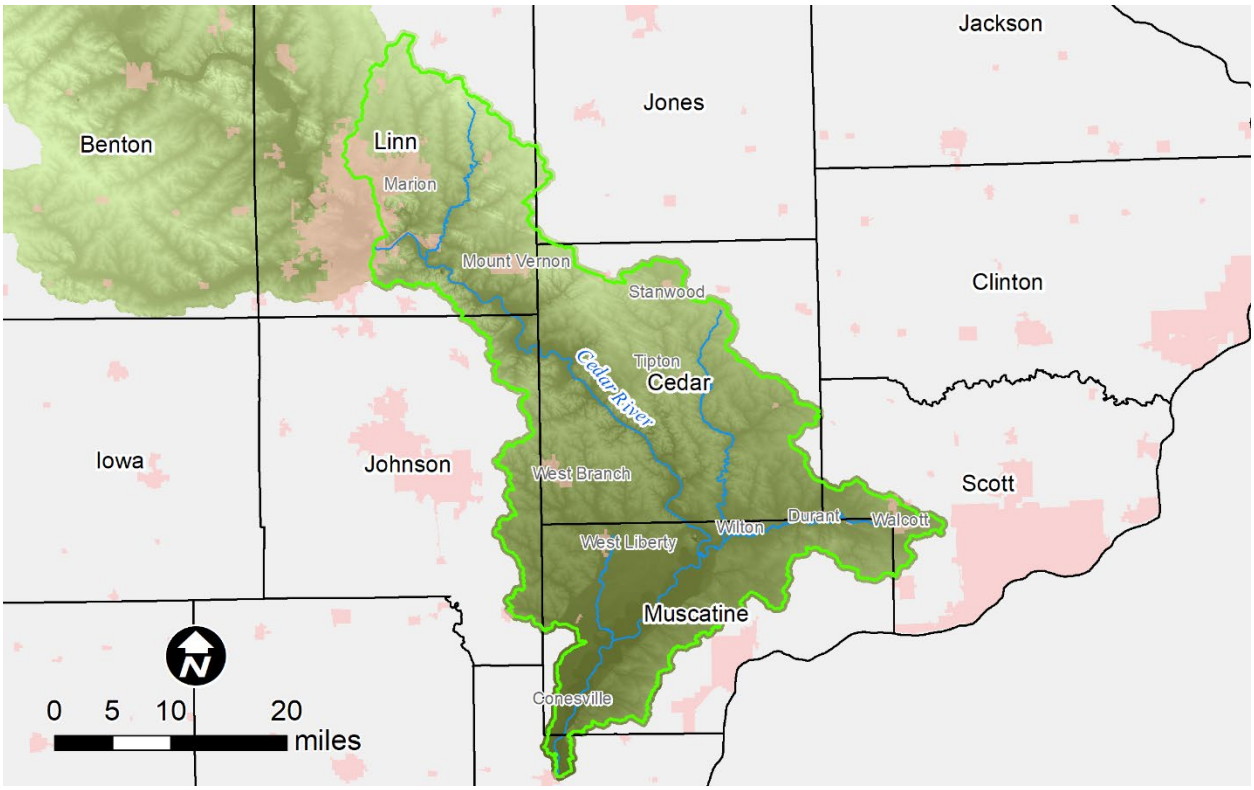

Figure 1-2. The Lower Cedar River Watershed crosses several political boundaries, falling within 7 counties in total.

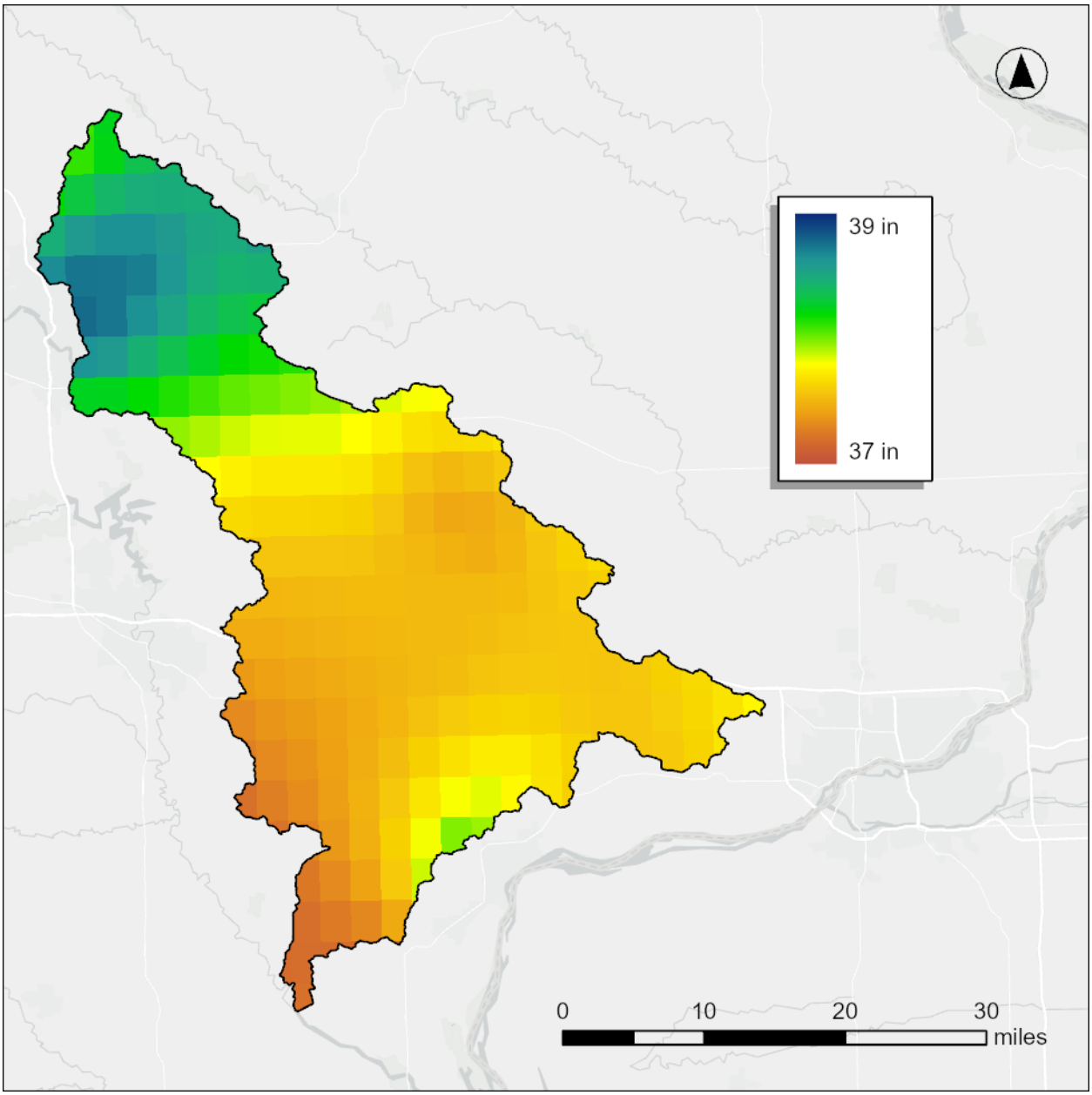

Figure 1-3. Average annual precipitation from PRISM 30-year precipitation normal (1981-2024). (PRISM Climate Group, Oregon State University, 2024)

1.2 Instrumentation/Data Records

The Lower Cedar River Watershed has instrumentation installed to collect and record stream stage, discharge, and precipitation measurements. Seven USGS-operated stage and discharge gauges and seven IFC stream-stage sensors are located within the watershed, as shown in Figure 1-4. There are several National Oceanic and Atmospheric Administration (NOAA) partnered precipitation gages within or near the watershed, some of which are also shown in Figure 1-4. The

operational period of many of these rain gages span the period from 1950-2022 (Wuertz, Lawrimore, & Korzeniewski, 2024). These long-term records are integral in evaluating long term water cycle trends for the watershed.

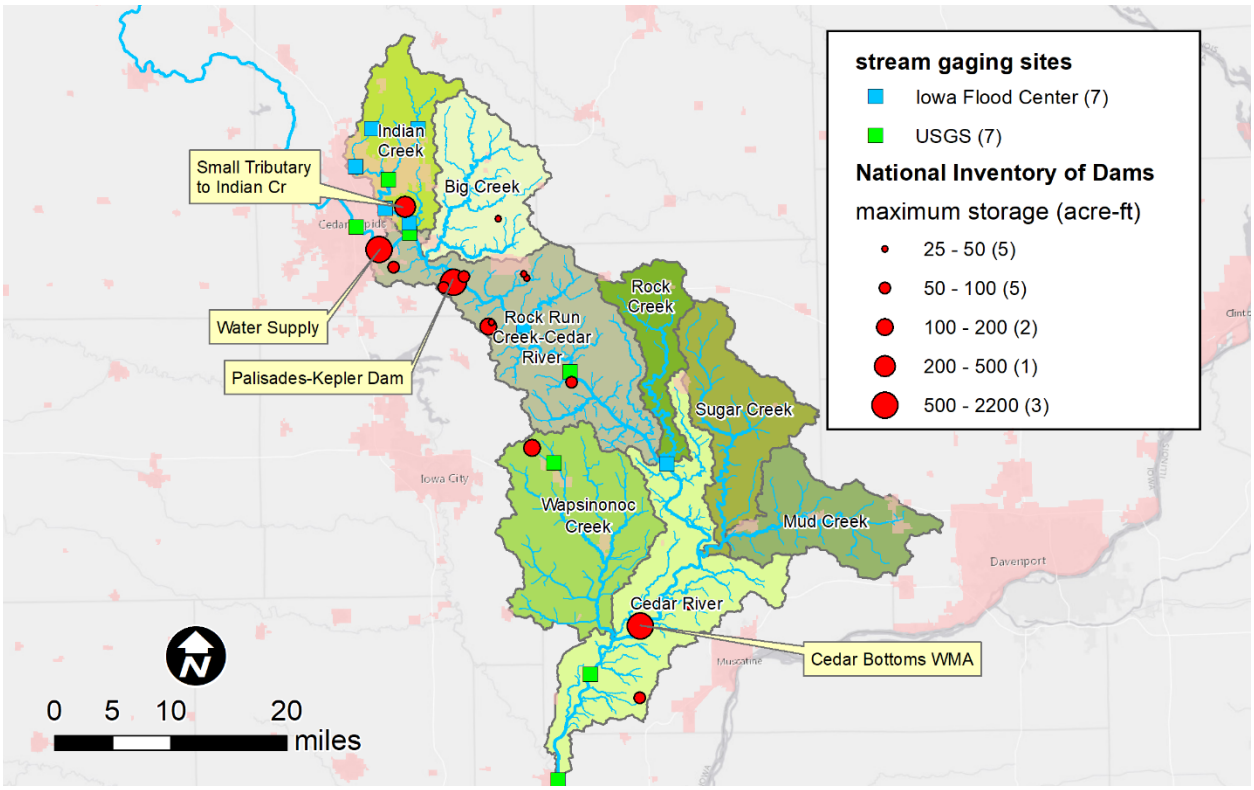

Figure 1-4. Eight digit Hydrologic Unit Code (HUC10) subwatersheds are within the Lower River Watershed. USGS discharge sensors and IFC stage sensors are shown, along with dam locations and maximum storage. Rain gages locationed near the watershed are also shown.

1.3 Geology and Soils

A landscape is a collection of terrain features or landforms (Iowa Geological & Water Survey, 2013). These combinations of surface features and underlying soils influence how water moves through the landscape. The Lower Cedar River Watershed is located within three distinct landform regions – the Iowan Surface, the Southern Iowa Drift Plain, and the Iowa-Cedar Lowland. Each landform region has a unique influence on the rainfall-runoff stream network characterization.

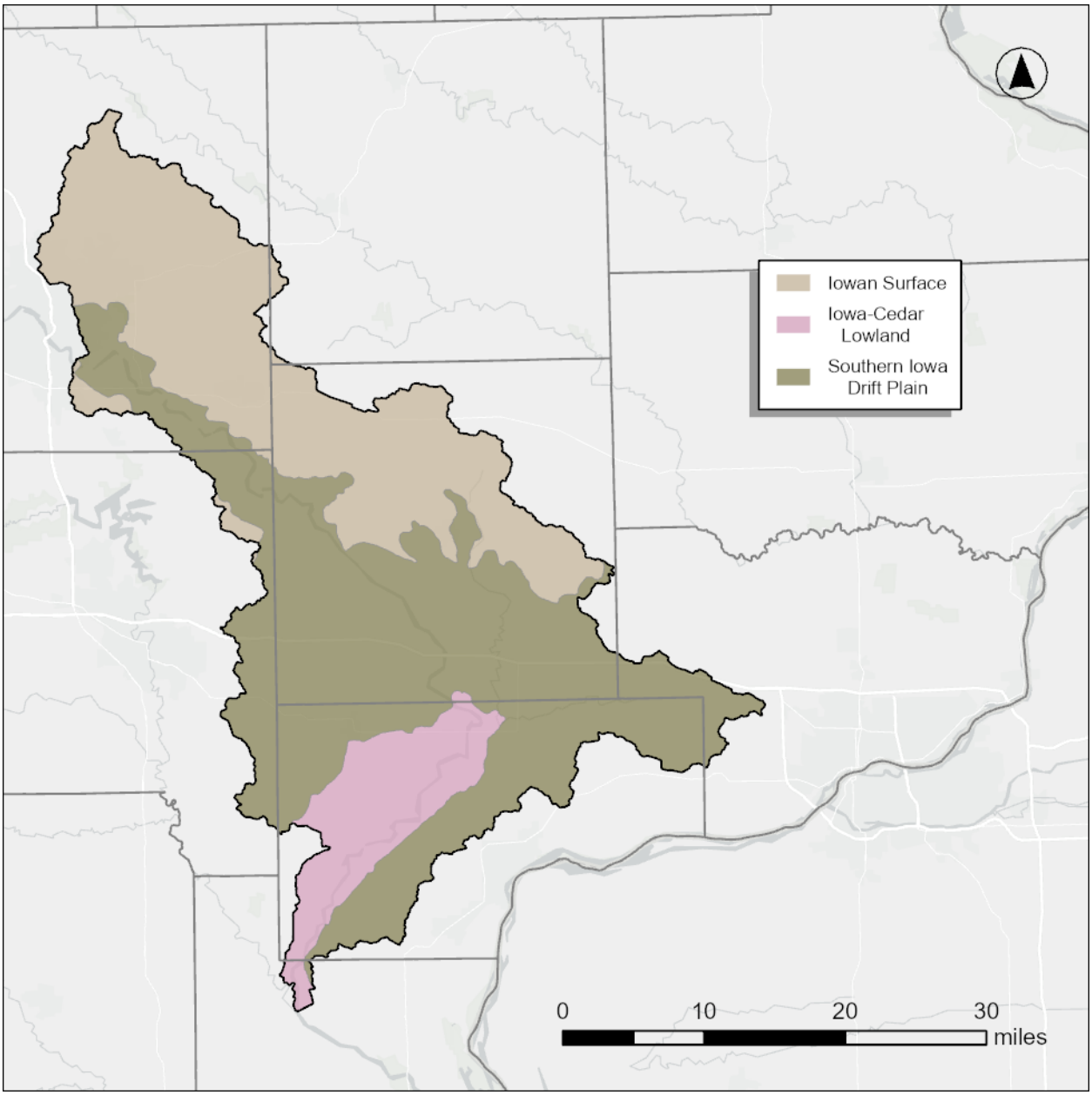

Figure 1-5. The majority of the Lower Cedar River Watershed lies within three Iowa Landform Regions – the Iowan Surface and Southern Iowa Drift Plain, and Iowa-Cedar Lowland.

The Iowan Surface encompasses much of northeast Iowa and is an area that was subjected to intense cold between 21,000 to 16,500 years ago during the last glacial advance into Iowa. The proximity to the Des Moines Lobe ice margin resulted in tundra and permafrost conditions, and as a result wind and water action significantly eroded the landscape. Characteristic features include gently rolling topography, common glacial 'erratics' (rocks and boulders not native to Iowa that

have been transported by glaciers), and loess-mantled paha (northwest to southeast trending uneroded upland remnants of the former landscape) (Prior & Hutchinson, 2024). A typical cross-section of the Iowa Surface landform region is shown in Figure 1-6. Glacial materials at the surface consist of poorly consolidated glacial deposits with the potential for extensive local sand bodies. In areas where the depth to bedrock is shallow, these materials provide limited protection from surface water infiltrating into bedrock. Shallow limestone bedrock can be seen in the form of karst features, including sinkholes, which are cavities in the underlying Devonian limestone that have collapsed (Prior & Hutchinson, 2024). Figure 1-7 shows known sinkhole locations along with karst bedrock materials within the watershed. There are a relatively small number of sinkholes compared to other areas in Iowa. Sinkhole locations are concentrated in the northern side of the watershed, collocated with karst material. The abundant limestone and dolomite deposits are typically shallowly buried by glacial materials within the Iowan surface. As a result, karst materials can be hydrologically connected to groundwater and can make the region especially vulnerable to groundwater contamination.

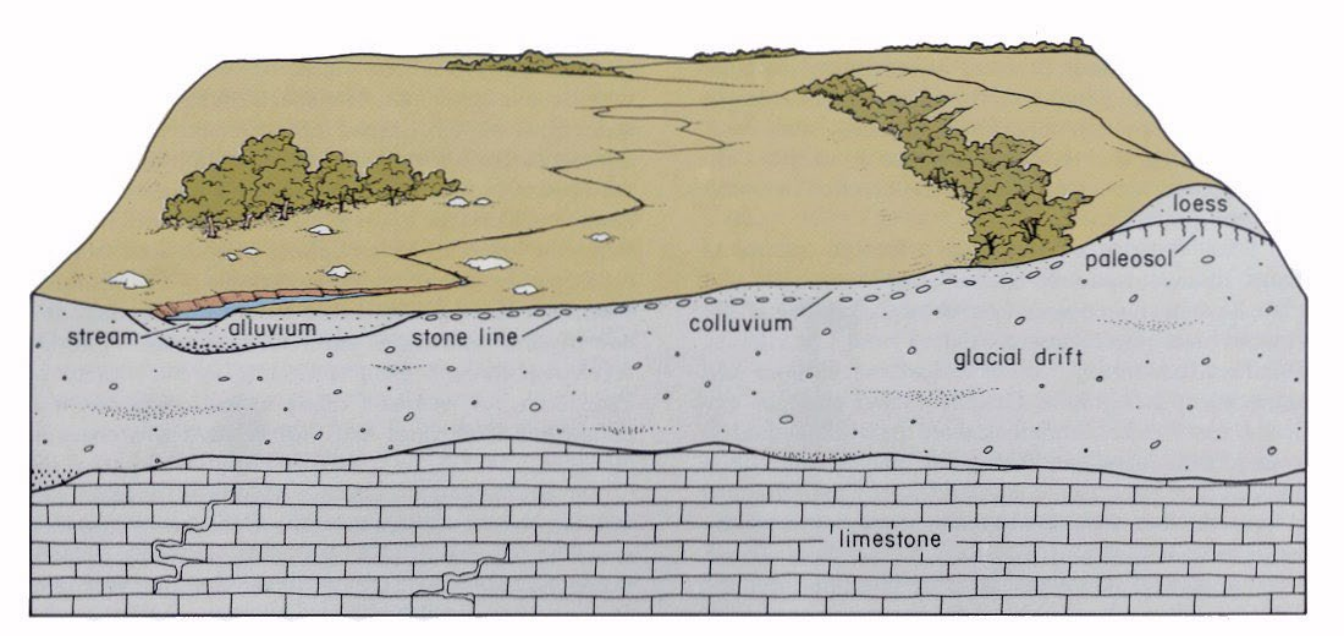

Figure 1-6. Typical Iowan Surface cross-section (Prior & Hutchinson, 2024).

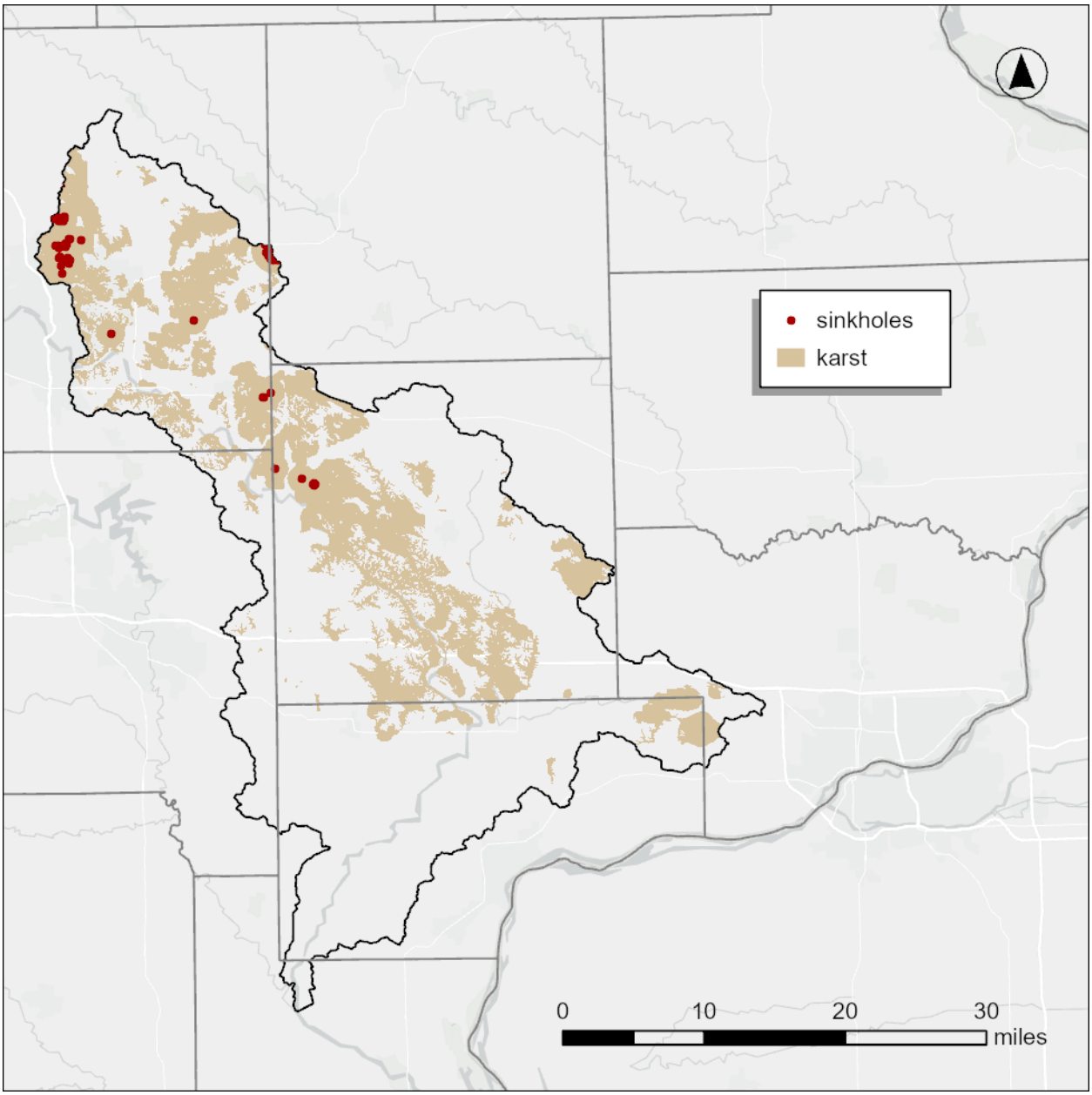

Figure 1-7. Areas of karst material and sinkhole locations in the watershed.

The Southern Iowa Drift Plain experienced numerous episodes of glaciation between 500,000 and 2.6 million years ago. Since that time, periods of relative landscape stability and soil formation have alternated with episodes of erosion, shaping the land surface we see today. The landscape is characterized by steeply rolling topography and well-developed drainage divides. A typical cross-section of the Southern Iowa Drift Plain landform region is shown in Figure 1-8. Features from episodes of historic glaciation have been obliterated by time (Prior & Hutchinson,

2024). The terrain has significant local relief, a result of many deepening episodes of stream erosion removing the glacial deposits. The summits of the undulating landscape are the oldest landscape features in the region. They seem to return to a uniform elevation at each peak, evidence of the original geologic landscape. They have broad, loess-mantled uplands and are largely uneroded remnants of the last Pre-Illinoian drift plain.

The Iowa Geological Survey (IGS) developed a depth to bedrock surface for the state. Depth to bedrock varies from 0–500 feet throughout the watershed, as shown in Figure 1-9. There are areas of shallow depth to bedrock throughout the watershed. There are likely numerous instances of exposed bedrock, which are distributed nearly identically to the karst areas. There are also relatively deep linear features resembling prehistoric stream channels.

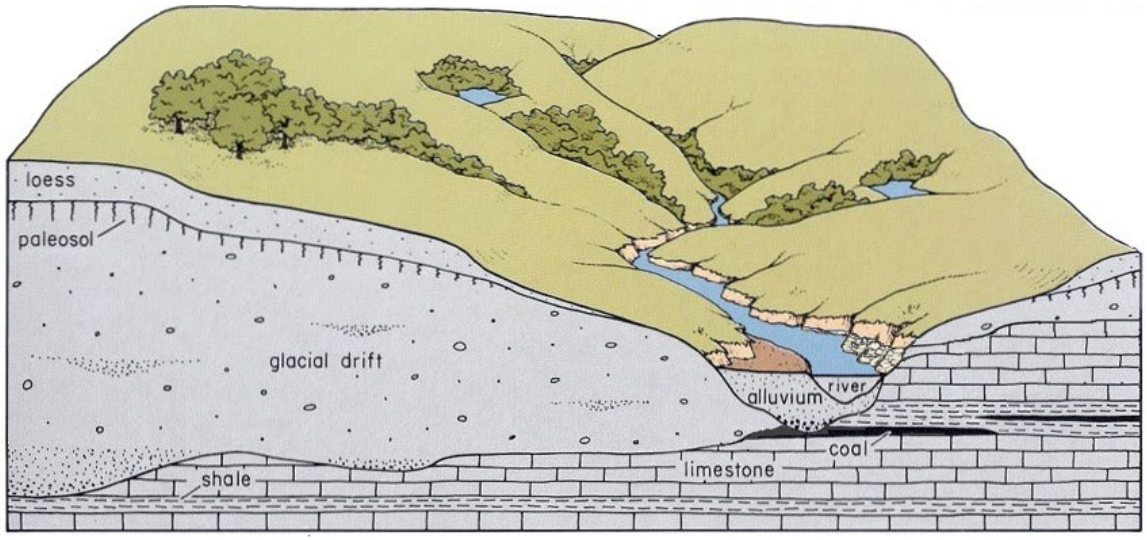

Figure 1-8. Typical Southern Iowa Drift Plain cross-section (Prior & Hutchinson, 2024).

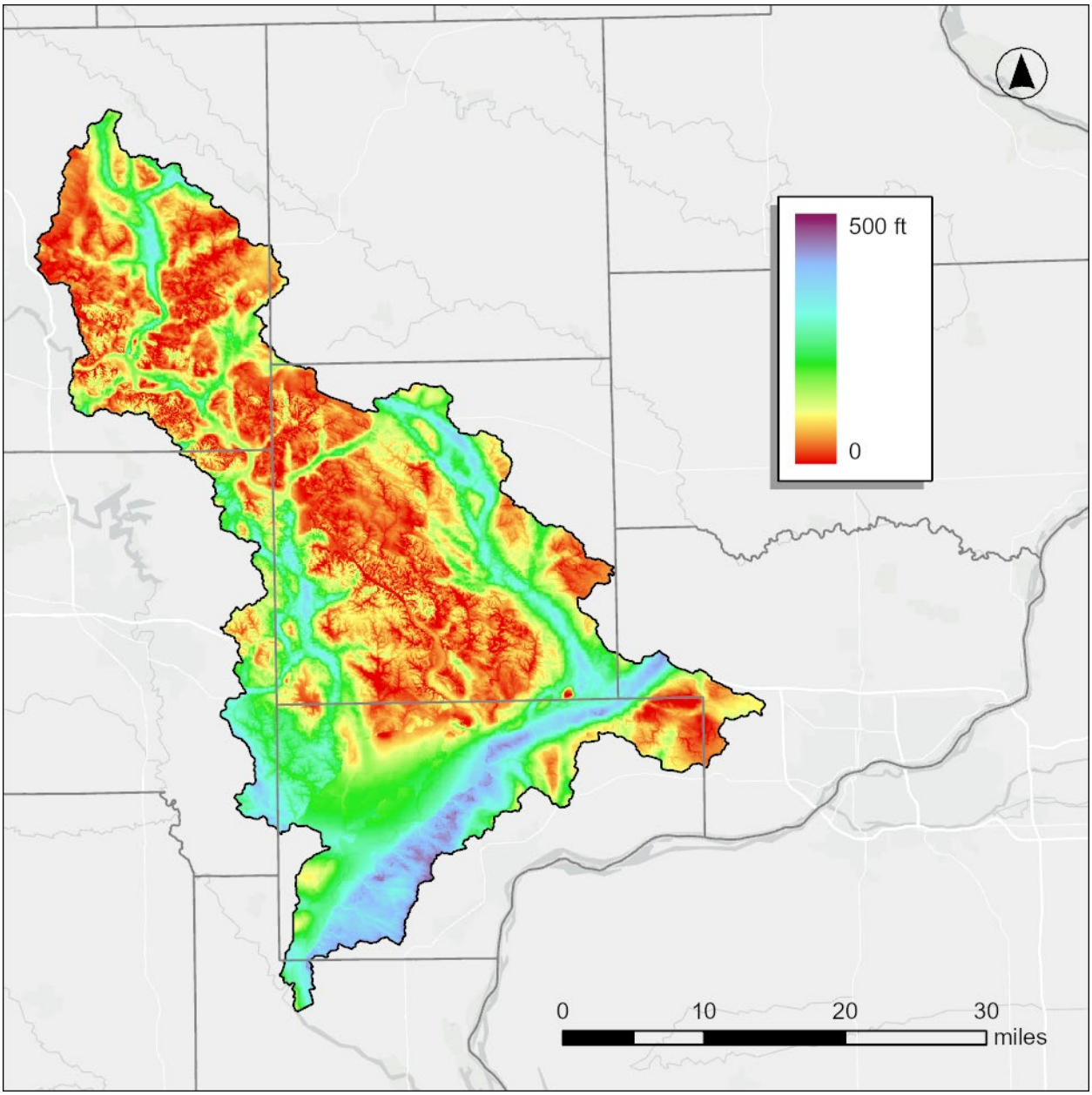

Figure 1-9. Depth to bedrock in the Lower Cedar River Watershed.

1.4 Topography

The topography of the Lower Cedar River Watershed reflects its geologic past. As previously mentioned, much of the watershed lies within the Iowan Surface and Southern Iowa Drift Plain. Figure 1-10 shows topography provided by Iowa DNR in the form of bare-earth light detection and ranging (LiDAR) data. Elevations range from approximately 950 feet above sea level in the uppermost part of the watershed upstream of Marion, to 590 feet at the Cedar River outlet

at the Iowa River. Typical land slopes are between 1.2% and 7.7% (25th and 75th percentiles), with the steepest areas occurring in along the Cedar River, as shown in Figure 1-11. The watershed is generally flat or gently sloping. The Iowa DNR has delineated locations, shown in Figure 1-12, that likely require artificial drainage to maximize row crop yields based on terrain, water table, and soil types (Iowa DNR, 2024). There are several clusters that meet the criteria for likely relying on artificial drainage tile to maximize row crop yields.

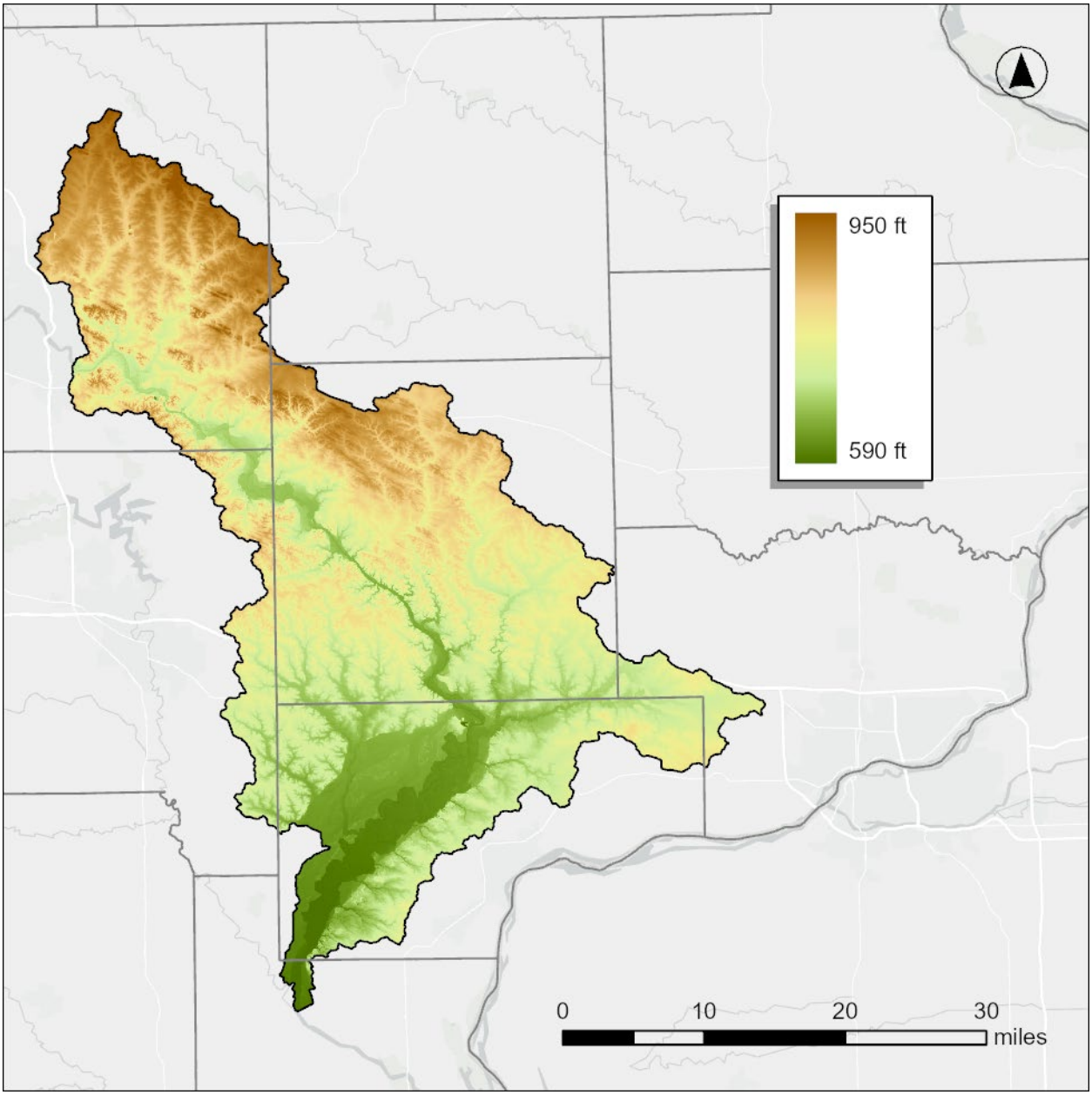

Figure 1-10. Iowa statewide LiDAR topography collected 2019-2020.

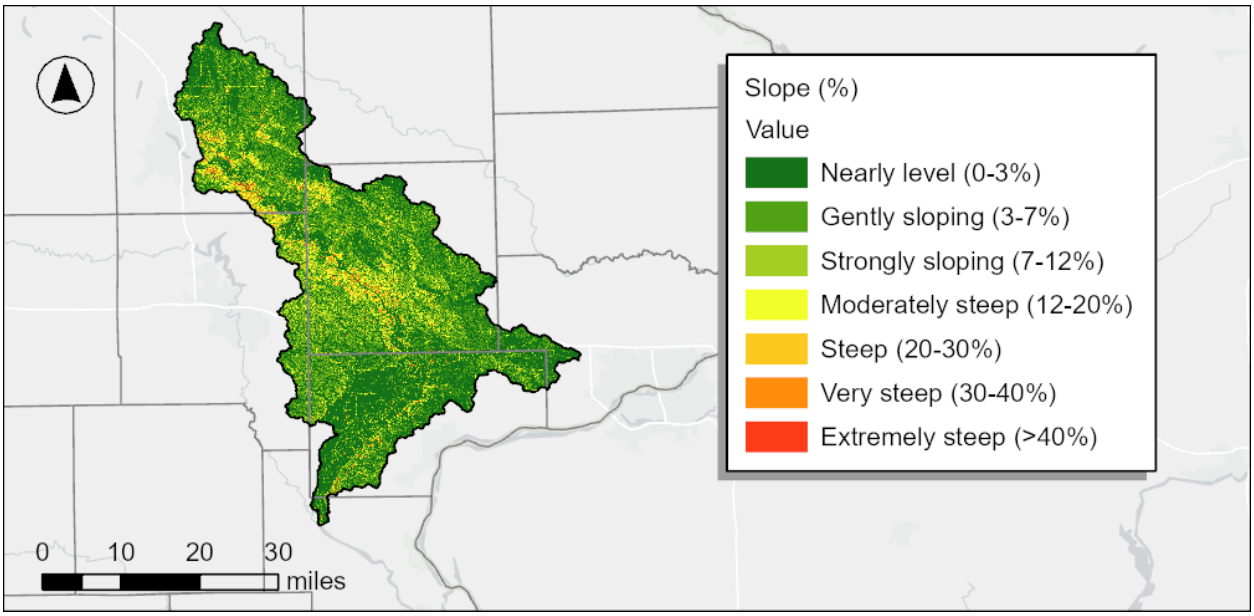

Figure 1-11. Topography slope classifications.

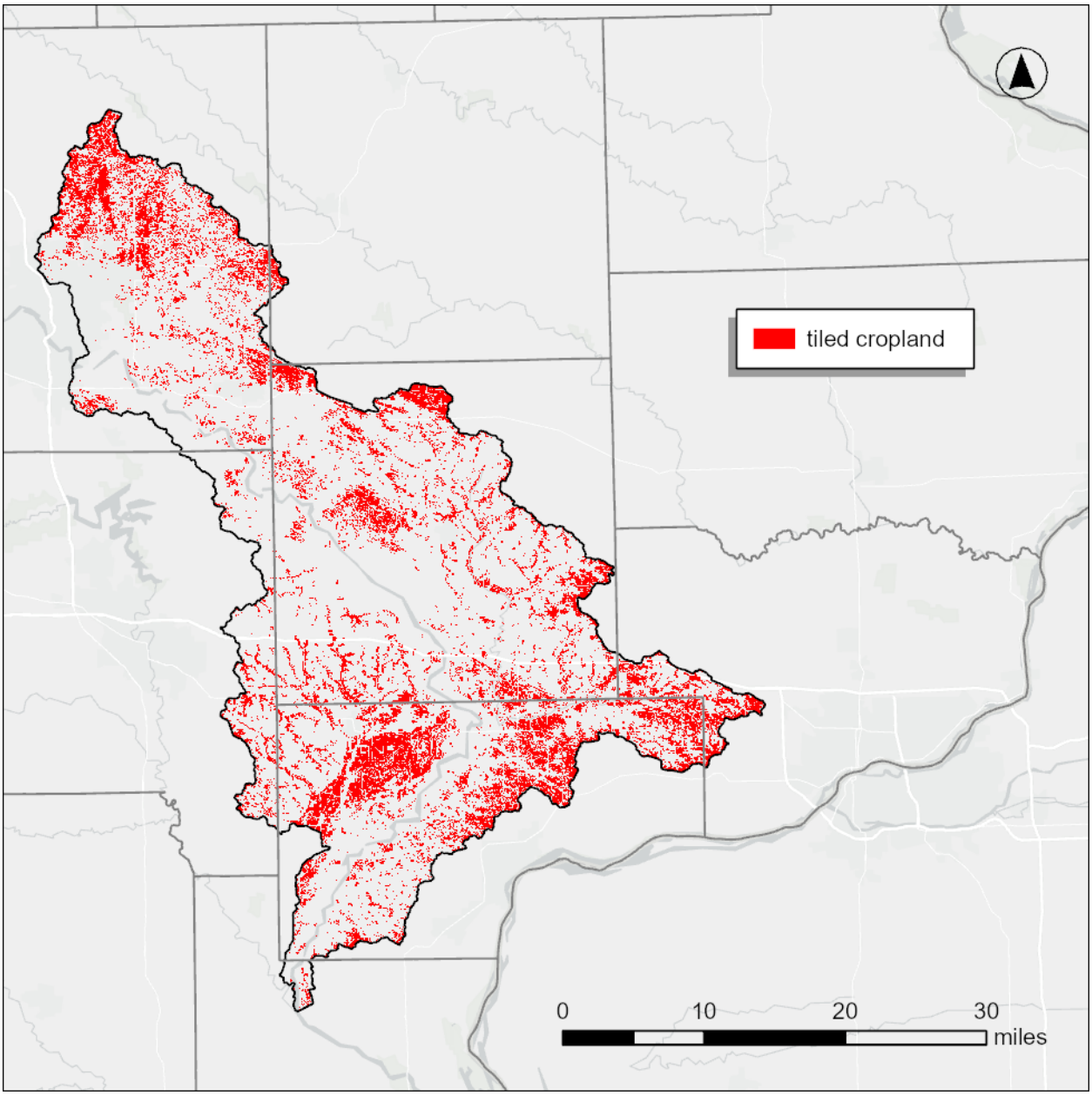

Figure 1-12. Soils that require artificial drainage to maximize yields (Iowa DNR, 2024).

1.5 Land Cover

Land use in the Lower Cedar River Watershed is predominantly agricultural, dominated by cultivated crops (corn/soybeans) on approximately 69.8% of the acreage (approximately 490,550 acres), followed by grass/hay/pasture at approximately 7.8%. The remaining acreage in the watershed is about 8.8% forest (primarily deciduous forest), 8.1% developed land, and 5.3%

open water and/or wetlands, per the 2023 National Land Cover Database (U.S. Geological Survey, 2023). Figure 1-13 shows the spatial distribution of land cover in the watershed.

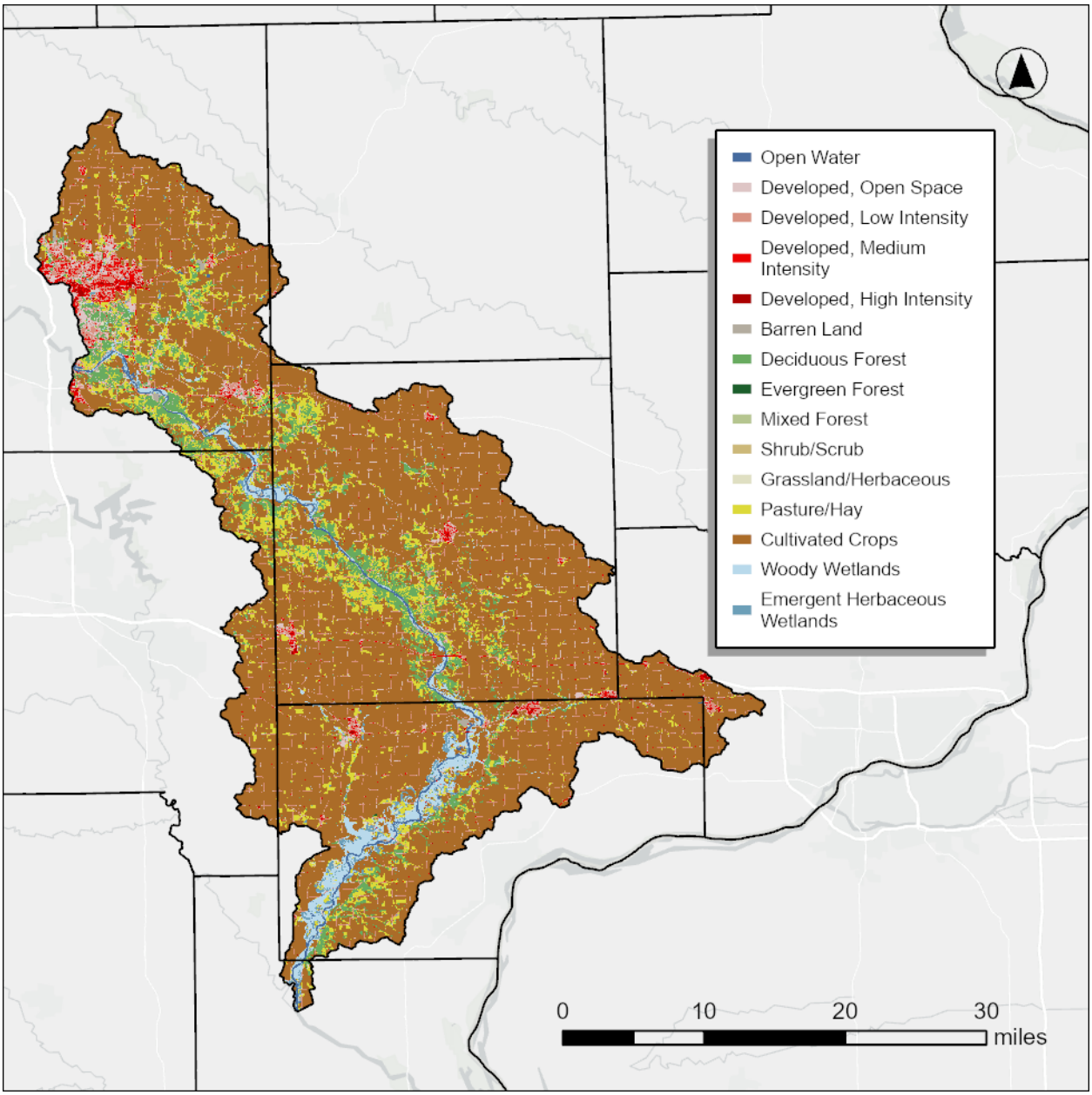

Figure 1-13. 2023 National Land Cover Database classifications (U.S. Geological Survey, 2023).

1.6 Best Management Practices

The Iowa Best Management Practices (BMP) Mapping Project was a collaborative effort led by the Iowa State University Geographic Information Systems (GIS) Facility that was active

from 2017-2019. It was completed in association with the Iowa DNR, Iowa Flood Center, Iowa Department of Agriculture and Land Stewardship, Iowa Nutrient Research Center, National Laboratory for Agriculture and the Environment, and the Iowa Nutrient Research and Education Council. The goal of the project was to provide a complete baseline set of BMPs during the 2007–2010 timeframe for use in watershed modeling, historic documentation, and future practice tracking. These practices included terraces, water and sediment control basins (WASCOBs), grassed waterways, pond dams, contour strip cropping, and contour buffer strips. The data has been manually digitized for each HUC 12 using LiDAR products, color-infrared (CIR) imagery, National Agriculture Imagery Program imagery, and historic aerial photography. Figure 1-14 summarizes individual BMPs at the HUC8 scale. The individual BMPs can also be viewed in an online interface that allows for better visualization – bensonvip.gis.iastate.edu/IA_BMPs/.

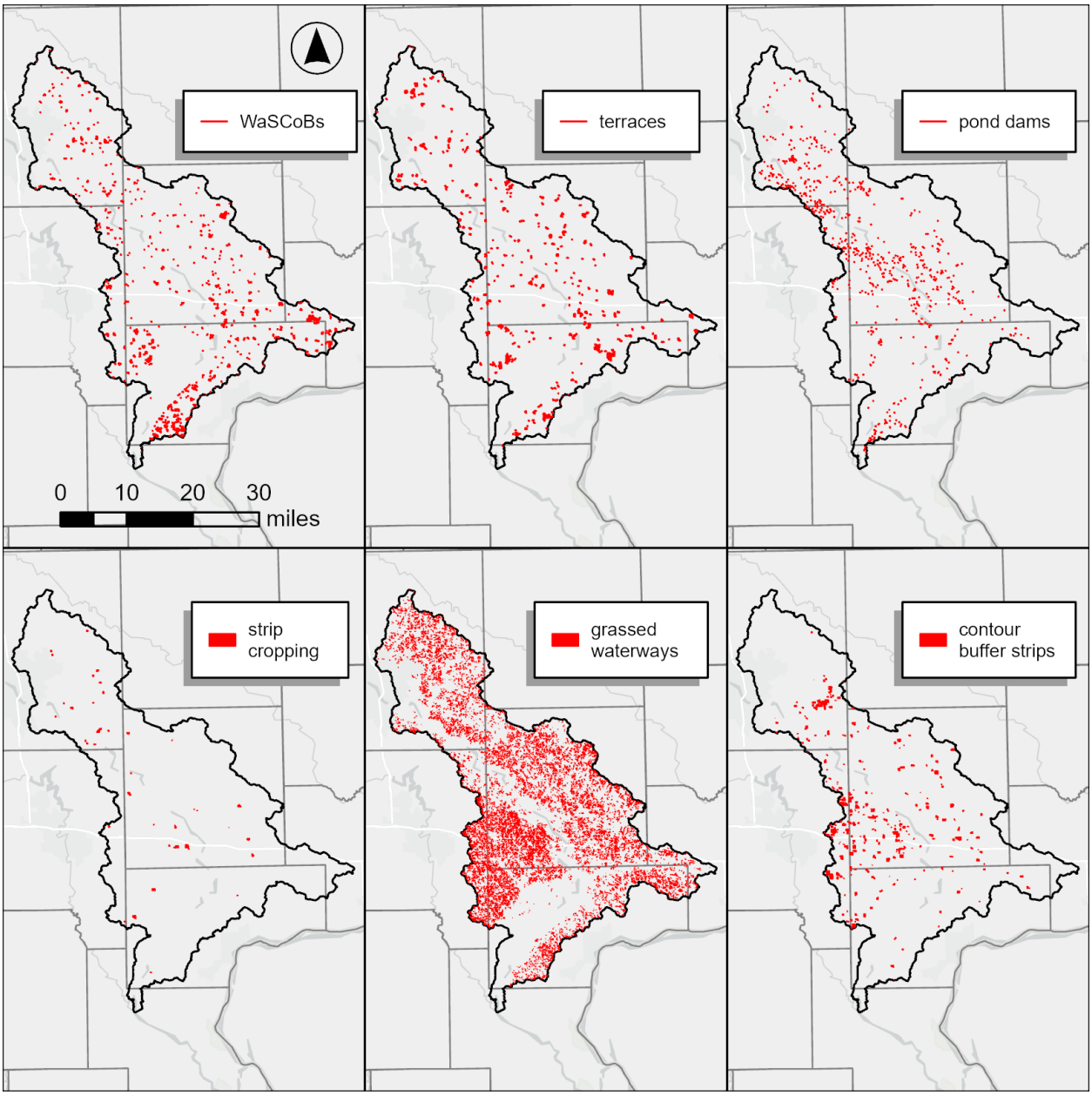

Figure 1-14. Best Management Practices in the watershed during 2007-2010. From the Iowa Best Management Practices (BMP) Mapping Project.

1.7 Soils

Soil infiltration and storage capacity are major factors in hydrologic response of the watershed. Soil properties are available in the Soil Survey Geographic Database (SSURGO). This database has been developed by the National Cooperative Soil Survey over the course of a century and is made available through the U.S. Department of Agriculture (USDA) and the Natural Resources Conservation Service (NRCS) (Soil Survey Staff, NRCS, USDA, 2024). An example

of the spatial detail of the soil database can be seen in the soil taxonomic classes shown in Figure 1-15.

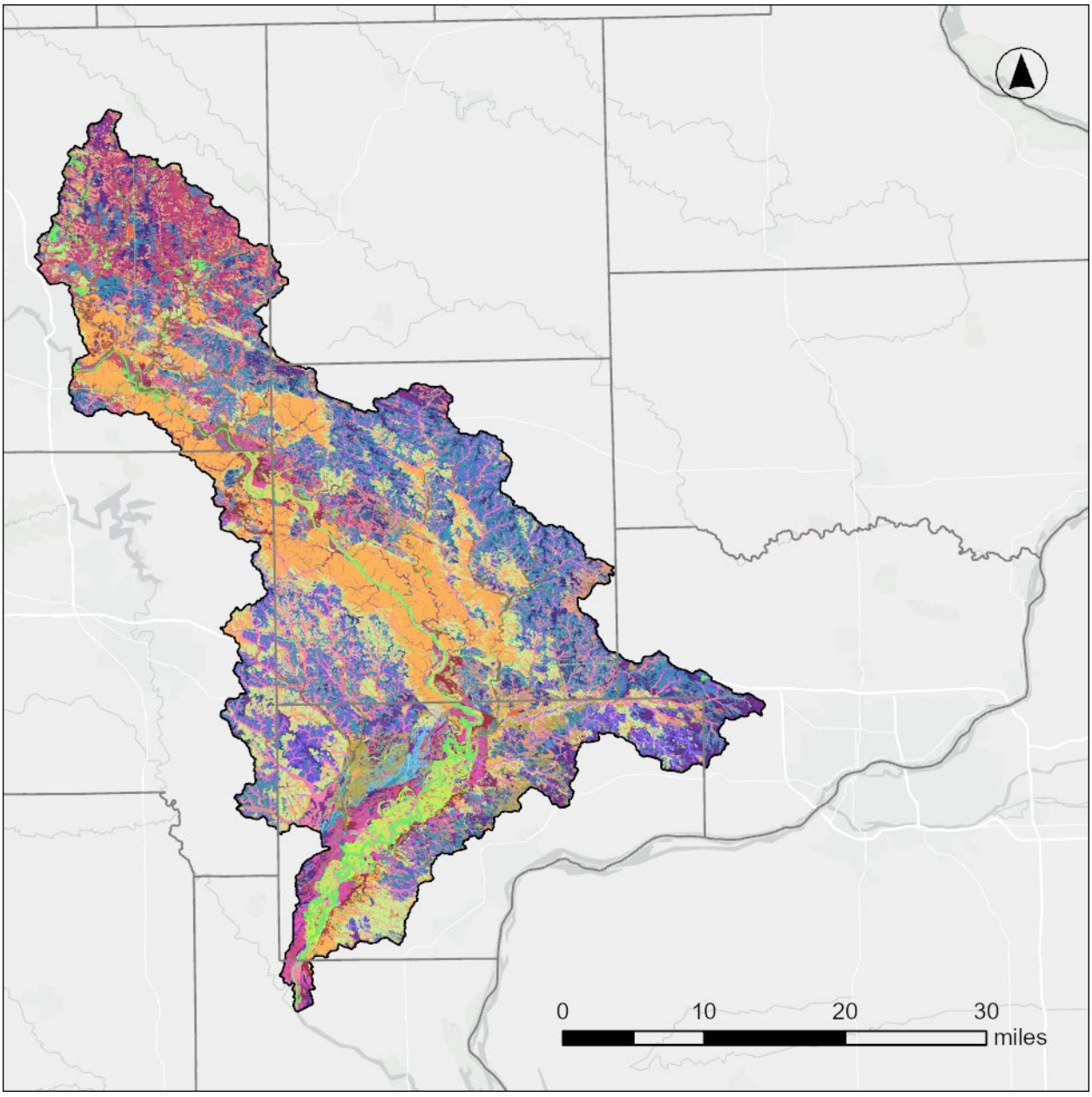

Figure 1-15. SSURGO soil taxonomic classes (Soil Survey Staff, NRCS, USDA, 2024).

The NRCS classifies SSURGO soils into four hydrologic soil groups (HSG) based on the soil's runoff potential. The four HSGs are A, B, C, and D, where A-type soils have the lowest runoff potential, and D-type have the highest. In addition, there are dual code soil classes A/D, B/D, and C/D that are assigned to certain wet soils. For these soil groups, even though the soil

properties may be favorable to allow infiltration (water passing from the surface into the ground), a shallow groundwater table (within 24 inches of the surface) typically prevents much from doing so. For example, a B/D soil will have the runoff potential of a B-type soil if the shallow water table were to be drained away, but the higher runoff potential of a D-type soil if it is not. Table 1-2 summarizes some of the properties generally true for each HSG (A-D). This table is meant to provide a general description of each HSG and is not all-inclusive. Complete descriptions of the HSGs can be found in USDA-NRCS National Engineering Handbook, Part 630 – Hydrology, Chapter 7.

The spatial distribution of HSGs in the Lower Cedar River Watershed are shown in Figure 1-16. The watershed is dominated by HSG C and C/D type soils. Isolated areas near the main river reaches generally have higher infiltration rates – HSG A and B types. Many areas along valleys and drainageways are classified as C/D. As discussed previously and shown in Figure 1-12, many areas have had drainage tile installed to drain away shallow groundwater. Viewing the soil distribution at this map scale is difficult, but the map does illustrate how much soils vary in space and the noticeable difference in soil types of the main river channel area versus moving further outward towards the watershed boundary. Table 1-2 shows the approximate percentages by area of each soil type for the watershed.

Table 1-2. Soil properties and characteristics generally true for hydrologic soil groups A-D.

Hydrologic Soil Group	Runoff Potential	Soil Texture	Composition	Minimum Infiltration Rate[1] (in/hr)
A	Low	Sand, gravel	< 10% clay > 90% sand/gravel	>5.67
B	Moderately low	Loamy sand, sandy loam	10–20% clay 50–90% sand	1.42-5.67
C	Moderately high	Loam containing silt and/or clay	20–40% clay <50% sand	0.14–1.42
D	High	Clay	>40% clay <50% sand	<0.14

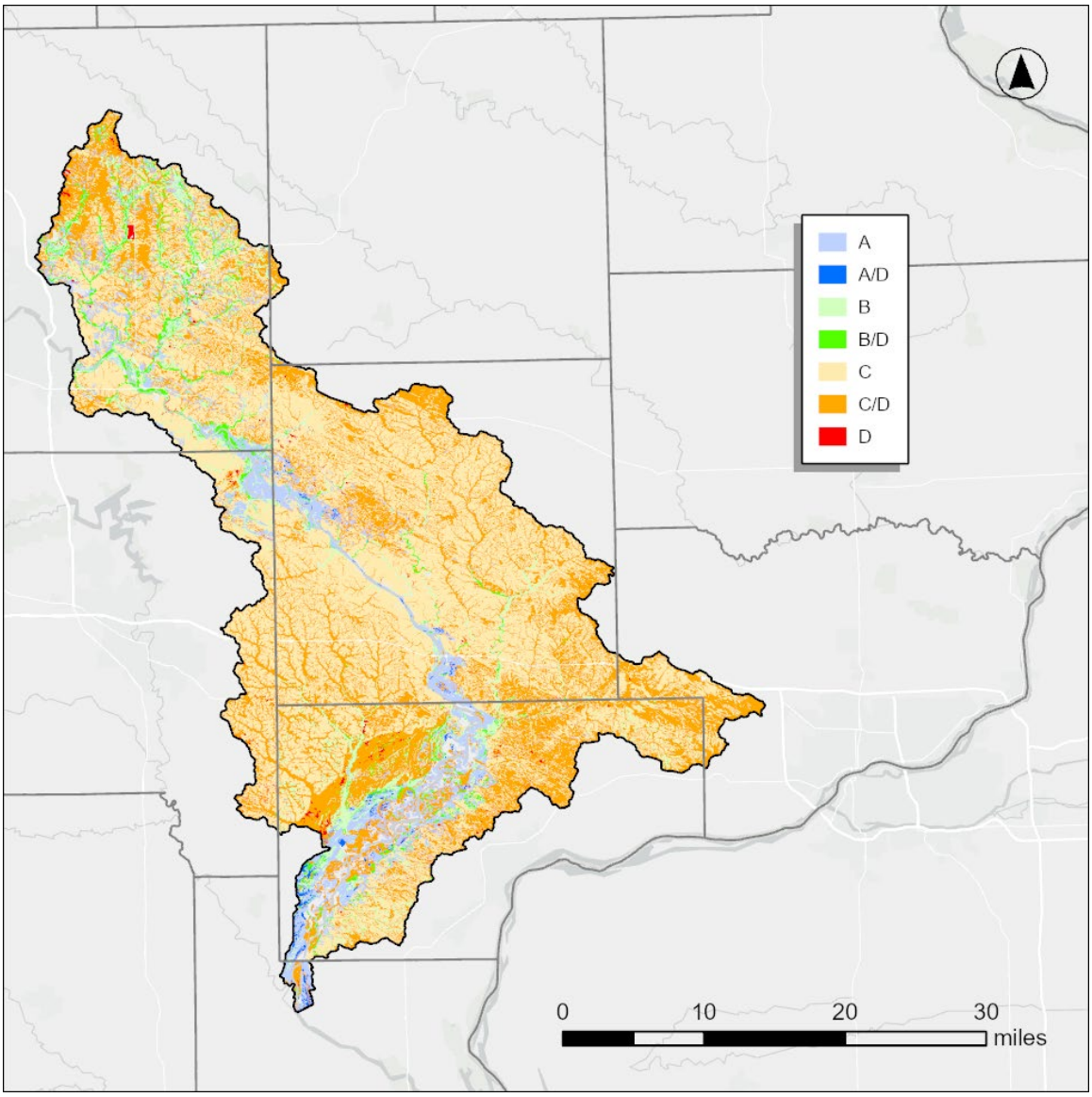

Figure 1-16. Distribution of Hydrologic Soil Groups. Hydrologic Soil Groups reflect the degree of runoff potential a particular soil has, with Type A representing the lowest runoff potential and Type D representing the highest runoff potential.

Table 1-3. Hydrologic Soil Group percentages by area of the watershed.

Hydrologic Soil Group	% of Watershed
A	7.9
A/D	0.5
B	5.5
B/D	3.0
C	47.1
C/D	32.6
D	3.3

1.8 Baseflow and Runoff Historic Trends

Annual precipitation volumes were estimated for each water year (October 1–September 30) from 1950 to 2024 using daily precipitation records near Conesville, Iowa. Total annual discharge for each water year was also calculated at Conesville, using daily discharge observations from USGS gaging stations 05465000. Using these historical precipitation and discharge records, it is possible to estimate partitioning of precipitation into baseflow and direct runoff on an annual basis. Using the local minimum method, daily discharges were separated into baseflow and runoff. The times series of annual precipitation upstream of Conesville, along with streamflow, baseflow, and runoff at Conesville are shown in Figure 1-18. Trendlines of annual precipitation, streamflow, baseflow, and runoff at Conesville, Iowa are shown in Figure 1-17. All datasets have a slight positive trend, with low correlation values.

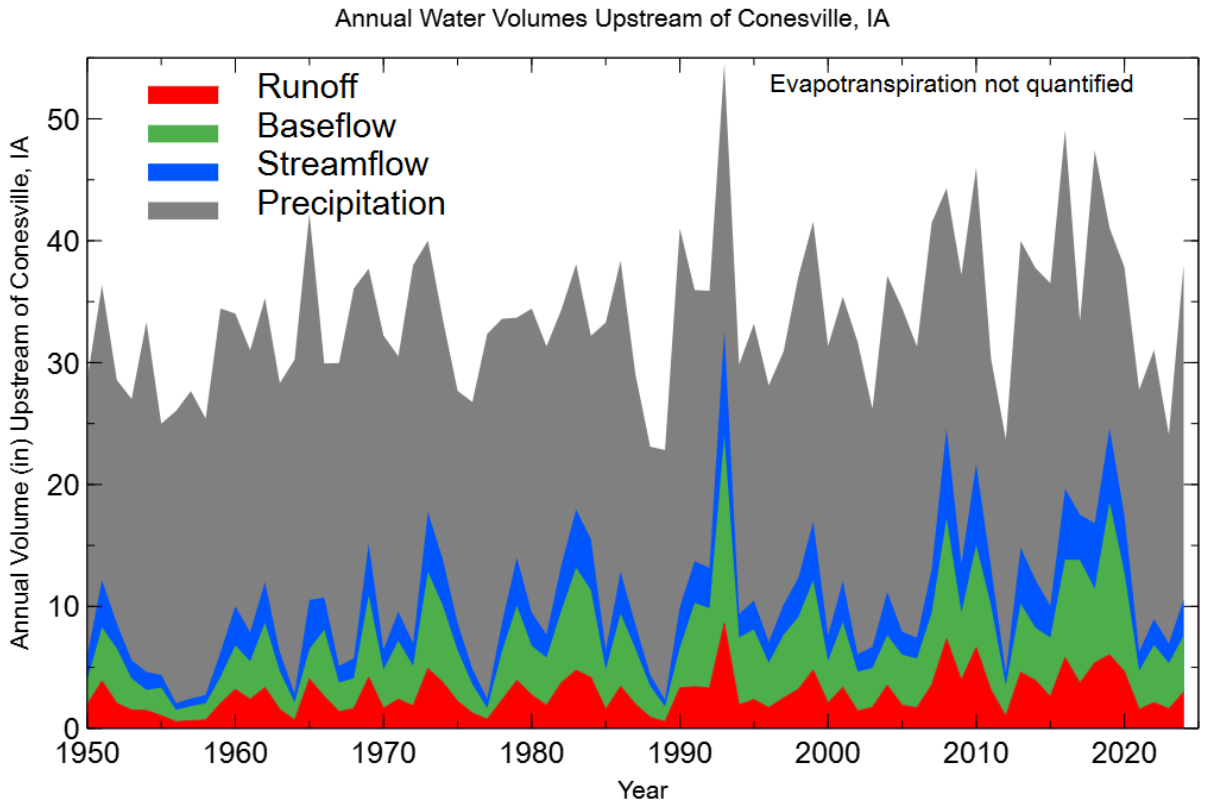

Figure 1-17. Annual volumes of precipitation, streamflow, baseflow, and runoff in inches of depth for watershed area upstream of Conesville, Iowa.

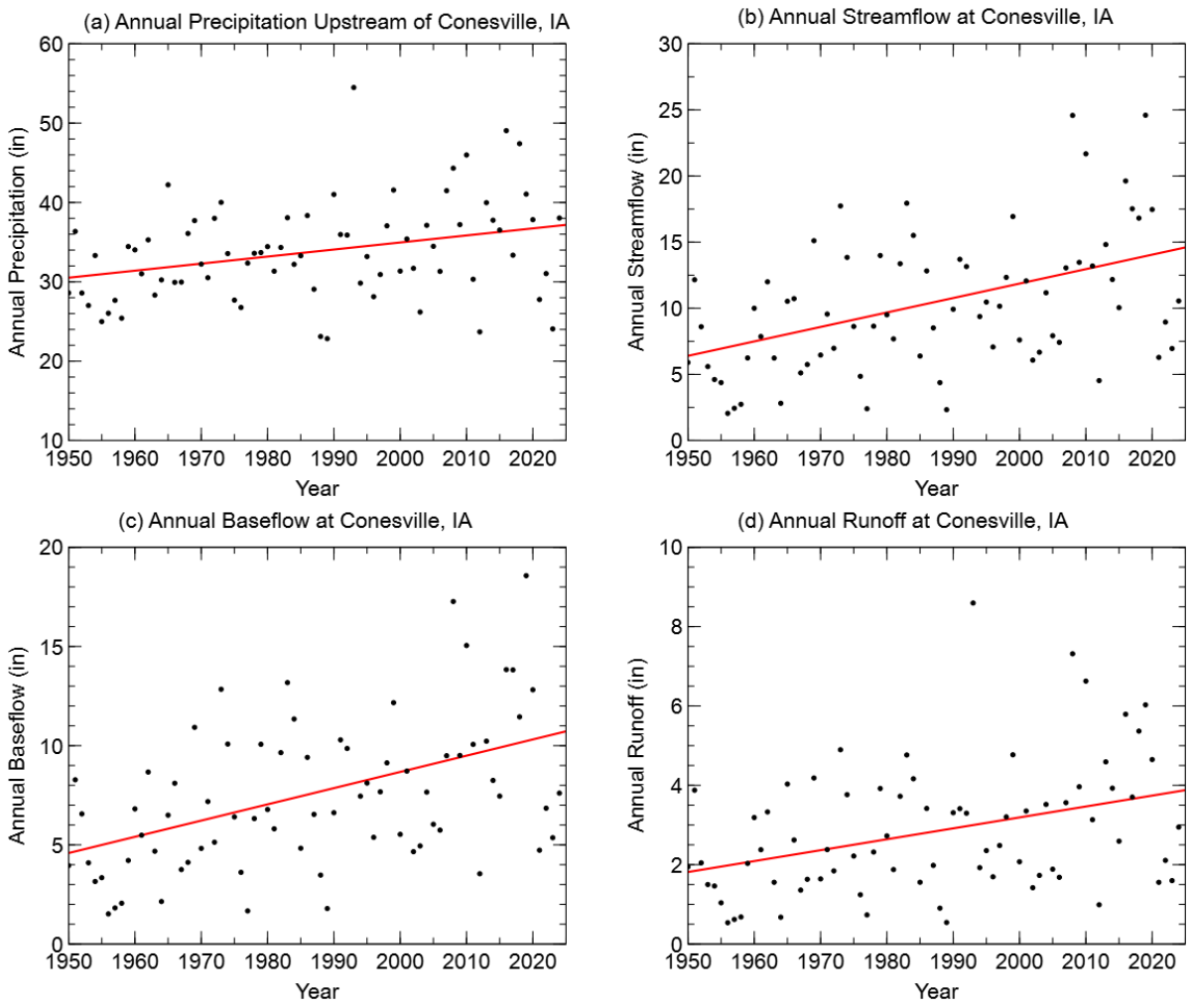

Figure 1-18. Annual totals for: (a) precipitation; (b) streamflow; (c) baseflow; and (d) runoff at Conesville, IA.

Cumulative mass curves were developed to further visualize and investigate any historic trends associated with these data. Cumulative mass curves allow visualization of long-term discharge or precipitation trends, with changes in slope indicating possible historical change points. Cumulative mass curves at Conesville were created for precipitation, streamflow, baseflow, and runoff by summing each consecutive annual total volume (inches) and are shown in Figure 1-17. Cumulative annual precipitation closely follows a linear, with no significant change in long-term total precipitation. There are slight change points around 1970-1990 for streamflow, baseflow and runoff. It is worth noting that the 1993 water year appears to contribute to an abrupt departure from the historic trend.

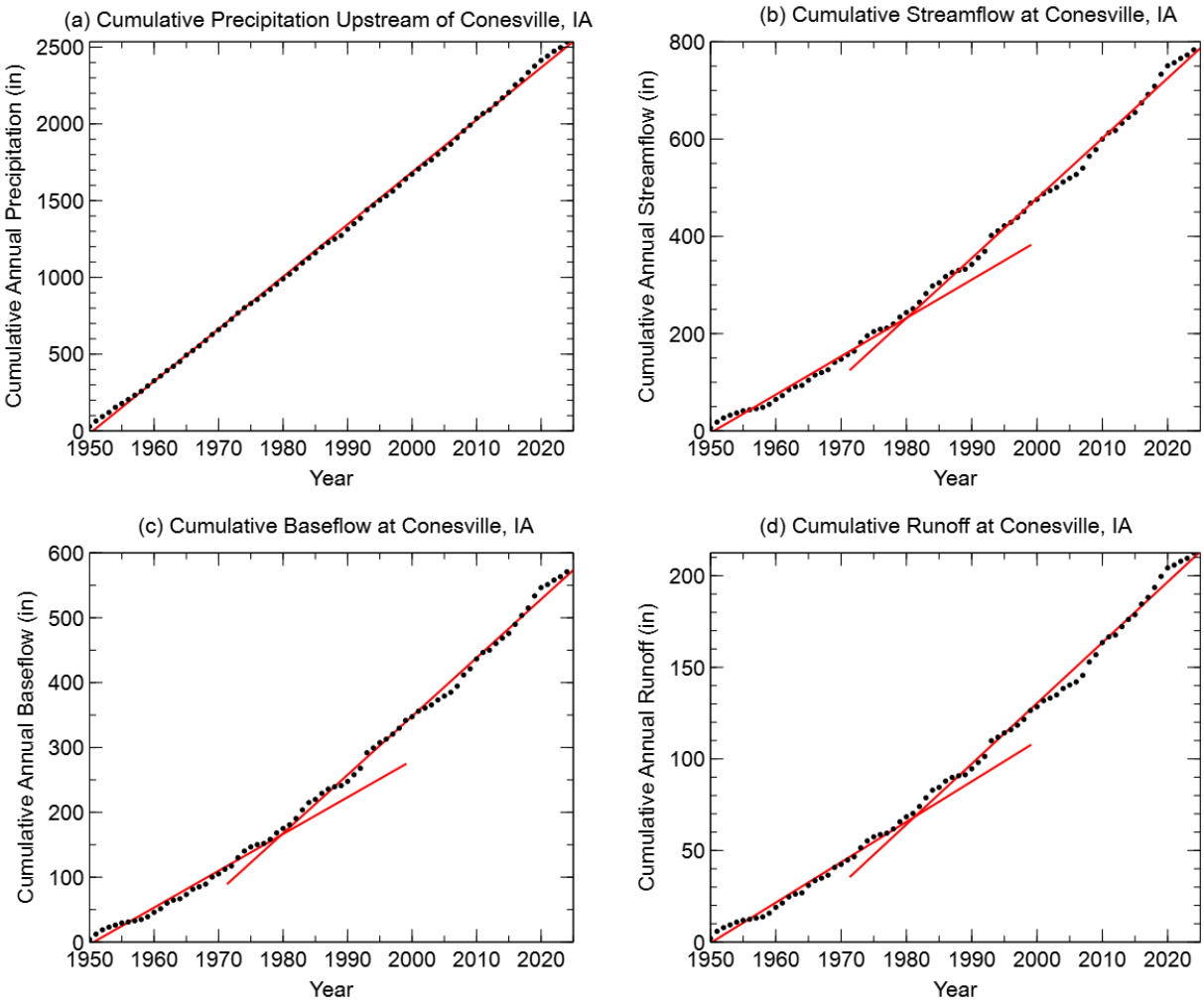

Figure 1-19. Cumulative annual totals for: (a) precipitation; (b) streamflow; (c) baseflow; and (d) runoff at Conesville, Iowa. Flow trendlines show a change in slope around 1980.

The influence of extremely wet years, such as 1993, on the linear trend can be accounted for using a double-mass curve. A double-mass curve based on a plot of two cumulative quantities during the same period will follow a straight line if the proportionality between the qualities remains unchanged (Gao, et al., 2017). Figure 1-20 shows double mass curves of cumulative precipitation with cumulative streamflow, baseflow, and runoff at Conesville. This plotting method shows a slight change point around 1970-1990 for these double mass curves. This means the relationship between long term precipitation and streamflow appear to have changed over the period of record. This change could be attributed to changes in precipitation and/or baseflow beginning in the 1970s, with the largest changes occurring in the last two decades. The reason for changes in streamflow in Iowa continues to be investigated (Mora et al. 2013, Frans et al. 2013,

Yiping et al. 2013); likely drivers include improved conservation practices promoting infiltration, greater artificial drainage, increasing row crop production, and channel incision (Schilling and Libra, 2003).

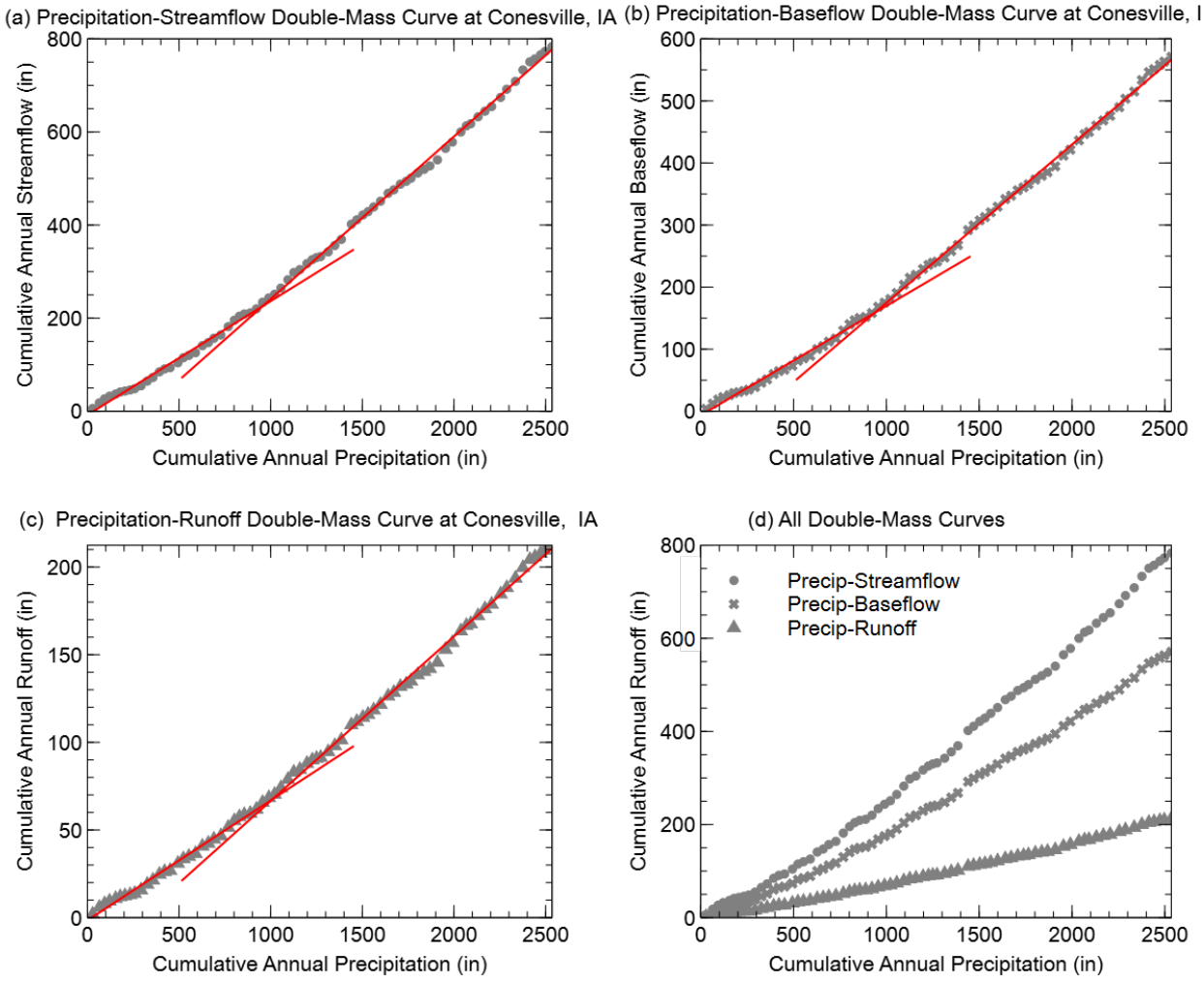

Figure 1-20. Double-mass curves using cumulative annual precipitation with cumulative annual (a) streamflow, (b) baseflow, and (c) runoff, and (d) all data at Conesville, Iowa.

1.9 Monthly Water Cycle

Using historic USGS streamflow and precipitation records, the average monthly stream flow and upstream precipitation at Conesville was calculated for the period 1950-2024. Monthly averages are shown in Figure 1-21. Precipitation amounts are lowest during the winter months. However, this precipitation is likely snowfall, which accumulates before melting in the warmer spring temperatures. A large increase in the average precipitation occurs in the spring months, before peaking in the months of May through July. Streamflow follows a different trend; the largest

monthly average streamflow occurring in March through June. Precipitation slowly decreases through late summer and early fall and streamflow drops accordingly after the summer months.

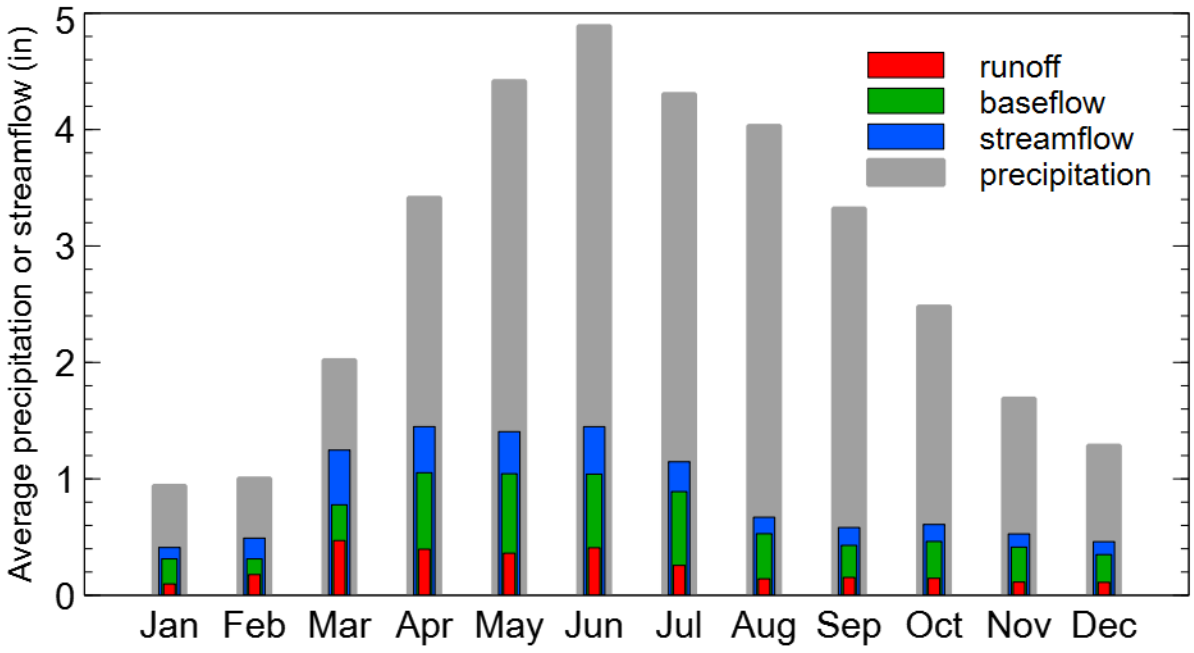

Figure 1-21. Average monthly water cycle for the Cedar River Watershed at Conesville, Iowa. The plots show the average monthly precipitation, streamflow, baseflow, and runoff in inches, based on the period 1950–2024.

1.10 Floods of Record

Meaningful analysis of flood observations requires a long period of record. The Cedar River at Conesville is the only gaging station with a significantly long record within the Lower Cedar River Watershed. Figure 1-22(a) shows the annual maximum peak discharges observed at the Conesville USGS gaging station. While these are annual maximum, many were not flood events. Calculating the mean annual peak discharge by averaging all annual peak observations can serve as a reasonable threshold for flooding occurrences. Of the 84 annual maximum peak discharges at Conesville, Iowa, 32 peaks were greater than the mean annual peak discharge.

Further analyses of these annual maximum peak discharges reveal the seasonal flood pattern for the Lower Cedar River Watershed. Figure 1-22(b) shows the calendar day of occurrence for each of the annual maximum peak discharges at Conesville. There is cluster of flooding events in the late winter early spring. There is an abrupt drop in annual maximum around in the month of May, before increasing again in June. This is further visualized in Figure 1-22(c) with the number

of flood occurrences for each month. Most flooding events occur during the months of March and April, likely driven by snowmelt.

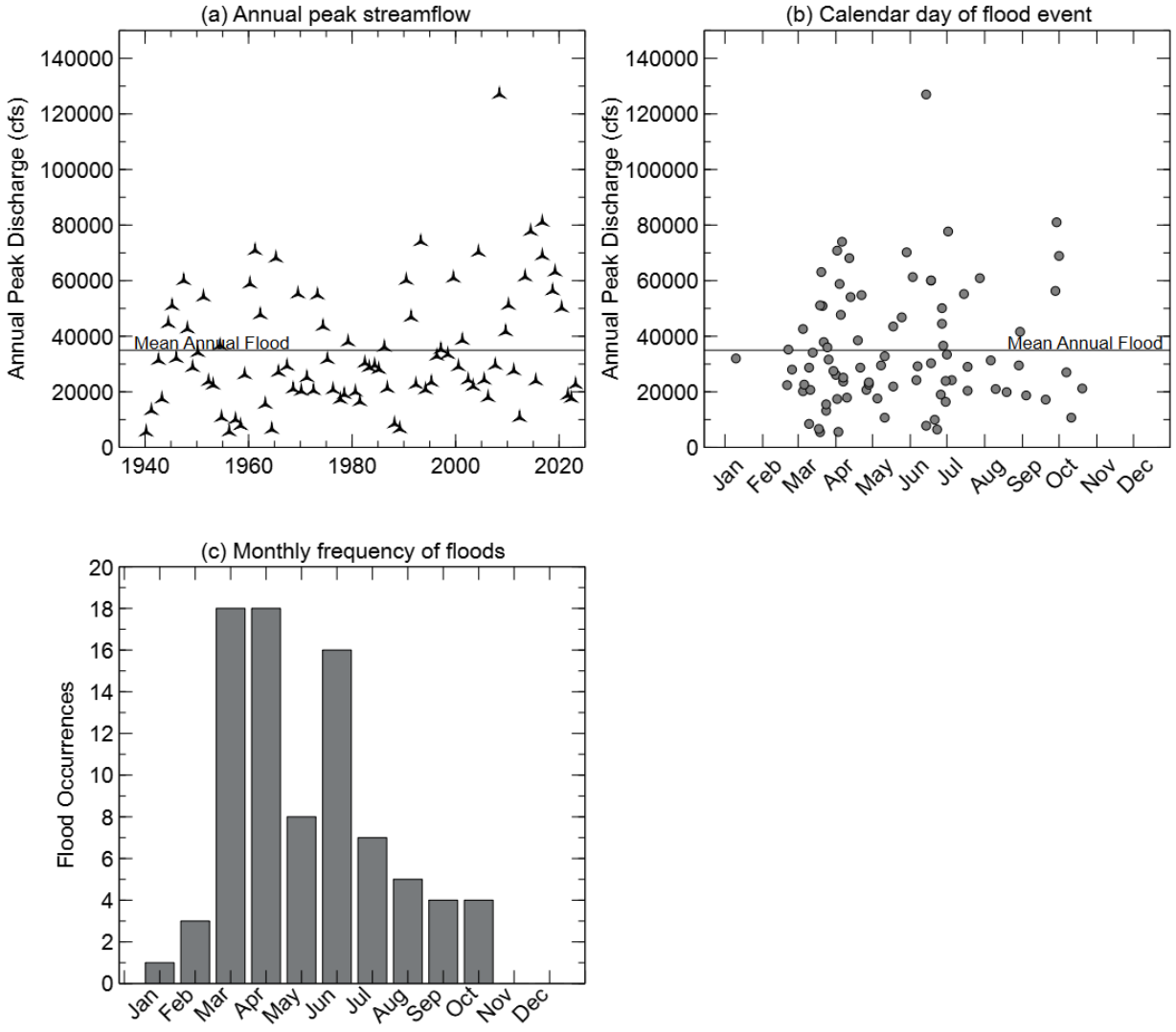

Figure 1-22. (a) Annual maximum peak discharge, (b) flood occurrences by month, and (c) calendar day of flood occurrence for the Cedar River at Conesville, Iowa.

Table 1-4 shows the five largest discharges at USGS gaging stations on the Cedar River at Conesville, Indian Creek at Marion, and the Wapsinonoc Creek at West Branch. The gaging stations at Marion and West Branch have limited sets of observations, so the largest peaks were likely not measured.

Table 1-4. Discharges from the five largest flow events at USGS Gaging Stations in the Lower Cedar River Watershed.

Cedar R at Conesville (1940 - Present)	6/14/2008 127,000 cfs	9/29/2016 81,000 cfs	7/2/2014 77,700 cfs	4/6/1993 74,000 cfs	4/2/1961 70,800 cfs
Indian Cr at Marion (2013 – 2015, 2021 - Present)	7/1/2014 4,590 cfs	3/11/2013 3,160 cfs	6/26/2021 2,170 cfs	6/12/2015 2,160 cfs	6/25/2022 981 cfs
Wapsinonoc Cr at West Branch (2016 - Present)	10/6/2018 859 cfs	9/5/2018 563 cfs	7/8/2022 510 cfs	6/9/2020 307 cfs	8/12/2016 233 cfs

1.11 Flood Frequency Estimates

Flood frequency estimates for Cedar River at Conesville were generated using a Bulletin 17C Analysis of USGS observed annual peak discharges and are shown in Table 1-5. Flood frequency estimates at Indian Creek at Marion and Wapsinonoc Creek at West Branch were generated using USGS StreamStats tools (USGS, 2024). These estimates represent the percent annual chance exceedance probability of the discharge occurring in any given year. For example, the 1-percent annual chance exceedance event has a probability of 1 in a 100 chance of occurring in any given year, hence it has been frequently referred to as the "100 Year Flood". However, when you consider longer periods, like a typical 30-year home mortgage, the 1-percent annual chance exceedance event has a 26% chance of occurring at least once over that 30-year period. There is significant uncertainty associated with lower probability event flows.

Table 1-5. Flood frequency estimates at Conesville, Marion, and West Branch, Iowa.

Percent Annual Chance Exceedance	Return Period	Estimated[1] Flowrate at Conesville, IA, cfs	Estimated[2] Flowrate at Marion, IA, cfs	Estimated[2] Flowrate at West Branch, IA, cfs
0.2	500	140,036	17,100	2,840
0.5	200	121,161	15,700	2,590
1	100	107,038	12,200	1,990
2	50	93,043	10,400	1,670
4	25	79,157	8,580	1,360
10	10	60,878	5,780	889
20	5	46,932	3,940	582
50	2	27,450	1,960	277

[1]HEC-SSP Bulletin 17C Analysis
[2]USGS StreamStats, Peak Iowa Region 2, 2013 Equations (USGS, 2024)

2. MODEL DEVELOPMENT

This chapter summarizes the development of the model used in the Hydrologic Assessment of the Lower Cedar River Watershed. Researchers used the U.S. Army Corps of Engineers' (USACE) Hydrologic Engineering Center's Hydrologic Modeling System (HEC-HMS), Version 4.12.

HEC-HMS is designed to simulate rainfall-runoff processes of a watershed. It is applicable in a wide range of geographic areas and for watersheds ranging in size from very small (a few acres) to very large (the size of the Lower Cedar River Watershed or larger). Figure 2-1 illustrates the water cycle and major hydrologic processes that occur in a watershed. The physical processes of the Lower Cedar River Watershed explicitly modeled with HEC-HMS include the partitioning of precipitation into infiltrated and overland flow volumes, transformation of excess runoff to subbasin outflow, downward groundwater movement, and flood wave routing. The model is mass conserving.

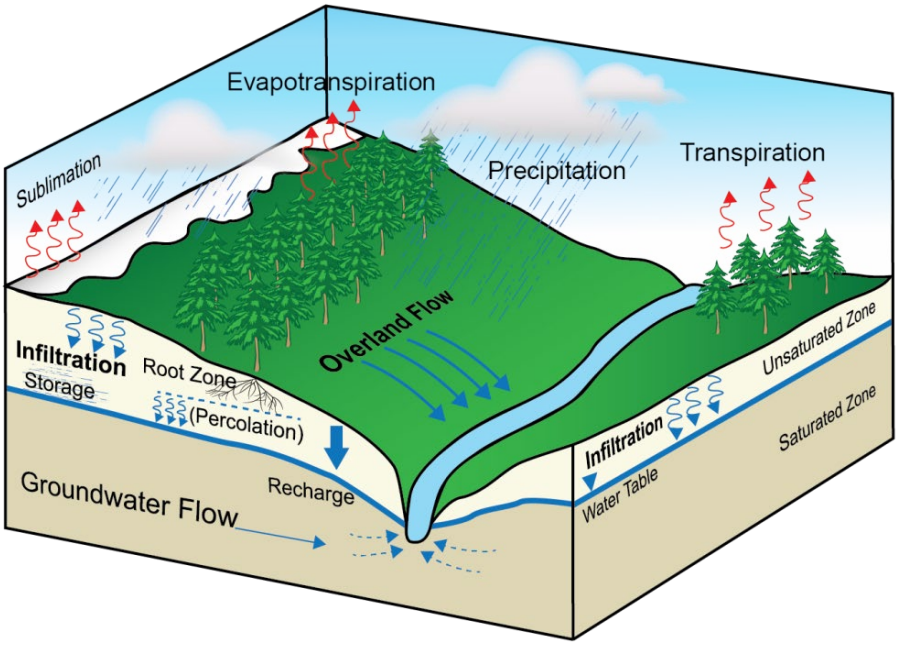

Figure 2-1. Hydrologic processes that occur in a watershed. Modeling considered the precipitation, infiltration, evapotranspiration, percolation, base flow and overland components of the water cycle.

HMS is a mathematical, lumped parameter, coupled surface subsurface model. The authors of this report will briefly discuss each of these characteristics. HMS is a mathematical model,

which implies that it represents the different hydrologic processes with simplified models that are often empirically developed to best describe observations or controlled experiments. HMS is also a lumped parameter model, meaning physical characteristics of the watershed, such as land use and soil type, are "lumped" together into a single representative value for a given land area, often referred to as a "subbasin". Once HMS establishes these averaged values, they remain constant throughout the simulation, rather than varying over time. The infiltration methods utilized are coupled, meaning that it solves different hydrologic processes simultaneously. Finally, HMS is a surface water model, meaning that it works best to simulate large storm events or when the ground is nearly saturated because overland flow is expected to dominate the partitioning of rainfall in both cases. Due to the model structure and prevalence of subsurface drainage infrastructure in this watershed, storm events that do not result in overland flow dominating rainfall partitioning are not ideal.

The two major components of the HMS hydrologic model are the basin model and the meteorologic model. The basin model defines the hydrologic connectivity of the watershed and how rainfall is converted to runoff, as well as how water is routed from one location to another. The meteorologic model stores the precipitation data that define when, where, and how much it rains over the watershed. Simulated hydrographs from HMS can be compared to discharge observations.

2.1 Subbasin Delineation

The Lower Cedar River Watershed modeled and described herein comprises approximately 1,100 square miles. The Cedar River flows through the Lower Cedar Watershed before meeting the Iowa River, at Columbus Junction, Iowa. For modeling, the watershed was divided into 670 smaller units, called subbasins in HMS. These have an average area of approximately 1.6 square miles but can be as large as 7.0 square miles. Figure 2-2 illustrates subbasin delineation of the Lower Cedar River Watershed as implemented in HMS. Subbasins were developed to ensure a junction point was created where USGS stream gaging stations were located. Figure 2-3 shows the distribution of subbasin areas for the model.

The newest versions of HEC-HMS have GIS toolsets available for terrain preprocessing, creating flow direction and flow accumulation grids, defining the stream network, and delineating the subbasins. The stream network was defined by channels draining at least 1.5 square miles;

subbasins were created such that a subbasin was defined upstream of all stream confluences. GIS-defined subbasins were further split manually to create an outlet point at each USGS gauge location, as well as the discharge point of incorporated structures.

In HMS, the model performs the averaging previously described for lumped parameter models within the boundary of each subbasin. Each subbasin was assigned a single value for the parameter being developed.

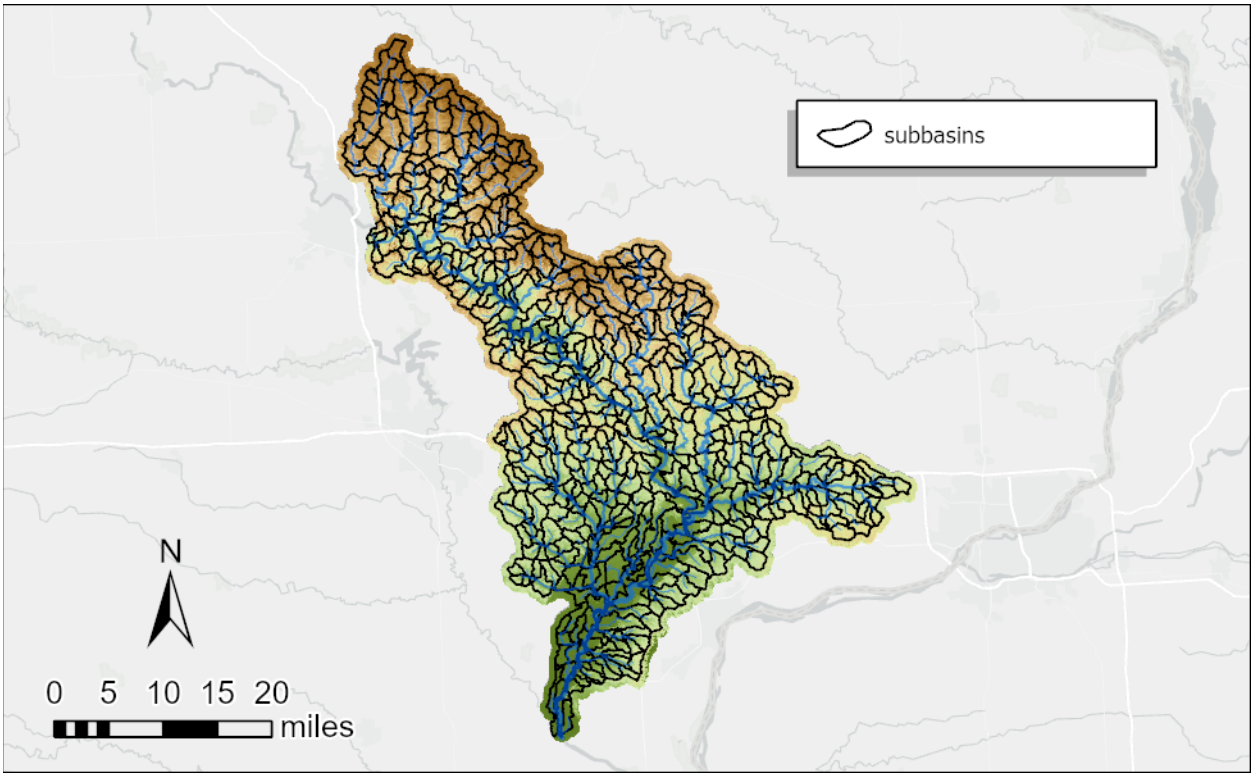

Figure 2-2. HMS model development of the Lower Cedar River Watershed. The watershed was divided into 670 subbasins for modeling.

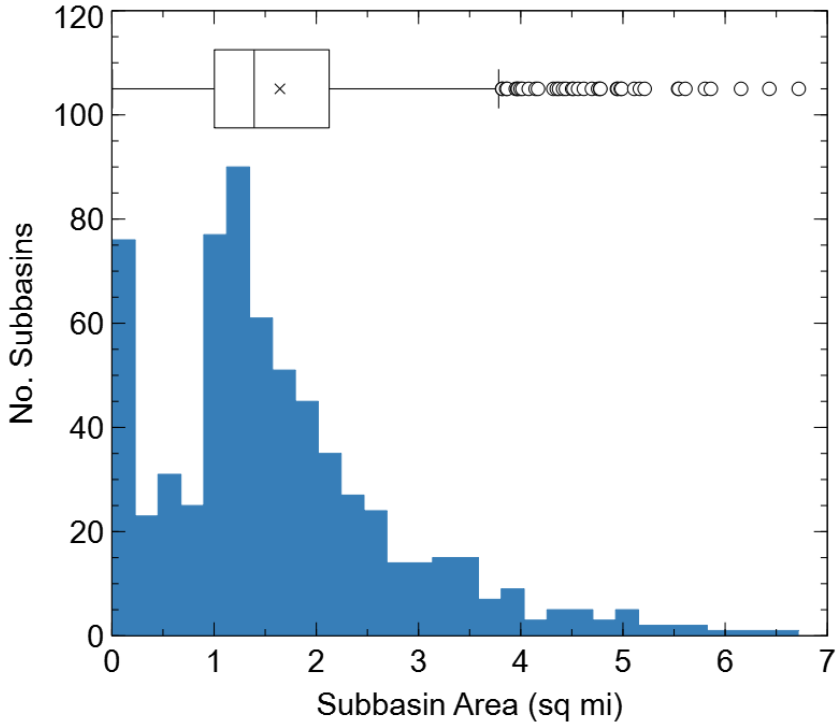

Figure 2-3. HEC-HMS model subbasin area histogram and boxplot

2.2 Soil Moisture Accounting Loss Model

Within the HEC-HMS software, we applied the Soil Moisture Accounting (SMA) model to simulate hydrologic processes within each model subbasin. The SMA model simulates vertical movement and storage of water between the atmosphere, vegetative canopy, ground surface, soil, and groundwater, characterized by storage volumes and rate equations. A conceptual schematic of the SMA model in shown in Figure 2-4. A brief description of SMA model components is presented below. A more detailed description of the SMA model can be found in HEC 2024.

2.2.1 Canopy Storage

Precipitation introduced to a model subbasin is first intercepted by the vegetative canopy. Each subbasin has a maximum canopy storage volume, which varies according to the type of vegetative cover. We used the NLCD land cover data to estimate subbasin averaged maximum canopy storage values. Canopy storage water can also be lost to the atmosphere through evapotranspiration. See section 2.2.5 for a description of evapotranspiration component of the model. When canopy storage is exceeded, excess water is transferred to surface storage.

2.2.2 Surface Storage

Surface storage is water held in shallow surface depressions across the landscape. Surface storage receives excess canopy storage water. Surface storage can be infiltrated into the soil at a rate which is dependent upon soil characteristics and degree of saturation. Surface storage water can also be lost to the atmosphere through evapotranspiration. See section 2.2.5 for a description of evapotranspiration component of the model. If the surface storage volume is exceeded, then excess volume becomes direct surface runoff. Routing of surface runoff to the receiving stream is calculated outside the SMA model in the runoff transform component of HEC-HMS. The runoff transform model is discussed in section 2.3.

2.2.3 Soil Profile Storage

Soil profile storage is water held the top layer of soil. Soil profile storage receives water from surface storage via infiltration and loses water through percolation into groundwater or evaporation. Soil profile storage is divided into two parts: tension storage and upper zone storage. Tension storage is the proportion of soil profile water attached to soil particles by surface tension, while upper zone storage is the proportion of soil profile water held in soil pores. In the SMA model, tension storage is filled before infiltrated water is added to upper zone storage. Conversely, water is only evaporated from tension storage once upper zone storage is empty. Water in tension storage cannot percolate and only leaves the soil though evapotranspiration. See section 2.2.5 for a description of evapotranspiration component of the model.

2.2.4 Groundwater storage

In our application, we use two vertical groundwater storage layers. The upper layer receives water from soil profile storage through percolation. Water from the upper layer is transferred to the lower layer through percolation and transferred to the receiving stream through a linear reservoir as interflow. Water in the lower layer is transferred to deep groundwater through percolation or to the receiving stream through a second linear reservoir as baseflow.

2.2.5 Evapotranspiration

If no precipitation occurs during a given model timestep, water can leave the canopy, surface, or soil through evapotranspiration. To meet potential evapotranspiration, the SMA model first draws from the canopy storage, followed by surface storage, then upper zone storage, and

finally tension storage. Evapotranspiration occurs simultaneous with other modeled processes. Details of each evapotranspiration process can be found in HEC 2024.

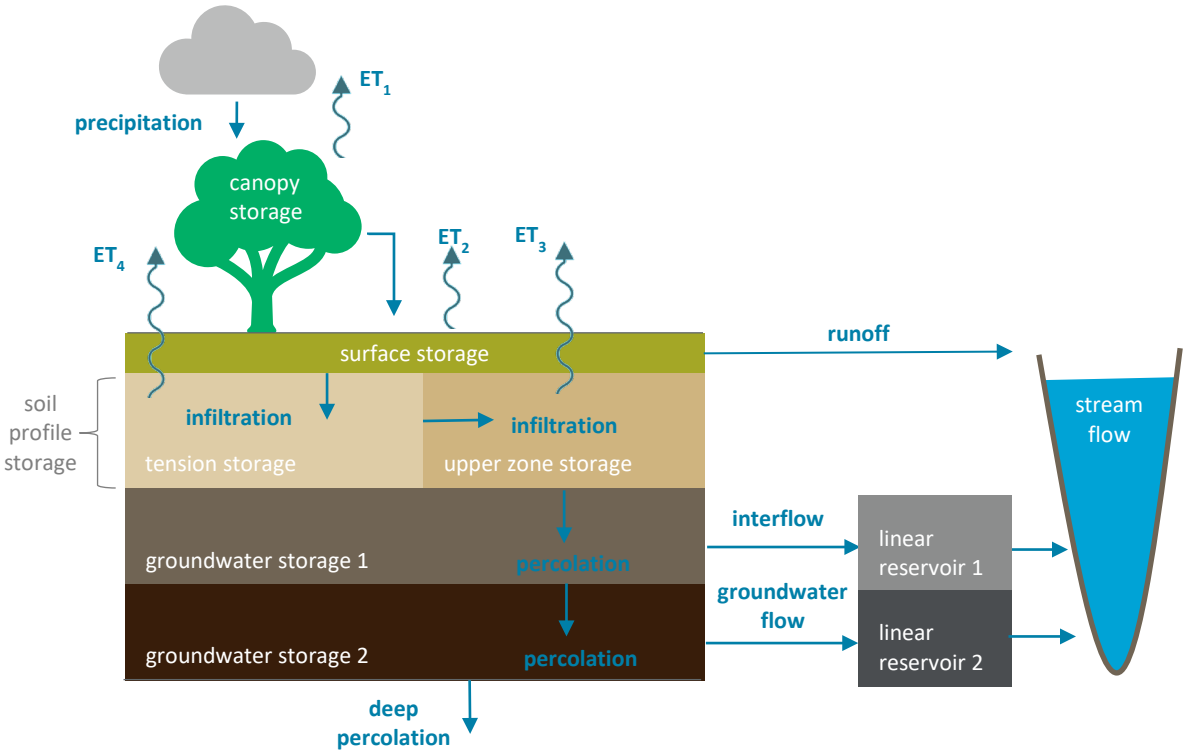

Figure 2-4. Soil Moisture Accounting (SMA) model

2.3 Runoff Transform

When surface storage capacity is exceeded, direct runoff is generated. Subbasin runoff hydrograph routing to the subbasin outlet is simulated using the Clark Unit Hydrograph transform method. Further details of the Clark Unit Hydrograph method can be found in the HEC-HMS technical reference manual (Hydrologic Engineering Center, 2024). The Clark Unit Hydrograph method was used to convert excess precipitation into a direct runoff hydrograph for each subbasin. This unit hydrograph method accounts for translation (delay) and attenuation (reduction) of the peak subbasin hydrograph discharge due to travel time of the excess precipitation to the subbasin outlet and temporary surface storage effects. The hydrograph is routed through a linear reservoir to account for temporary storage effects.

The Clark unit hydrograph method requires two inputs — time of concentration and a time storage coefficient. The time of concentration is the time required for water to travel from the hydraulically most remote point in the subbasin to the subbasin outlet.

2.4 Channel Routing

Once water enters a stream as runoff, interflow, or baseflow, it is routed through the model stream network using the kinematic wave method. This method approximates the full unsteady flow equations by neglecting inertial and pressure forces (Hydrologic Engineering Center, 2024). Required parameters include the reach length, bottom slope, Manning's n roughness, number of subreaches, an index method, and a cross-section shape/dimensions (Hydrologic Engineering Center, 2024).

2.5 Baseflow

A mass conserving linear reservoir baseflow method was utilized in conjunction with the SMA model. The lateral outflow from the SMA groundwater layer 1 is connected to the linear reservoir groundwater layer 1. Similarly, the lateral outflow from the SMA groundwater layer 2 is connected to the linear reservoir groundwater layer 2. The linear reservoirs can be used to further store and attenuate groundwater layer outflows.

2.6 Model Inputs and Parameters

2.6.1 Elevations

Iowa's 2019-2021 statewide LiDAR dataset provided elevation data to parameterize the basin model. The USGS has performed quality assurance testing on these LiDAR data at quality level QL2, which have reported vertical positional accuracy of +/- 10 cm, and a nominal pulse density of 2 points per square meter. The LiDAR product used had a resolution of 3-meters and was processed as a bare earth product, with structures and vegetation removed. Using ESRI ArcGIS, LiDAR data was clipped the to the watershed boundary and mosaicked into a seamless digital elevation model. The Iowa State Plane North geographic coordinate system was used, referencing the North American Datum of 1983 (NAD 83). All elevation values are in feet and are referenced to the North American Vertical Datum of 1988 (NAVD 88).

2.6.2 Soil Properties

Initial soil properties parameters were developed using USDA SSURGO soils data. Soil properties included maximum infiltration rates, soil storage, tension storage, and soil percolation rates. Many of these parameters were adjusted during calibration by region.

2.6.3 Surface Storage

Initial storage depth estimates were provided by the ACSE Design & Construction of Urban Stormwater Management Systems (The Urban Water Resources Research Council , 1992). Initial surface storage depths were parameterized using land use classifications provided by the National Land Cover Database (NLCD). These surface storage depths were adjusted by during calibration by region.

Table 2-1. Initial depression storage estimates from ASCE (The Urban Water Resources Research Council , 1992)

Land Cover	Storage Depth (in)
Impervious surfaces	0.05 – 0.10
Lawns	0.10 – 0.20
Pasture	0.20
Forest Litter	0.30

2.6.4 Runoff Hydrographs

An initial estimate of time of concentration was generated using equation (2-1) (Hydrologic Engineering Center, 2024). An initial estimate of Clark unit hydrograph storage coefficient was generated using equation 3-2 (Hydrologic Engineering Center, 2024)

$$T_c = 2.2 * \left(\frac{L * L_c}{\sqrt{Slope_{10-85}}} \right)^{0.3} \quad (2\text{-}1)$$

Where L = longest flow path length
L_c = centroidal longest flowpath length

$Slope_{10\text{-}85}$ = average slope of the flowpath represented by 10-85 percent of the longest flowpath

$$R = 16.4 * L^{-0.342} Slope_{10-85}{}^{-0.79} \quad (3\text{-}2)$$

Figure 2-5 illustrates the NRCS methodologies for runoff depth estimation and how this runoff depth is converted to discharge (using one of the Clark unit hydrograph methods).

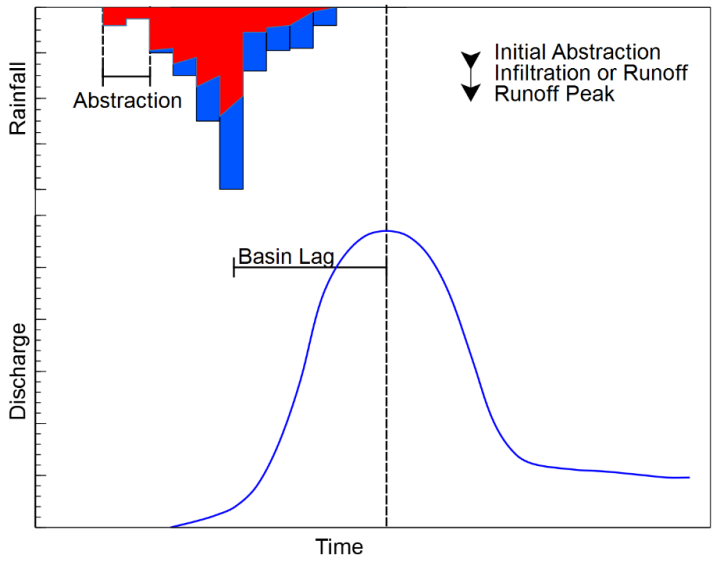

Figure 2-5. Subbasin runoff hydrograph conceptual model. Rainfall is partitioned into a runoff depth according to the Soil Moisture Accounting model, which is then converted to discharge using the Clark unit hydrograph method.

2.6.5 Channel Routing

The kinematic wave routing model was parameterized using GIS methods to estimate reach length and bottom slope from bare-earth LiDAR elevation data. The stream order of each reach was used to make assumptions about cross-section width. Manning's n roughness, number of sub reaches, and index celerity method were adjusted during calibration.

2.6.6 Baseflow

Baseflow and groundwater parameters were estimated by analyzing observed stream flow data from USGS gaging stations. The receding limbs of multiple storms were analyzed to estimate storage volumes and timing for groundwater, runoff and interflow influences. These analyses were used to calculate groundwater layers 1 and 2 recession coefficients and storage depths. Further adjustments occurred during calibration.

3. MODEL FORCING

3.1 Precipitation

We used NOAA Office of Water Prediction Analysis of Period of Record for Calibration (AORC) data to force our model. AORC is a historical gridded precipitation product developed from several sources, specifically for the purpose of hydrologic model calibration (Fall, et al., 2023). AORC provides 4-kilometer (2.5-mile) resolution, hourly precipitation for the continental United States over the period from 1979 to present. We used AORC data for the period from 2000 to 2021 to calibrate and validate our model, as well as to evaluate management practices. The AORC grid is shown superimposed on the Lower Cedar River watershed in Figure 3-1. Locations of USGS gaging stations, temperature stations, and rain gauge locations used in this analysis are also shown. For most simulations, observed streamflow on the Cedar River at Cedar Rapids was used as an upstream boundary condition.

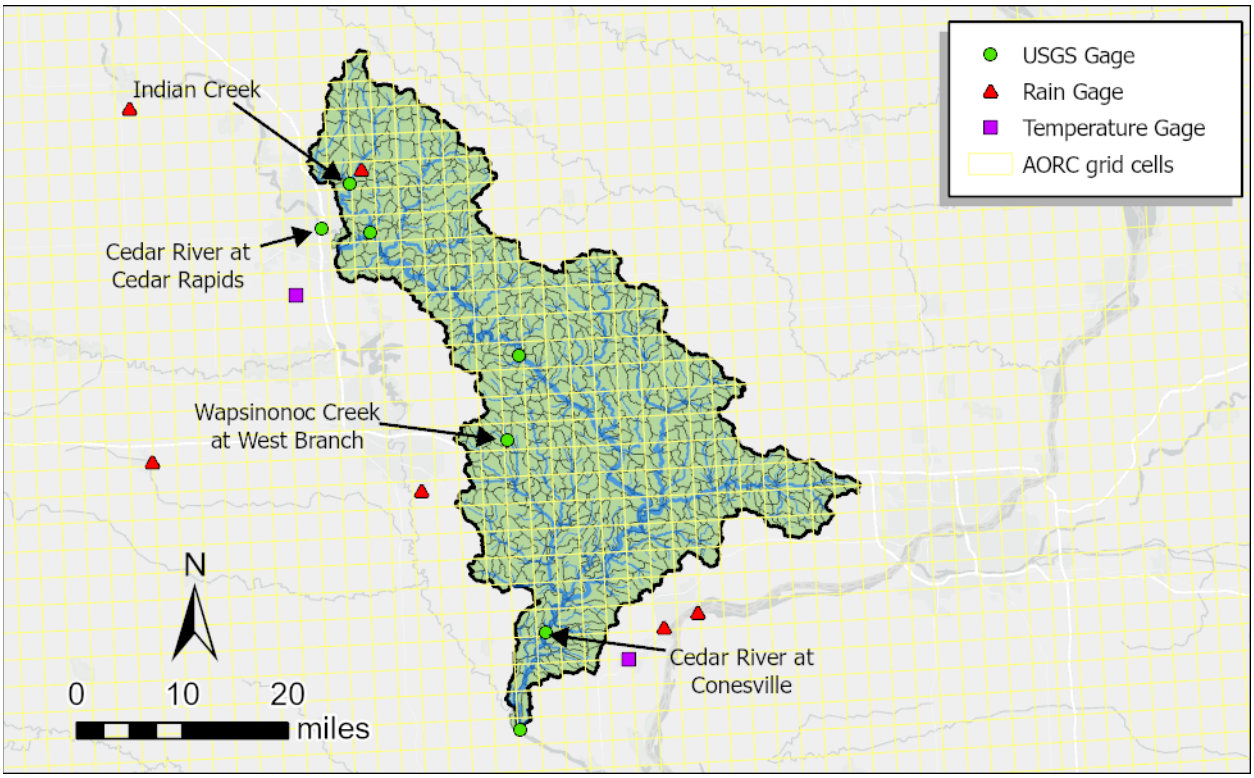

Figure 3-1. AORC gridded radar precipitation and temperature observations were used to force the model simulations.

A hypothetical storm was developed for comparative analyses, such as potential runoff generation, increased infiltration capacity, and increased distributed storage within the watershed. The hypothetical storm applies a uniform depth of six inches of rainfall across the entire watershed with the same timing everywhere. A Soil Conservation Service (SCS) Type-II distribution, 24-hour storm was used for the hypothetical storm. Rainfall does not typically occur uniformly across the entire watershed. However, the hydrologic response of subbasins can be compared and analyzed more easily if all the subbasins are subject to the same rainfall depth and timing.

3.2 Temperature

We utilized Automated Surface Observing System (ASOS) temperature datasets from Cedar Rapids and Muscatine archived by the Iowa Environmental Mesonet (Iowa State University, 2024). We created a spatially interpolated temperature dataset for the watershed within HEC-HMS using inverse distance weighting as the interpolation method. The temperature model is vital component of the evapotranspiration and snowmelt models.

4. MODEL CALIBRATION

To calibrate a model, the initial set of parameters are developed for a hydrologic model are adjusted so the model's simulated results match an observed time series as closely as possible. Typically, this is stream discharge at a gaging station. Importantly, modelers should not make extreme adjustments to parameters just to manipulate the end results to match the observed time series. If this is necessary, the model does not reasonably represent the watershed, and it is requisite upon the modeler to change methods used within the model or find out which parameter(s) might be needed to better represent the watershed's hydrologic response. A significant source of uncertainty when attempting to simulate historic events is the radar rainfall used for forcing. Even if the watershed hydrology is well represented by model parameters, the radar rainfall could be higher or lower than actual precipitation amounts for any given event.

The Lower Cedar River Watershed HMS model was calibrated to the 2012-2016 water years by adjusting several model parameters – maximum infiltration rate, soil percolation, groundwater storage depths and timing coefficient, and deep percolation rates. Many of these adjustments were necessary to account for the likely influence of artificial drainage and karst within the watershed. Several intense rainfall events occurred during the 2012-2016 period, resulting in several large flow events to calibrate the model to, specifically Indian Creek upstream

of Marion. Global adjustments to the maximum infiltration rates, surface storage, and subbasin time of concentration and storage coefficients, and groundwater storage coefficients were completed within each region to best match observed discharge time series at each USGS discharge gauge location. However, some restraint was exercised due to the possibility that the radar rainfall was underpredicted.

Figure 4-1 shows flow time series for the calibration period for Indian Creek at Marion. Overall, simulation results match observations well at this location, mostly capturing recurring high-flow periods in terms of timing and magnitude. Selected peak flow events from this time series are better visualized in Figure 4-2. The largest flow event recorded at Marion occurred in June 2014 and the model significantly under predicted the peak flow. Model parameters were adjusted to reproduce this large event but were not successful. It appeared that the radar rainfall may a likely source of error. It is also worth noting the Indian Creek catchment is relatively small compared to the radar rainfall grid cells, so it is possible the rainfall was not accurately captured for this particular event. The other peak flow events in June 2013, June 2015 and July 2016 were reproduced well by the model. Table 4-1 shows common metrics used in hydrologic model performance evaluations. Based on Moriasi et al., (2007) model simulations can be judged as satisfactory if Nash-Sutcliffe efficiency (NSE) > 0.50, Percent bias (PBIAS) ± 25% for streamflow, and the coefficient of determination (R^2) values are close to 1. The Kling-Gupta Efficiency (KGE) metric is also included as an additional model performance metric and is generally judged as satisfactory if > 0 (Kling, Fuchs, & Paulin, 2012). In general, simulation results from the calibration period exceed these standard performance metrics. Observed and simulated monthly flow volumes normalized by upstream drainage area at Marion, shown in Figure 4-3, also show good agreement.

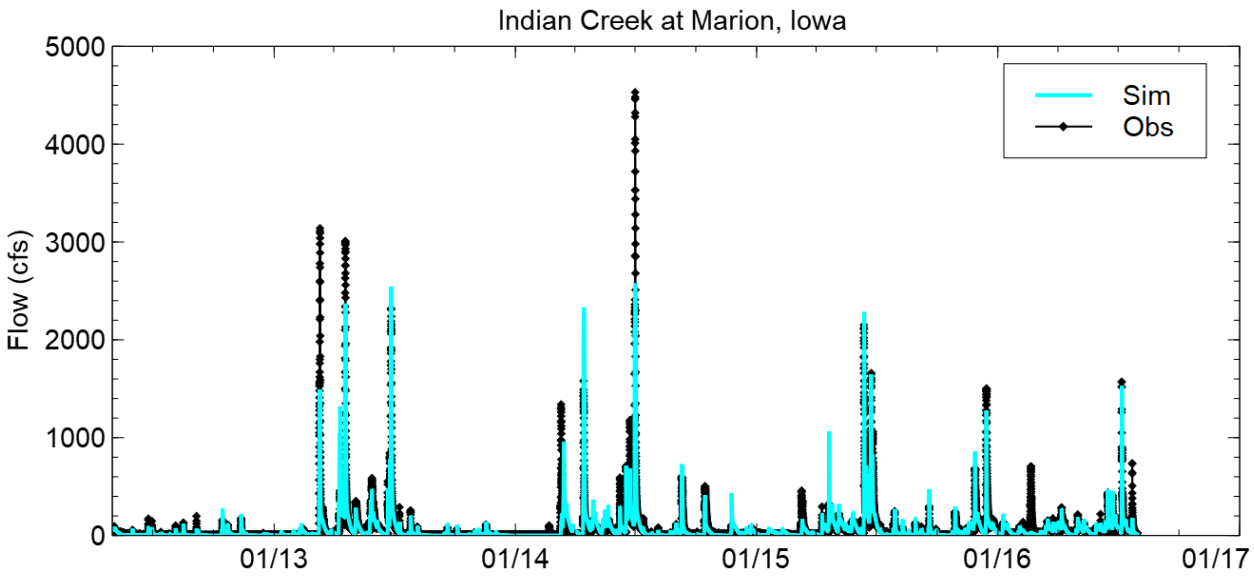

Figure 4-1. Observed and simulated flow hydrographs at USGS gaging station on Indian Creek at Marion for the calibration period.

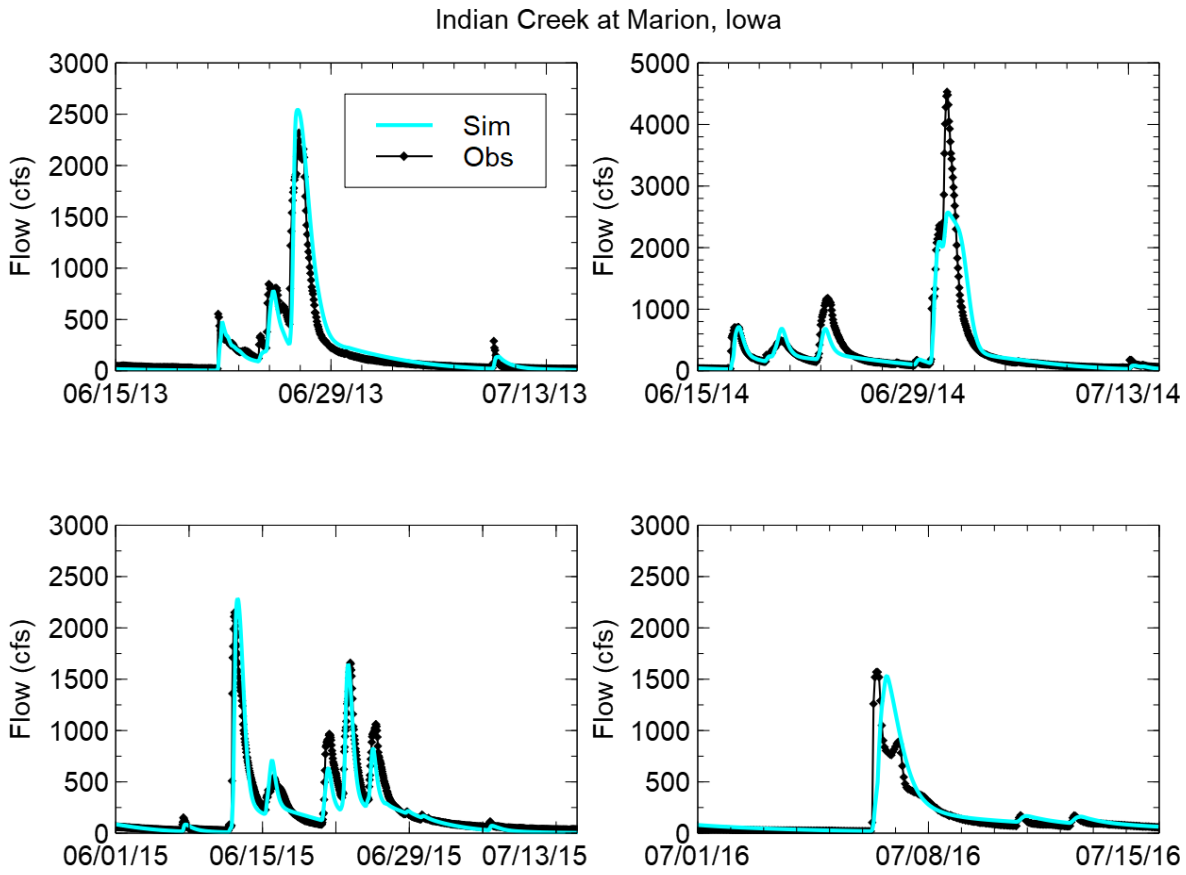

Figure 4-2. Selected peak flow events during the 2012-2016 calibration period.

Table 4-1. Simulation performance metrics for the 2012-2016 calibration period for Indian Creek at Marion. Root Mean Squared Error (RMSE), coefficient of determination (R^2). Nash-Sutcliffe efficiency (NSE), Percent bias (% Bias), and Kling-Gupta Efficiency (KGE).

Location	RMSE	R^2	NSE	% Bias	KGE
Indian Creek at Marion	84.5	0.78	0.77	-5.5%	0.84

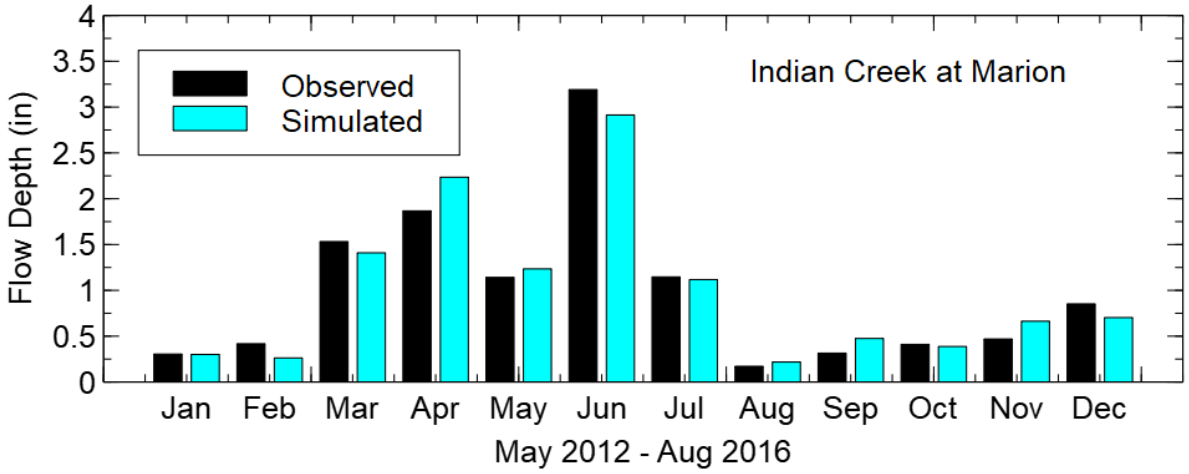

Figure 4-3. Monthly flow volume in depth (inches) for Indian Creek at Marion, May 2012 – Aug 2016, normalized by upstream drainage area.

Observed and simulated flow for the Cedar River at Conesville for the calibration period is shown in Figure 4-4. Flow observations for the Cedar River at Cedar Rapids were used as an upstream model inflow, so it is expected that simulation results match observations very closely at this location. Model performance metrics are shown in Table 4-2. In general, simulation results from the calibration period exceed standard performance metrics. Observed and simulated monthly flow volumes normalized by upstream drainage area at Conesville, shown in Figure 4-5, also show good agreement.

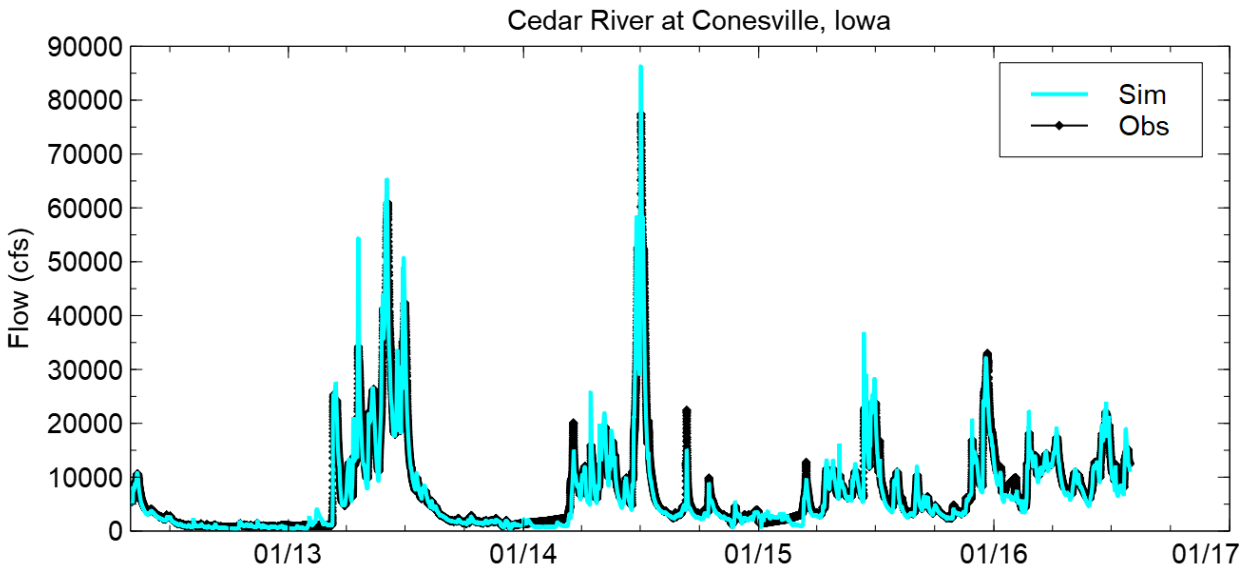

Figure 4-4. Observed and simulated flow hydrographs at USGS gaging station on the Cedar River at Conesville for the calibration period.

Table 4-2. Simulation performance metrics for the 2012-2016 calibration period for Cedar River at Conesville. Root Mean Squared Error (RMSE), coefficient of determination (R^2). Nash-Sutcliffe efficiency (NSE), Percent bias (% Bias), and Kling-Gupta Efficiency (KGE).

Location	RMSE	R^2	NSE	% Bias	KGE
Cedar River at Conesville	2148	0.94	0.93	-5.9%	0.90

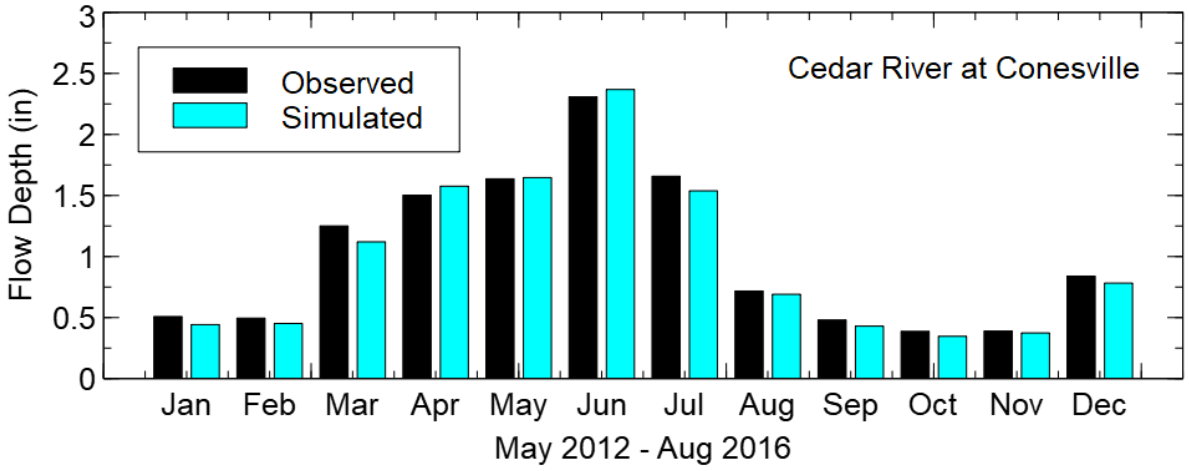

Figure 4-5. Monthly flow volume in depth (inches) for Cedar River at Conesville, May 2012 – Aug 2016, normalized by upstream drainage area.

5. MODEL VALIDATION

To validate a model, the calibrated model is used to simulate other events without changing any model parameters. If the calibrated model can reproduce the validation event reasonably well, then the model is validated.

5.1 May–Sep 2024 Validation Period

The 2024 water year had several flow events on Indian Creek that occurred during the spring and summer. The Cedar River also experienced a few relatively high flow events throughout 2024. Observed and simulated flow timeseries for the 2024 validation period are shown in Figure 5-1. Overall, simulation results match observations well through several events at both gaging locations. The flow peak magnitude and timing are well captured. The common metrics used in hydrologic model performance evaluations are show in Table 5-1. In general, simulation results from this validation period exceed those metrics. Observed and simulated monthly flow volumes normalized by upstream drainage area at Marion and Conesville, shown in Figure 5-2, also show good agreement.

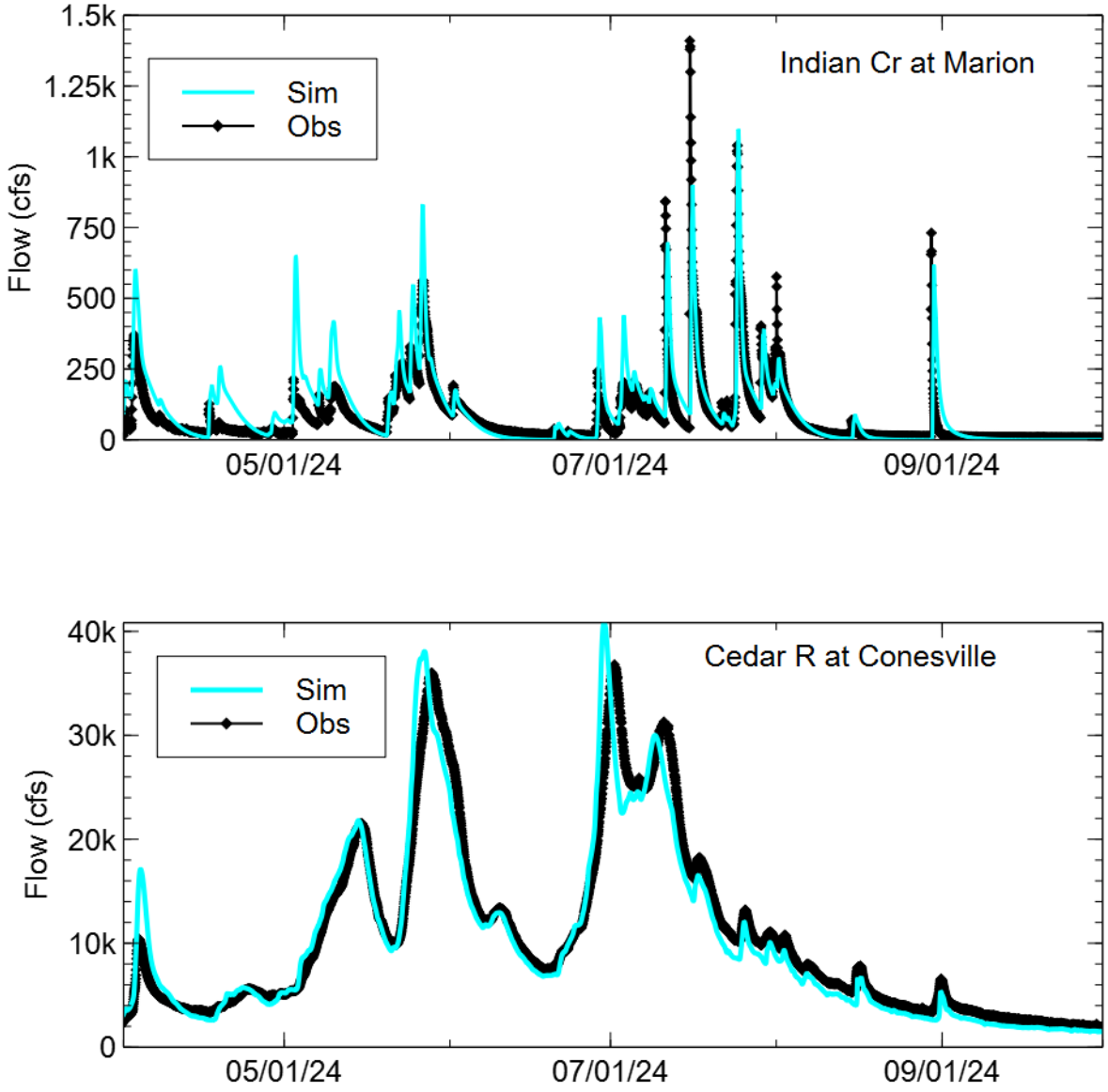

Figure 5-1. Simulated flow hydrographs with observed flow at USGS gaging stations for the 2024 validation period.

Table 5-1. Simulation performance metrics for the 2024 validation period. Root Mean Squared Error (RMSE), coefficient of determination (R^2). Nash-Sutcliffe efficiency (NSE), and Percent bias (% Bias).

Location	RMSE	R^2	NSE	% Bias	KGE
Indian Creek at Marion	57.8	0.83	0.78	+19.0	0.78
Cedar River at Conesville	2970.3	0.89	0.88	-3.4	0.89

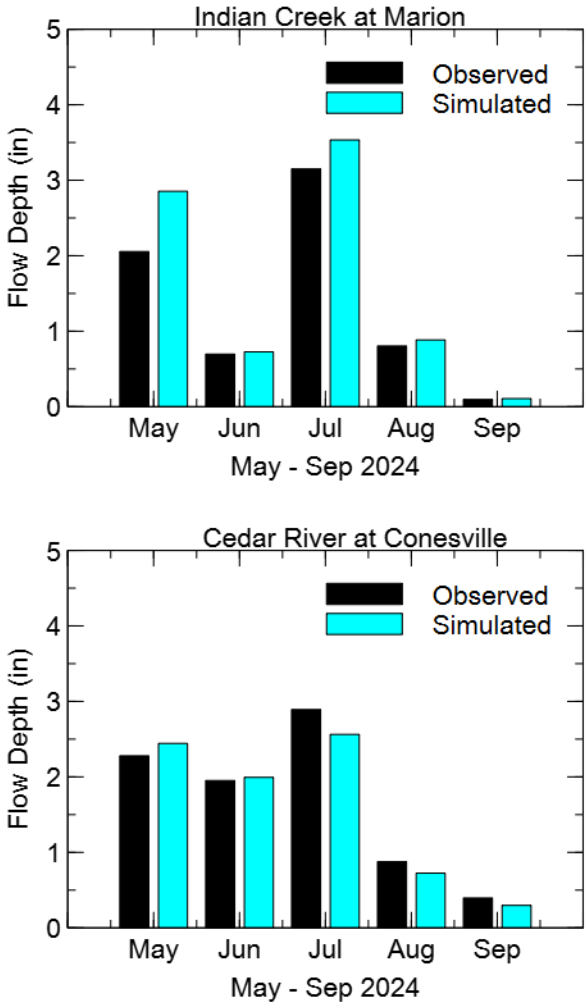

Figure 5-2. Monthly flow volume in depth (inches) at Marion (top) and Conesville (bottom) for May-Sep 2024, normalized by upstream drainage area.

6. WATERSHED MANAGEMENT ALTERNATIVES

The HEC-HMS model of the Lower Cedar River Watershed was used to identify areas in the watershed with high runoff potential and run simulations to help understand the potential impact of alternative flood mitigation strategies in the watershed. Scenarios were developed to help understand the impacts of: (1) increasing infiltration in the watershed; and (2) implementing a system of distributed storage projects (ponds) across the landscape. There are many BMPs not investigated in this report that could potentially increase infiltration or runoff storage at the watershed scale. However, the analysis was limited by the resolution and capability of the HEC-HMS model to simulate effects of BMPs aggregated across subbasin areas of several square miles. Therefore, the investigations were limited to distributed storage provided by ponds, which are relatively large BMP structures, and broad-scale land cover changes. Simulation of other much smaller BMP structures or field management practices would require considering many more individual structures to make any impact at the watershed scale, and a much higher degree of model resolution to reliably quantify impacts.

6.1 High Runoff Potential Areas

Identifying areas of the watershed with higher runoff potential is the first step in selecting mitigation project sites. High runoff areas offer the greatest opportunity to retain more water from large rainstorms on the landscape and to reduce downstream flood peaks.

In the HMS model of the Lower Cedar River Watershed, the runoff potential for each subbasin is a function of the surface, soil, and subsurface. The fraction of rainfall converted to runoff — also known as the runoff coefficient — is a convenient way to illustrate runoff potential. Areas with higher runoff coefficients have higher runoff potential. To evaluate the runoff coefficient, the HMS model simulates runoff from each subbasin area for the same rainstorm; a rainstorm was selected with a total accumulation of 6.0 inches in 24 hours (approximately 25-year average recurrence interval at small scales) (Perica, et al., 2013). The timing of the rainfall and example infiltration is shown in Figure 6-1. Applying this design storm across the Lower Cedar River Watershed results in unrealistic peak discharge values at many locations with moderate drainage area. However, subjecting each model subbasin to the same storm allows for direct comparison among them.

Estimated runoff coefficients at each subbasin generated from simulation of the SCS design storm are shown in Figure 6-2. The runoff coefficients are the percent of precipitation that is converted to runoff divided by the precipitation applied. From these results, the highest runoff potential is located within northeast and central west portion of the watershed. The lowest runoff potential areas appear to follow the Cedar River corridor, likely a result of influence of forested and sandy areas in the initial parameterization of the watershed model. Aggregations of subbasin results at the HUC 12 watershed scale are shown in Figure 6-3. These results appear to show the HUC 12 watersheds to the north (Indian and Big Creeks), east (Sugar Creek) and west (Wapsinonoc Creek) are general areas of high runoff potential.

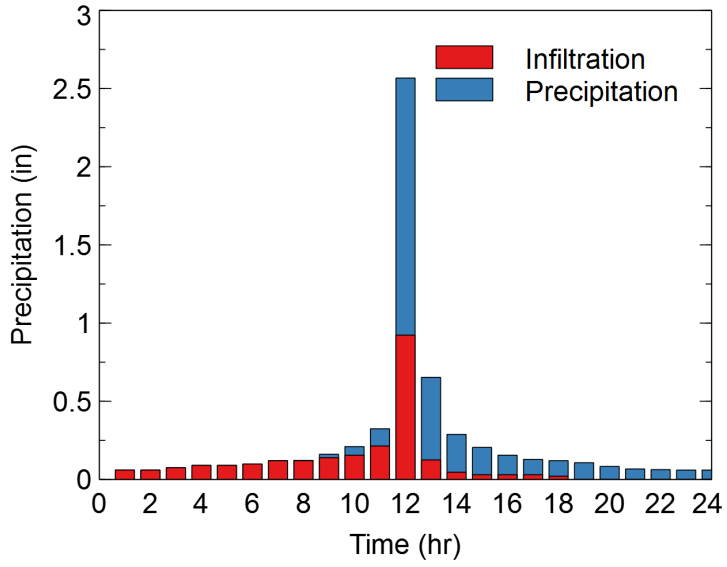

Figure 6-1. SCS design storm hyetograph, showing the timing of the rainfall and example infiltration for a given subbasin area.

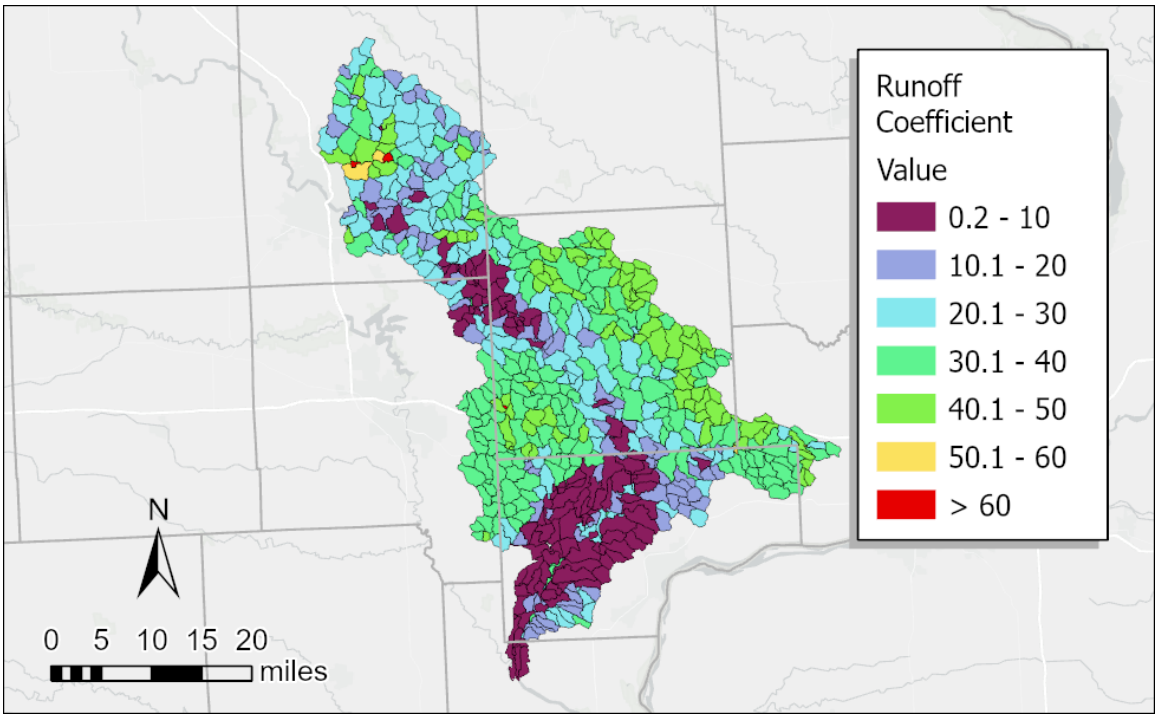

Figure 6-2. Modeled runoff coefficient using the SCS design storm at each HEC-HMS subbasin.

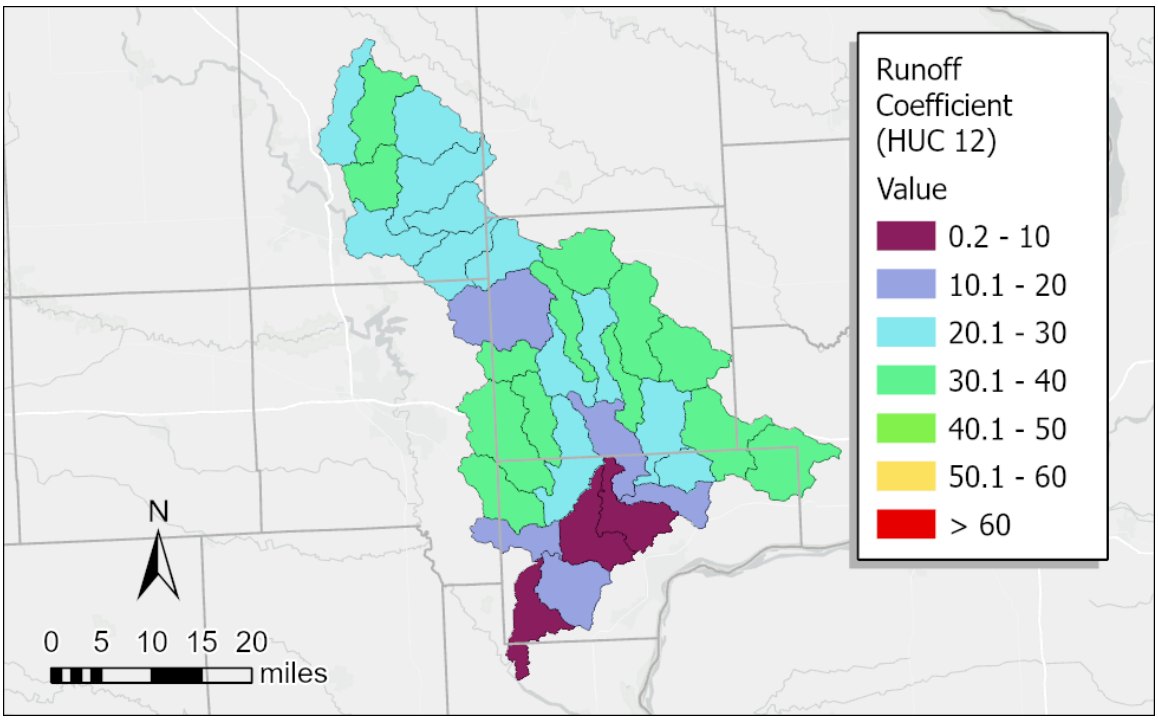

Figure 6-3. Modeled runoff coefficient using the SCS design storm aggregated at each HUC 12 watershed.

To further investigate high runoff potential areas without influence of model calibration, a spatial grid of SCS curve numbers was also generated, shown in Figure 6-4. The SCS curve number is a simple, widely used method for determining runoff potential. The curve number grid parameterizes runoff potential using spatial intersections of SSURGO hydrological soil groups (HSGs) and NLCD land cover data. Curve number values for these intersections of soil and land cover are provided by the NRCS TR-55 publication (Natural Resources Conservation Service, USDA, 1986). Curve numbers aggregated by model subbasin are shown in Figure 6-5. These show the highest runoff potential areas as the upland head water subbasins within the lowest runoff potential along the larger river corridors. Similar conclusions can be made from aggregations at the HUC 12 watershed scale shown in Figure 6-6.

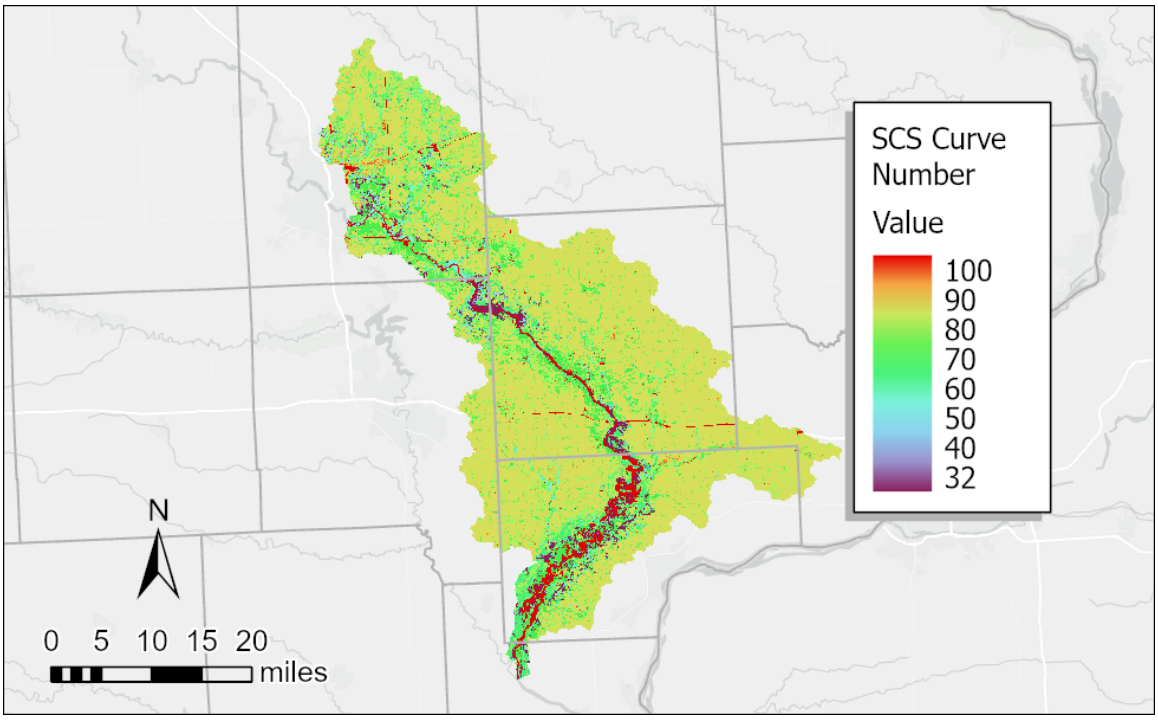

Figure 6-4. SCS curve number grid.

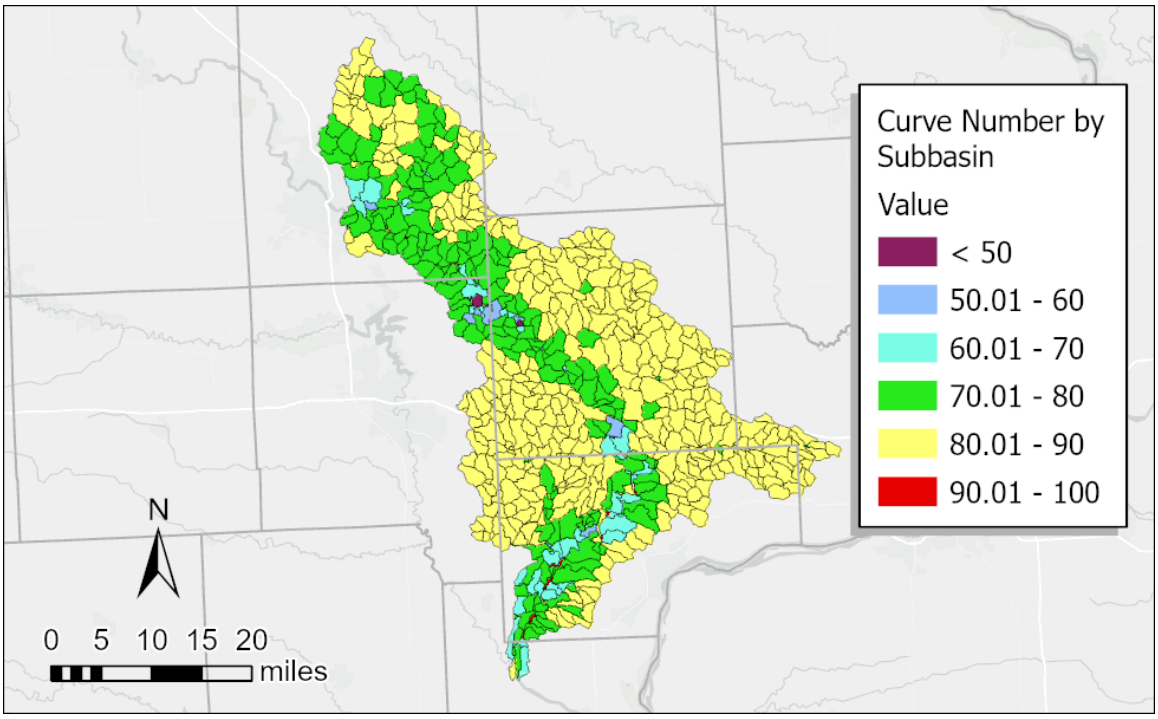

Figure 6-5. SCS curve number map by HEC-HMS subbasin.

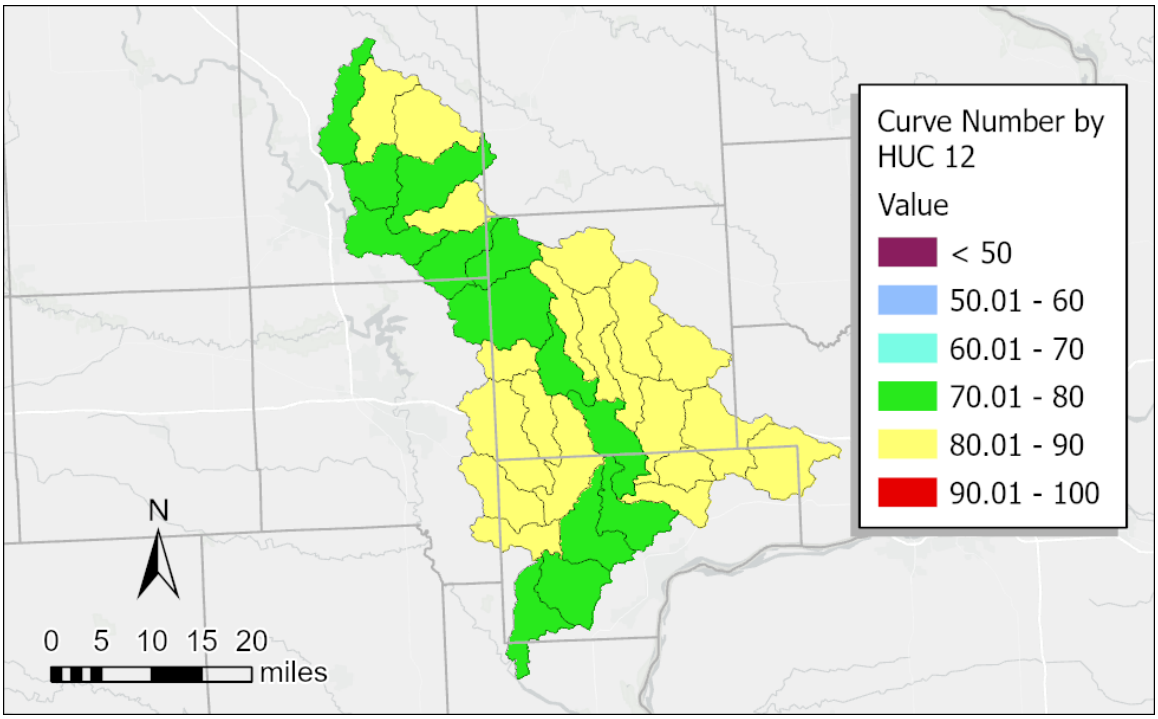

Figure 6-6. SCS curve number map by HUC 12 watershed.

6.2 Mitigating the Effects of High Runoff with Increased Infiltration

Runoff can be reduced from areas with high runoff potential by increasing how much rainfall infiltrates into the ground. Changes that result in higher infiltration reduce the volume of water that drains off the landscape during and immediately after the storm. The extra water that soaks into the ground may later evaporate ore transpire. Or it may slowly travel through the soil, either seeping deeper into the groundwater storage or traveling beneath the surface to a stream. Increasing infiltration has several benefits. Even if the infiltrated water reaches a stream, it arrives much later (long after the event has ended, and flooding has subsided). Also, its late arrival keeps rivers running during long periods without rain.

In this section, several different alternatives to reduce runoff through either land use changes or soil quality improvements were examined. One hypothetical land use change would be the conversion of row crop agriculture back to native tall-grass prairie. Another possible land use change would be improvements to agricultural conditions that would result from planting cover crops during the dormant season. These are hypothetical examples; they are meant to illustrate the potential effects on flood reduction. Hypothetical examples provide valuable benchmarks on the limits of flood reduction that are physically possible with broad-scale land cover changes.

6.2.1 Conversion of Row Crop Agriculture to Tall-Grass Prairie

Much has been documented about the historical water cycle of the native tall-grass prairie of the Midwest. Prior to the transformation to agricultural landscape, tall-grass prairies dominated the landscape. Historical vegetation classifications developed from surveys collected by the Government Land Office from 1832-1859 are shown in Figure 6-7. Most modern agricultural land in the Lower Cedar River Watershed was once native prairie or forest prior to European settlement. This ecosystem infiltrated, transpired, and stored extremely large volumes of water throughout the entire year (Mutel, 2010)(Hernandez-Santana, Zhou, Helmers, Kolka, & Tomer, 2013). The deep, loosely packed organic soils and the deep root systems of the prairie plants (Jackson, et al., 1996). allowed a high volume of the rainfall to infiltrate into the ground (Bharati, Lee, Isenhart, & Schultz, 2002). The soils retained the water instead of allowing it to travel rapidly to a nearby stream as surface flow. Once in the soils, much of the water was taken up by the root systems of the prairie grasses (Brye, Norman, Bundy, & Gower, 2000)

An analysis to quantify the impact of human-induced land use changes on the flood hydrology of the Lower Cedar River was completed. In this example, all current agricultural land use is converted to native tall-grass prairie with its much higher infiltration characteristics. Obviously, returning to this pre-settlement condition is unlikely to occur. Still, this scenario is an important benchmark to compare with any watershed improvement project considered.

To simulate the conversion to native tall-grass prairie with the HMS model, the model parameters affecting runoff potential across the landscape were adjusted to reflect the tall-grass prairie condition. Specifically, existing agricultural land use, which accounts for 70% of the watershed area, was redefined as tall-grass prairie. This broad-scale conversion was done by increasing several parameters - infiltration rates, soil storage, subbasin time of concentration and storage coefficients, as summarized in Table 6-1. The changes in Table 6-1 are applied based on weighting of current area row crop area within each model subbasin, e.g., parameters for a subbasin with 50 percent row crop area will be increased by 50 percent of values listed in Table 6-1. These changes reflect the lower runoff potential and slower runoff movement of runoff across native prairie. Following new assignment of subbasin parameters, the model was run using the design storm with total accumulation of 6.0 inches in 24 hours.

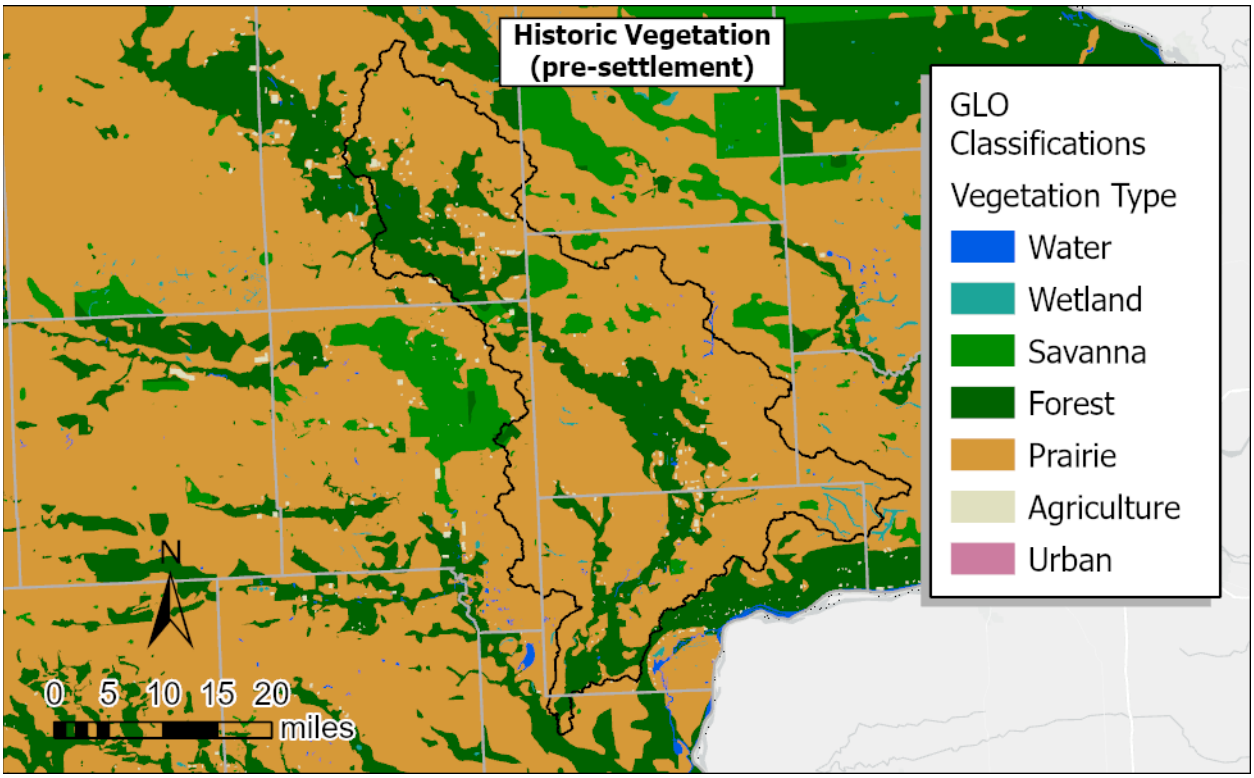

Figure 6-7. Historical vegetation prior to European settlement (Government Land Office plat maps, 1832-1859).

Table 6-1. Model parameter changes for 100% conversion of agricultural land to native prairie.

Model Parameter	% Change
Maximum infiltration rate	+60%
Soil Storage	+10%
Subbasin Time of Concentration	+100%
Subbasin Storage Coefficient	+100%

Six-Inch, 24-Hour SCS Design Storm

As expected, improving the infiltration of 70% of the watershed area by converting row crop agriculture to native tall-grass prairie has a significant effect on the flood hydrology. For the 6- inch design storm, the simulated tall-grass prairie infiltrates 0.4 inches more rainfall into the ground than does the current agricultural landscape. Additionally, the time of travel for the runoff is significantly increased, slowing down the watershed response. Discrete model index points, shown in Figure 6-8, were selected at ungaged head water locations and at USGS gaging stations to present simulation results at a range of spatial locations and drainage areas.

Figure 6-9 shows simulated flow hydrographs at model index locations for each scenario. The average peak flow reduction percentages are summarized in Figure 6-10 for each scenario and model index location. Most of the watershed experienced greater than a 30% reduction in subbasin peak discharge for the 100% conversion to native vegetation. This reduction is smaller at for the 25% and 10% conversion scenarios, but still relatively large considering the much smaller conversion percentage. Application of this design storm across the entire watershed produces somewhat unrealistic peak discharges at larger drainage areas, but still provide some context for the watershed scenarios.

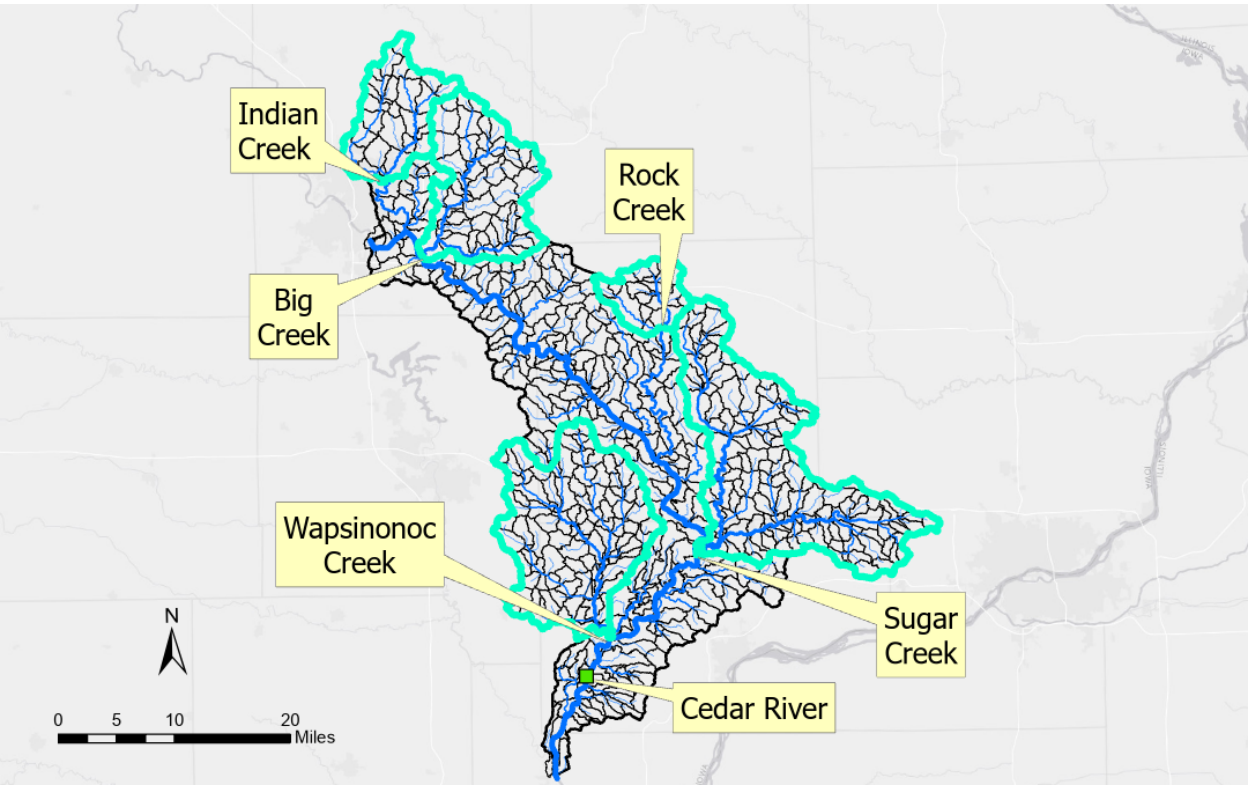

Figure 6-8. Model index locations selected for comparisons of hypothetical flood mitigation scenarios to current conditions.

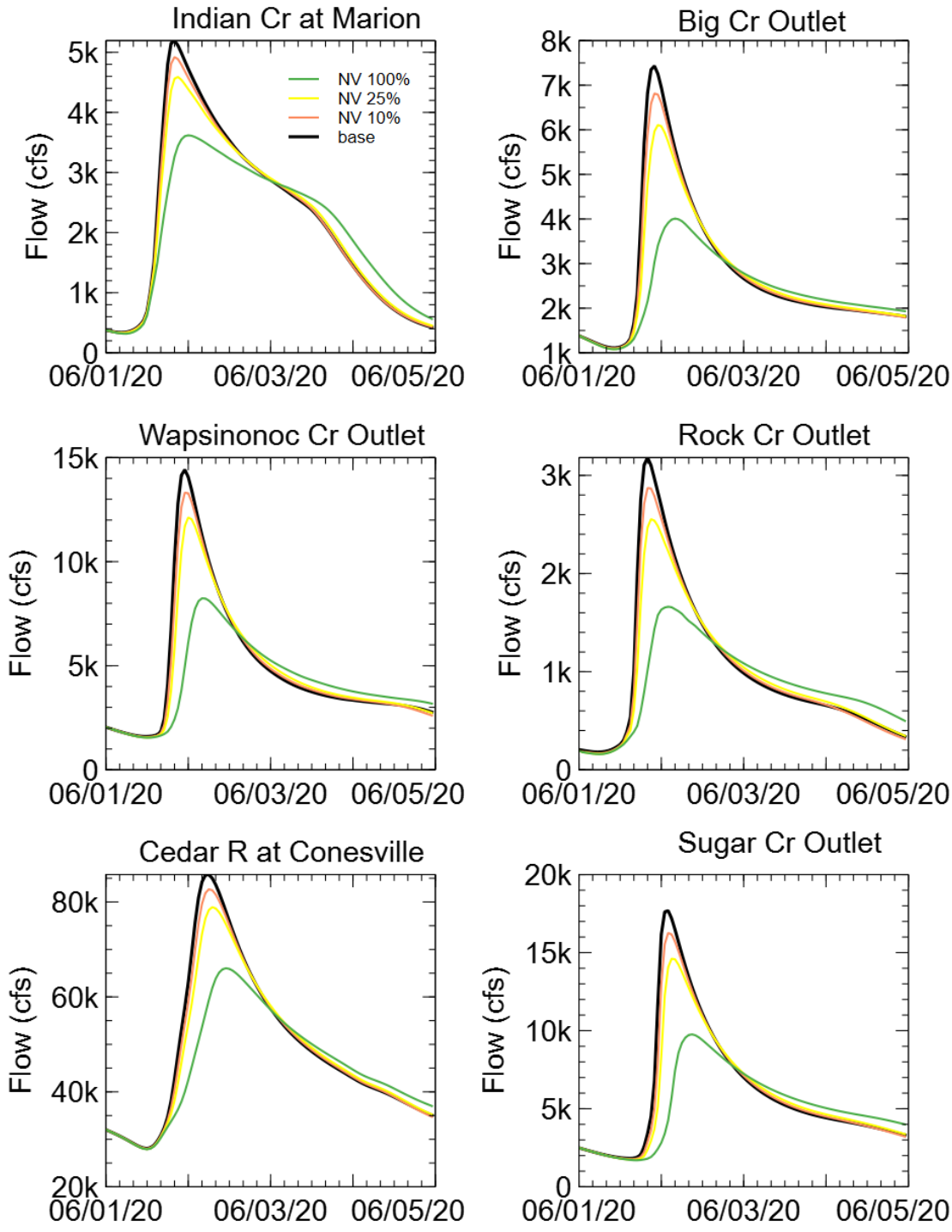

Figure 6-9. Simulated hydrographs at index locations for native vegetation scenario and SCS design storm.

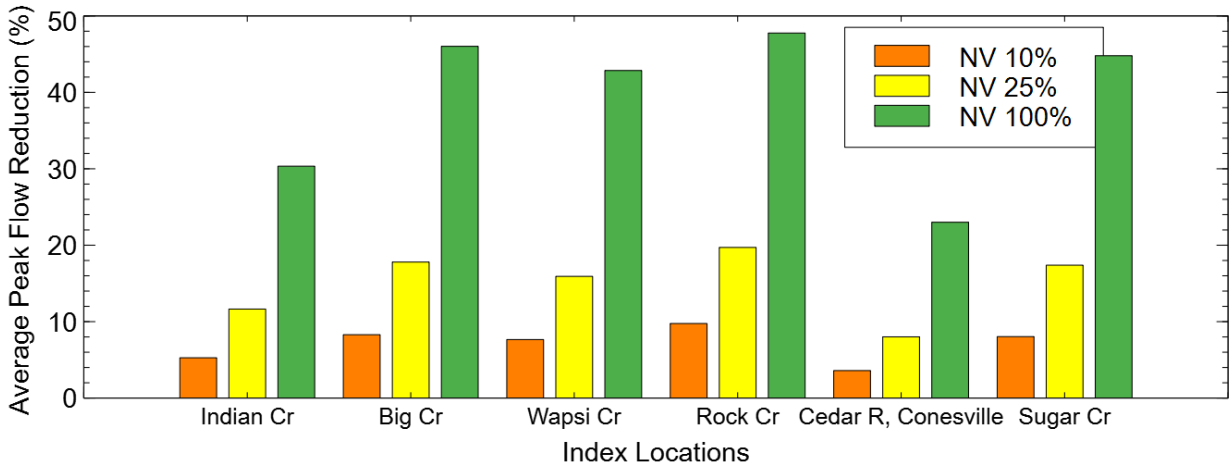

Figure 6-10. Average peak flow reductions for native vegetation scenarios and design storm.

6.2.2 Improved Agricultural Conditions from Planting Cover Crops

Cover crops can be an effective farming conservation practice that also enhances infiltration. Farmers typically plant cover crops after the harvest of either corn or soybeans and "cover" the ground through the winter until the next growing season begins. The cover crop can be killed off in the spring by rolling it or herbicide application; afterwards, row crops can be planted directly into the remaining cover crop residue. Cover crops provide a variety of benefits, including improved soil quality and fertility, increased organic matter content, increased infiltration and percolation, reduced soil compaction, and reduced erosion and soil loss. Cover crops also retain soil moisture and enhance biodiversity (Dabney, Delgado, & Reeves, 2001). One source suggests that for every one percent increase in soil organic matter (e.g., from 2% to 3%), the soil can retain an additional 17,000–25,000 gallons of water per acre (Archuleta, 2014). This estimate is highly dependent on soil types, but the holding capacity can certainly be improved significantly by increasing soil organic matter (Ontl, 2013). Examples of cover crops include clovers, annual and cereal ryegrasses, winter wheat, and oilseed radish (Dabney, Delgado, & Reeves, 2001).

The purpose of this hypothetical example is to investigate the impact improved agricultural management practices could have on reducing flood peak discharges throughout the watershed. It was hypothesized that planting cover crops across all agricultural areas in the watershed during the dormant (winter) season would lower the runoff potential of these same areas during the

growing season (spring and summer) because of increased soil health and fertility. To be clear, this scenario does not represent the conversion of the existing agricultural landscape (primarily row crops) to cover crops. Rather, the existing agricultural landscape is still mostly intact, but its runoff potential during the growing season has been slightly reduced by planting cover crops during the dormant season. This broad-scale conversion was done by increasing several parameters - infiltration rates, soil storage, subbasin time of concentration and storage coefficients, as summarized in Table 6-2. The changes in Table 6-2 are applied based on weighting of current row crop area within each model subbasin, e.g., parameters for a subbasin with 50 percent row crop area will be increased by 50 percent of values listed in Table 6-2. These changes reflect the lower runoff potential and slower runoff movement of runoff from improved agricultural management practices. Comparisons were made between current and cover crop simulations for the 6-inch, 24-hour SCS design storm.

Table 6-2. Model parameter changes for 100% utilization of cover crop/ improved soil health practice scenarios.

Model Parameter	% Change
Maximum infiltration rate	+40%
Soil Storage	+4%
Subbasin Time of Concentration	+50%
Subbasin Storage Coefficient	+50%

Six-Inch, 24-Hour SCS Design Storm

Improved agricultural management practices, represented by planting cover crops during the dormant season, reduces runoff and peak discharges less than the native tall-grass prairie simulation does. Figure 6-11 shows simulated flow hydrographs at model index locations for each scenario. The average peak flow reduction percentages for each scenario and model index location are summarized in Figure 6-12. Most of the watershed experienced a 15-35% reduction in subbasin peak discharge for the 100% utilization of cover crop/ improved soil health scenario. This reduction is drops to 5-10% and 2-5% for the 25% and 10% utilization scenarios, respectively. Application of this design storm across the entire watershed produces somewhat unrealistic peak discharges at larger drainage areas, but still provide some context for the watershed scenarios.

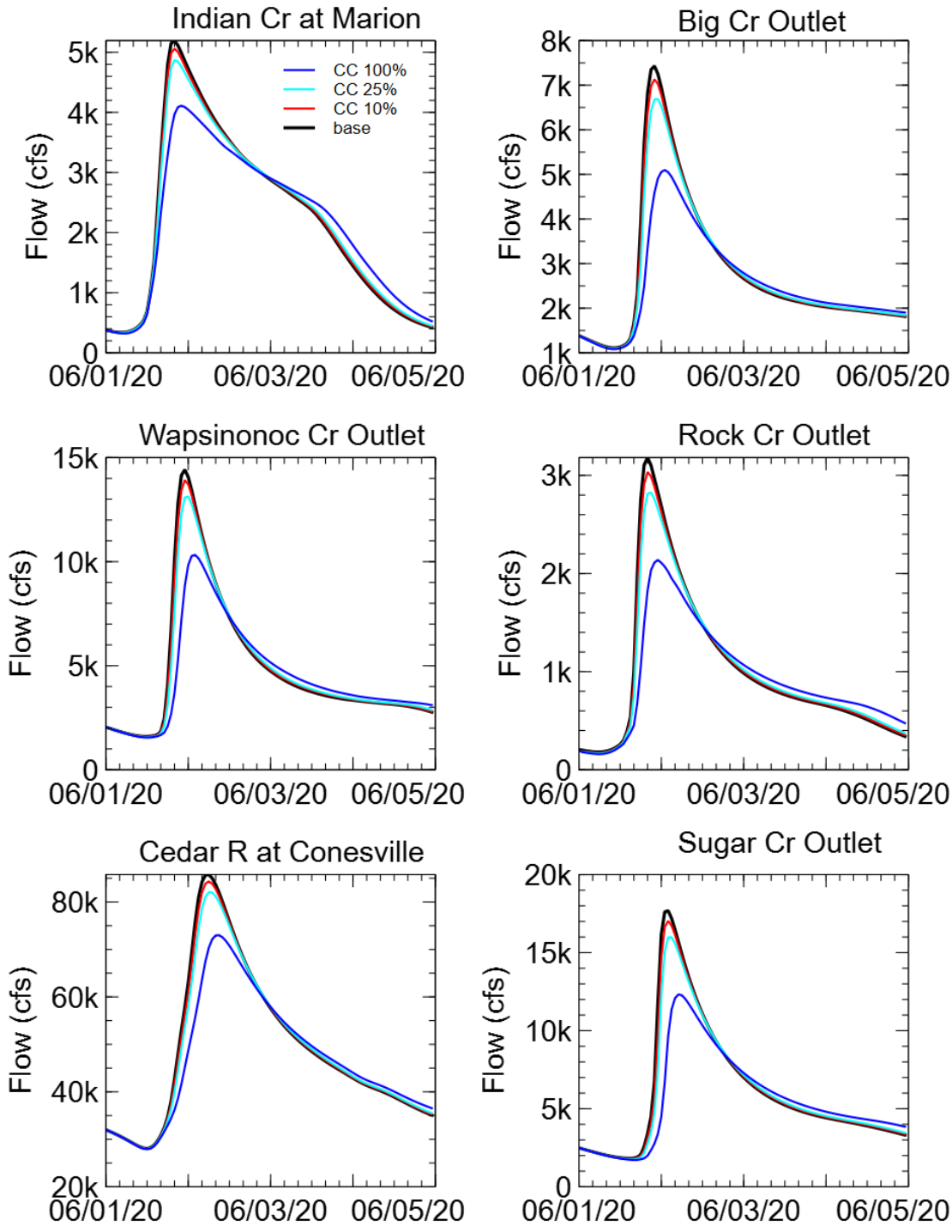

Figure 6-11. Simulated hydrographs at index locations for cover crop/ improved soil health scenario and SCS design storm.

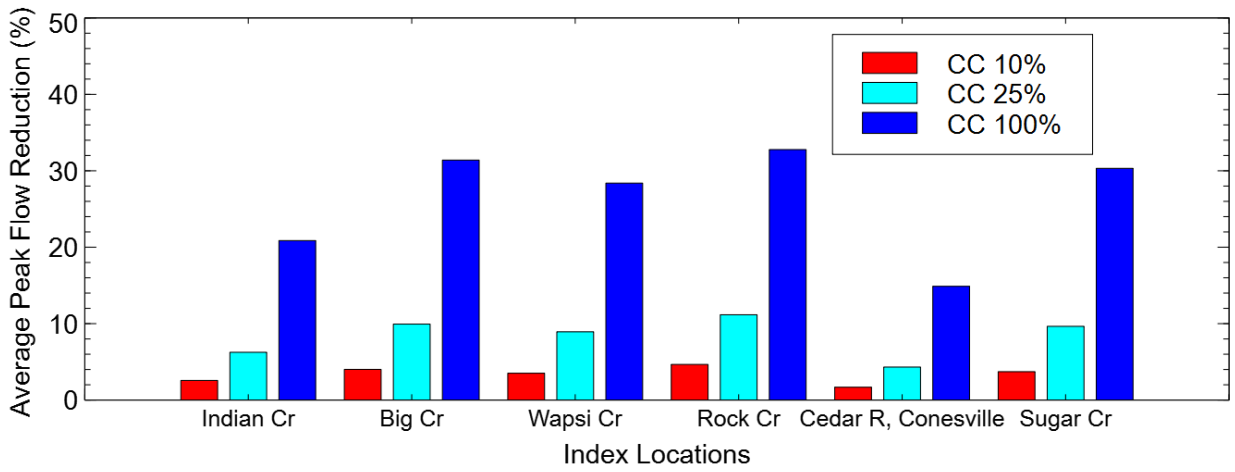

Figure 6-12. Average peak flow reductions for cover crop/ improved soil health scenario and SCS design storm.

6.3 Mitigating the Effects of High Runoff with Distributed Storage

In general, a system providing distributed storage, does not change the volume of water that runs off the landscape. Instead, storage ponds hold floodwater temporarily and release it at a slower rate. Therefore, the peak flood discharge downstream of the storage pond is lowered. The effectiveness of any one storage pond depends on its size (storage volume) and how quickly water is released. By adjusting the size and the pond outlets, storage ponds can be engineered to efficiently use available storage for large floods.

Generally, these ponds have a permanent storage area that holds water all the time. This is achieved by constructing an earthen embankment across a stream and setting an outlet (usually a pipe called the principal spillway) at some elevation above the floor of the pond. When a storm event occurs, runoff enters the pond. Once the elevation of the water surface is higher than the pipe inlet, water will pass through the pipe, leaving the pond at a controlled rate. Additionally, the earthen dam is built higher than the pipe, allowing for more storage capacity within the pond. An auxiliary or emergency spillway that can discharge water at a much faster rate than the pipe does is set at an elevation higher than the pipe. This auxiliary spillway is designed to release rapidly rising waters in the pond, so they do not damage the earthen embankment. The volume of water stored between the principal spillway and the emergency spillway is called flood storage.

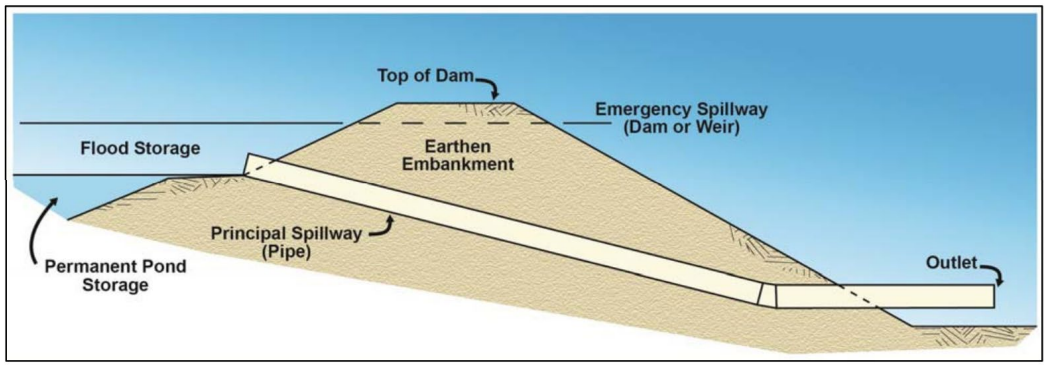

Figure 6-13. Schematic of a pond constructed to provide flood storage.

The hypothetical distributed storage analysis performed using Lower Cedar River Watershed model was based on the flood control concept developed by the Soap Creek Watershed located in south central Iowa. The Soap Creek Watershed Board formed in the 1980s when landowners banded together to reduce flood damage and erosion within their watershed. They adopted a plan to identify potential locations for 154 distributed storage structures (mainly ponds) that could be built within the watershed. As of 2018, 135 of these structures have been built (Stolze, 2024).

The Soap Creek Watershed drains approximately 250 square miles, equaling an average density of one pond for every 1.9 square miles of drainage area. Further analysis of the Soap Creek structures shows that most are constructed in the headwater areas of the watershed, which allows for smaller structures, rather than large, high-hazard class structures on the main rivers. The average pond density in the headwater areas where most of the ponds are sited is approximately 1 pond per 1.4 square miles of drainage area.

6.3.1 Siting of Ponds in the Lower Cedar River Watershed

Like the Soap Creek Watershed, a distributed network of detention ponds for 50, 100, and 250 sites were placed in headwater subbasins, shown in Figure 6-14. These scenarios assumed a typical 20 acre-feet detention pond was placed at the outlet of each selected subbasin. These typical ponds have 20 acre-feet of storage available for flood storage below the emergency spillway. A smaller principal spillway pipe with a diameter of 12 inches releases lower flows while also attenuating flood peaks by throttling flows and consuming pond storage. A scenario that blended the 25% utilization of cover crop/ improved soil health with 100 detention ponds was also included in this analysis.

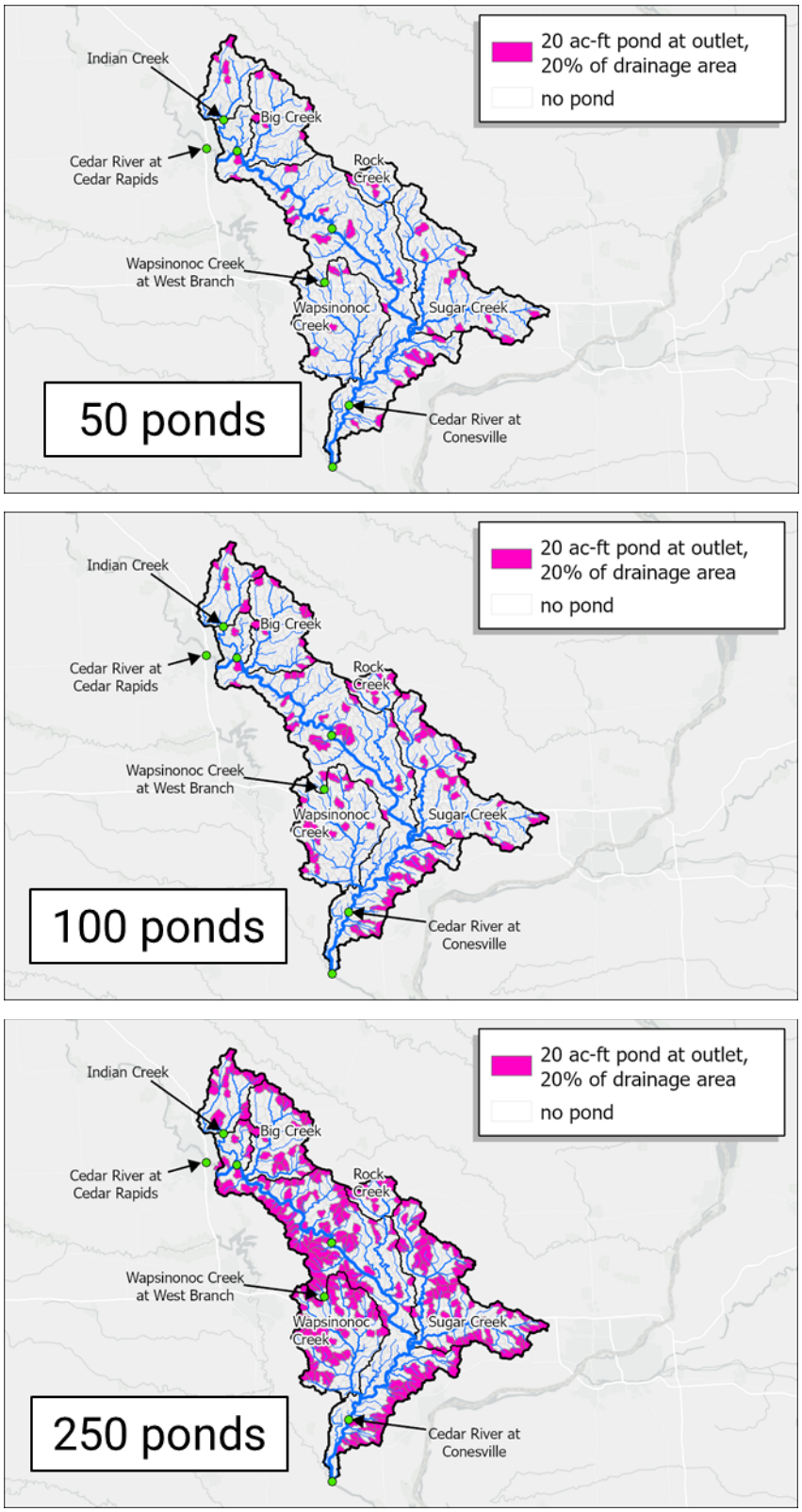

Figure 6-14. Distributed storage scenarios - 50 ponds (top), 100 ponds (middle), 250 ponds (bottom), placed at the outlet of headwater subbasins.

Additionally, the detention ponds were assumed to intercept 20% of the flow generated from their respective upstream subbasin given the small pond size relative to the subbasin area. This was accomplished using a diversion structure within HEC-HMS. Figure 6-15 shows a schematic demonstrating how areas draining to detention ponds are treated separately in HEC-HMS. While it is possible to aggregate several parallel ponds together, only one typical pond at the outlet its subbasin was used in this analysis.

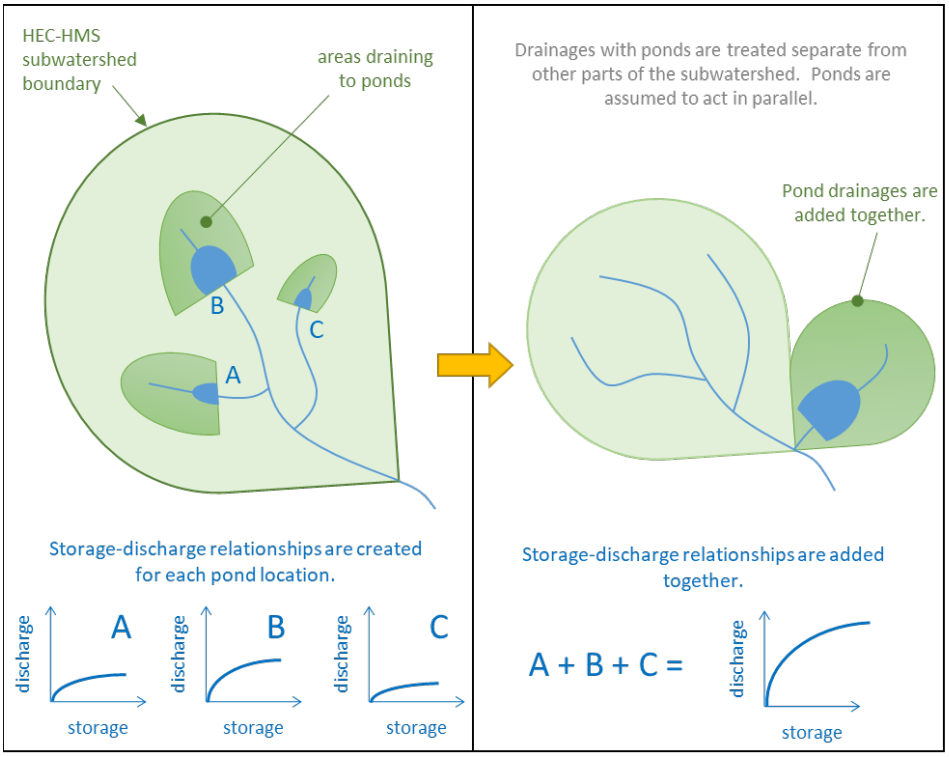

Figure 6-15. Aggregation of pond storage-discharge curves and drainage areas within a subbasin.

Six-Inch, 24-Hour SCS Design Storm

There are significant reductions in peak flow just downstream of individual detention pond projects. An example of inflow, outflow and resulting storage for a pond located within Sugar Creek is shown in Figure 6-16. However, at model index locations with larger unregulated drainage area, distributed storage is less effective than native vegetation and cover crops / soil health scenarios at reducing peak flows. Figure 6-17 shows simulated flow hydrographs at model index locations for each scenario. The average peak flow reduction percentages for each scenario and model index location are summarized in Figure 6-18. Most of the watershed experienced a 5-

10% reduction in peak discharge for the 250-pond scenario. This reduction is drops to 2-8% and 1-3% for the 100-pond and 50-pond scenarios, respectively. Interestingly, utilizing cover crops / soil health improvements along with the 100 ponds is provides a significantly higher peak flow reduction than the other scenarios. A large portion of this improvement can be attributed to the broad scale land use changes and infiltration improvements.

There are several reasons why the distributed detention ponds are less effective at the watershed scale than broad scale infiltration changes. Runoff volumes are the same at downstream locations because infiltration stays the same. While the detention ponds may provide significant peak flow reductions directly downstream, they are only intercepting 20% of the subbasin drainage area. Even if detention ponds were holding all the runoff many weeks after a storm event, the maximum flow reduction at the watershed scale will always be less than 20%. Another reason is that runoff originating from locations throughout the watershed arrive at vastly different times; some areas have ponds, others do not. The result is that the storage effect from ponded areas is spread out over time, instead of being concentrated at the time of highest flows. Hence, at larger drainage areas downstream in the watershed, the flood peak reduction of storage ponds diminishes.

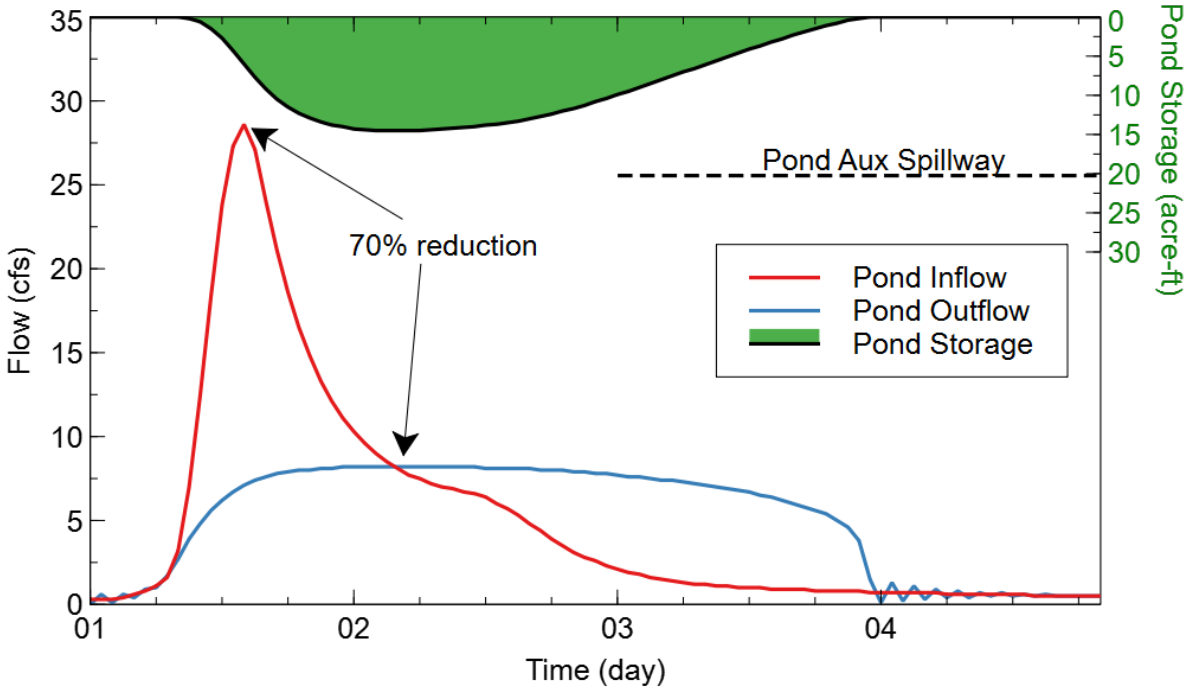

Figure 6-16. Individual detention pond inflow, outflow and storage behavior for the SCS Design Storm.

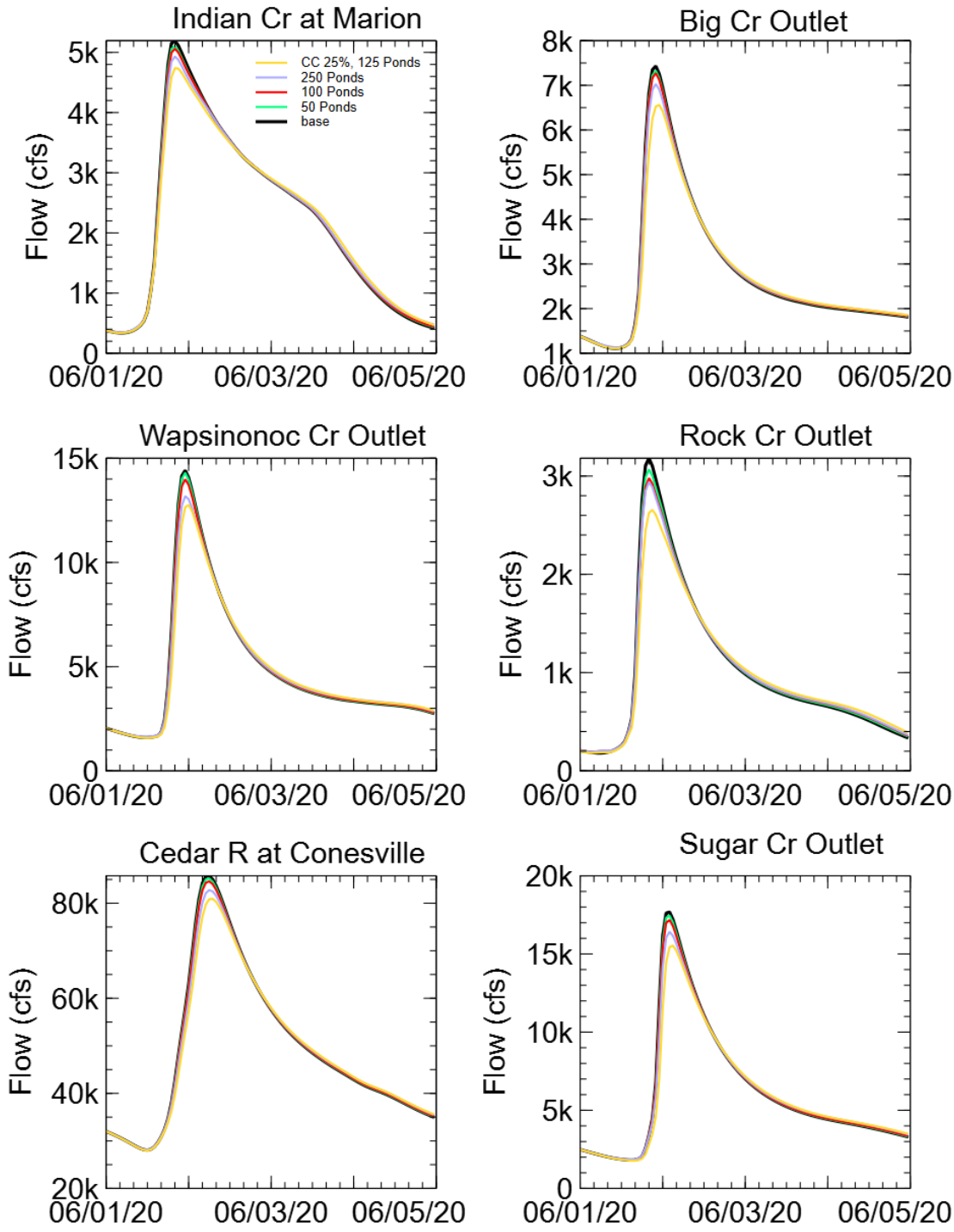

Figure 6-17. Simulated hydrographs at index locations for detention pond scenarios and SCS design storm.

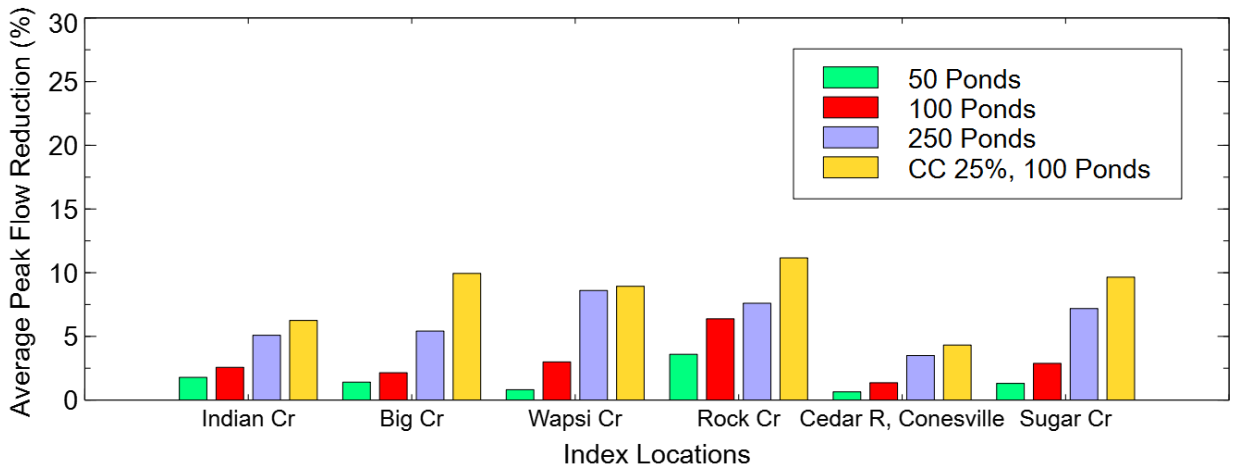

Figure 6-18. Average peak flow reductions for detention pond scenarios and SCS design storm.

6.4 Comparison of Watershed Scenarios for Historic Storm Events

In addition to the design storm event, watershed scenarios were compared through simulation of several historic storm events. Simulations of these historic events are more relevant to people than a design storm, and many likely remember the consequences of some of these events. In this section, the differences in simulation results at the model index locations, shown in Figure 6-8.

6.4.1 May – June 2008, Storm Event

Figure 6-19 shows the cumulative rainfall from May 25-June 15, 2008. The largest cumulative rainfall, totaling 10-12 inches, occurred primarily over the northern part of the Lower Cedar River Watershed, with most other areas receiving rainfall totaling 6-8 inches. There was also several significant rainfall events that occurred in the upper Cedar River Watershed that caused flooding of record along the Cedar River. Figure 6-20 shows simulated flow hydrographs at model index locations for the native vegetation scenarios. Figure 6-21 shows simulated flow hydrographs at model index locations for the cover crop / soil health improvement scenarios. Figure 6-22 shows simulated flow hydrographs at model index locations for the cover distributed pond scenarios. Average peak flow reductions for all scenarios for April – September 2008 are shown in Figure 6-23. As expected, broad scale changes in land cover result in large, broad-scale reductions in peak discharge. However, it is worth noting reductions on the main stem of the Cedar River at Conesville are negligible due to the scenarios only being applied within the Lower Cedar River Watershed. Additional simulations presented later in this report explore implementation of practices in the upstream portion of the Cedar River Watershed in addition to those in the Lower Cedar.

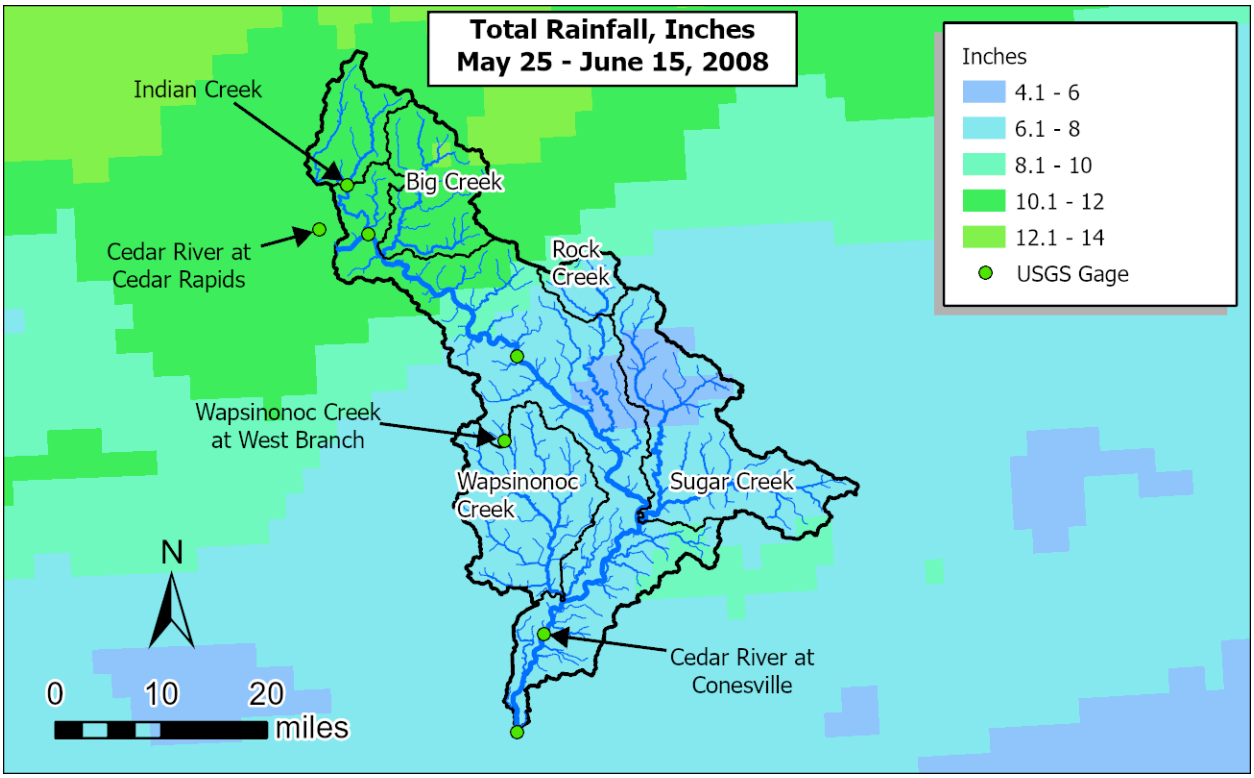

Figure 6-19. May 25 – June 15, 2008, cumulative rainfall used for simulating watershed scenarios

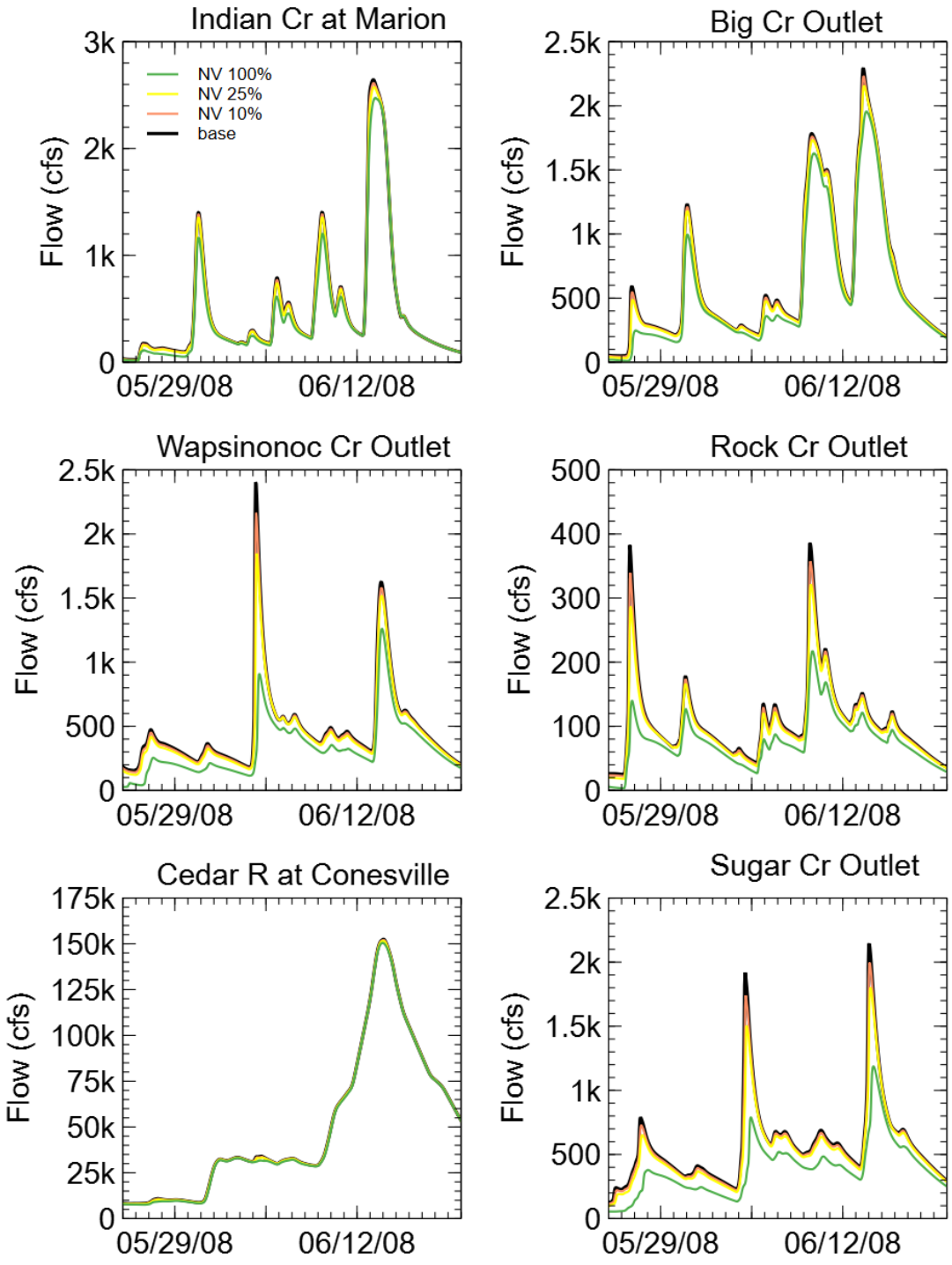

Figure 6-20. Simulated hydrographs at index locations for native vegetation scenario and May 25 – June 15, 2008, storm event.

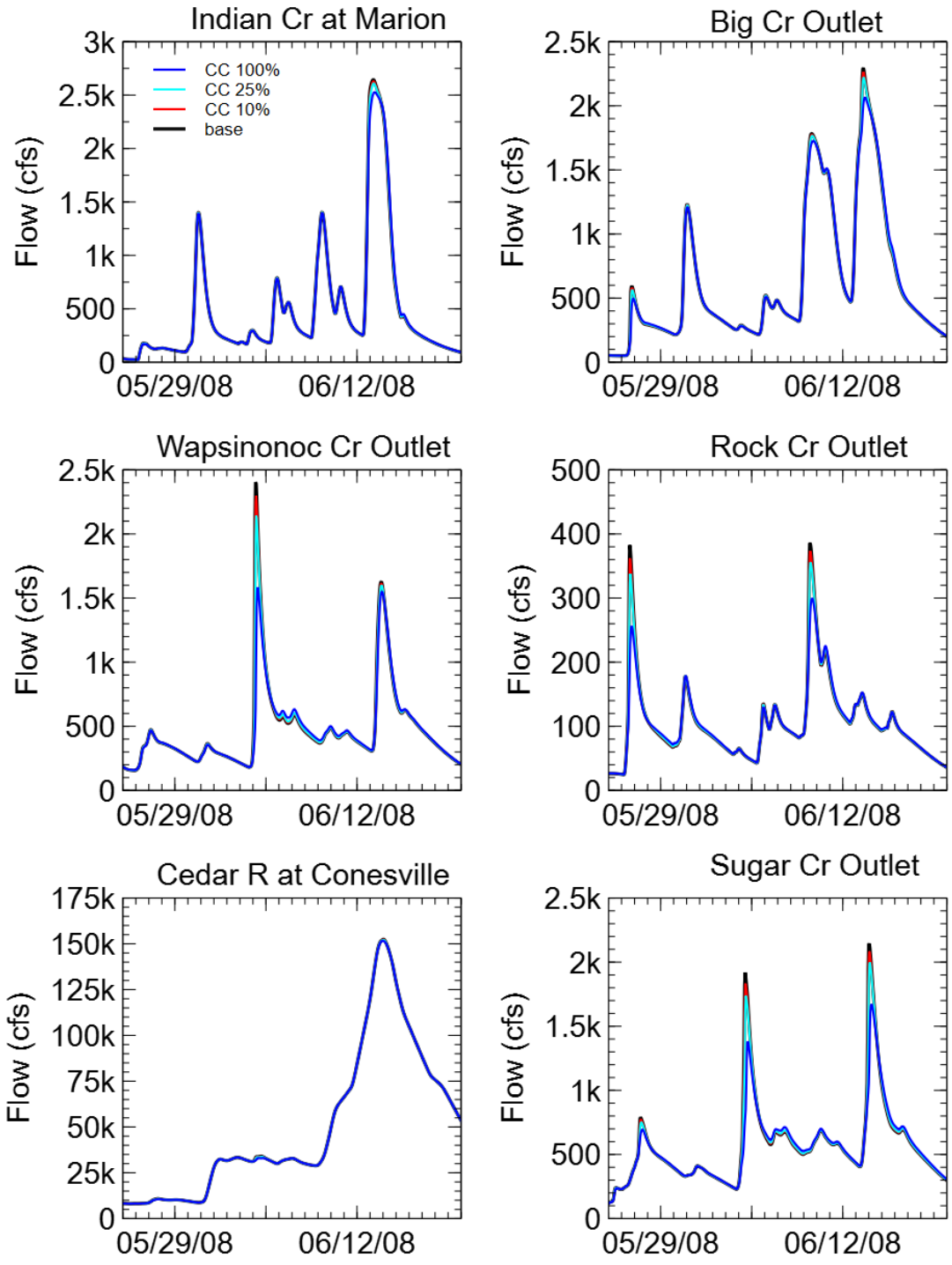

Figure 6-21. Simulated hydrographs at index locations for cover crops / soil health improvement scenario and May 25 – June 15, 2008, storm event.

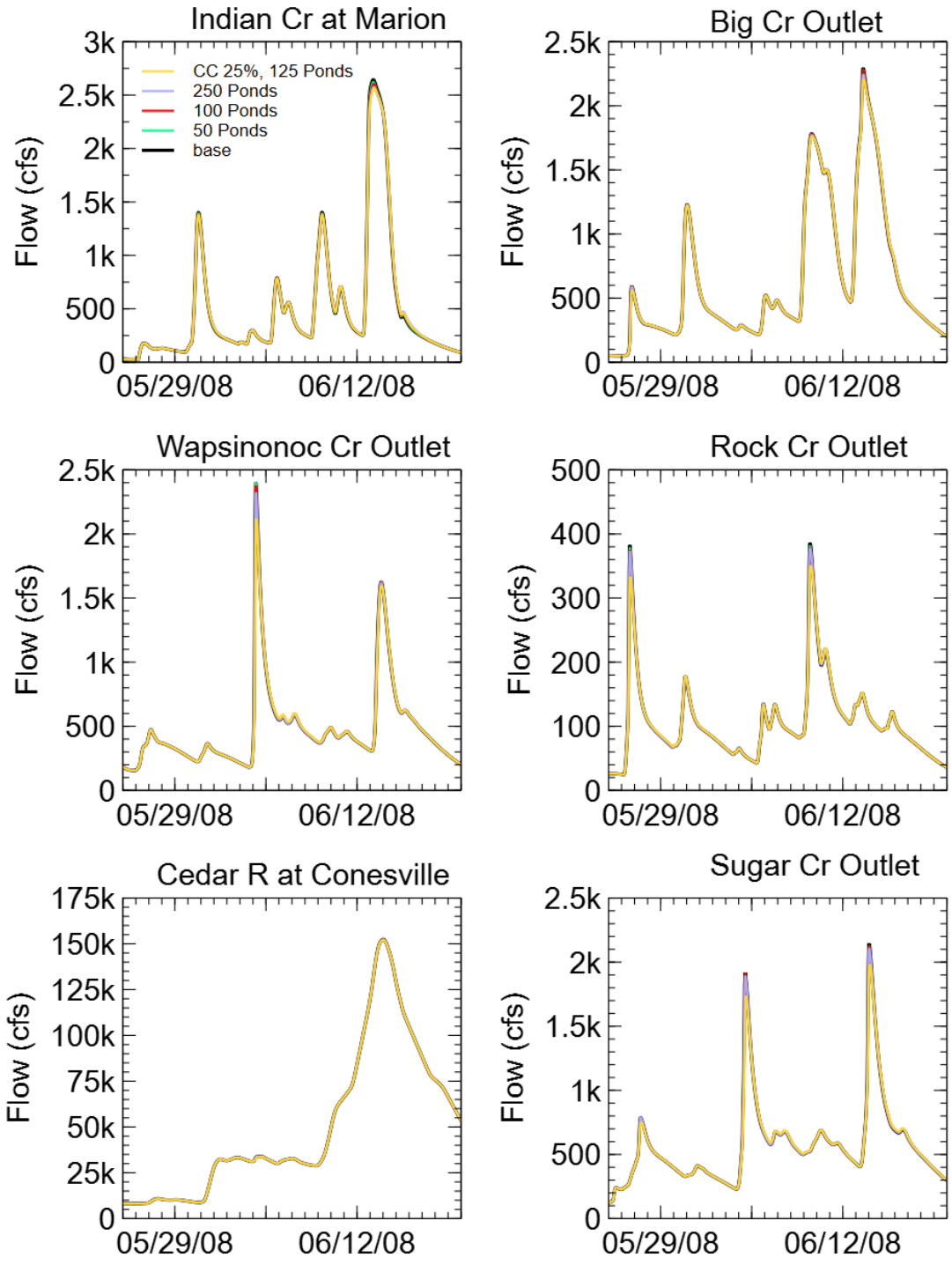

Figure 6-22. Simulated hydrographs at index locations for detention pond scenarios and May 25 – June 15, 2008, storm event.

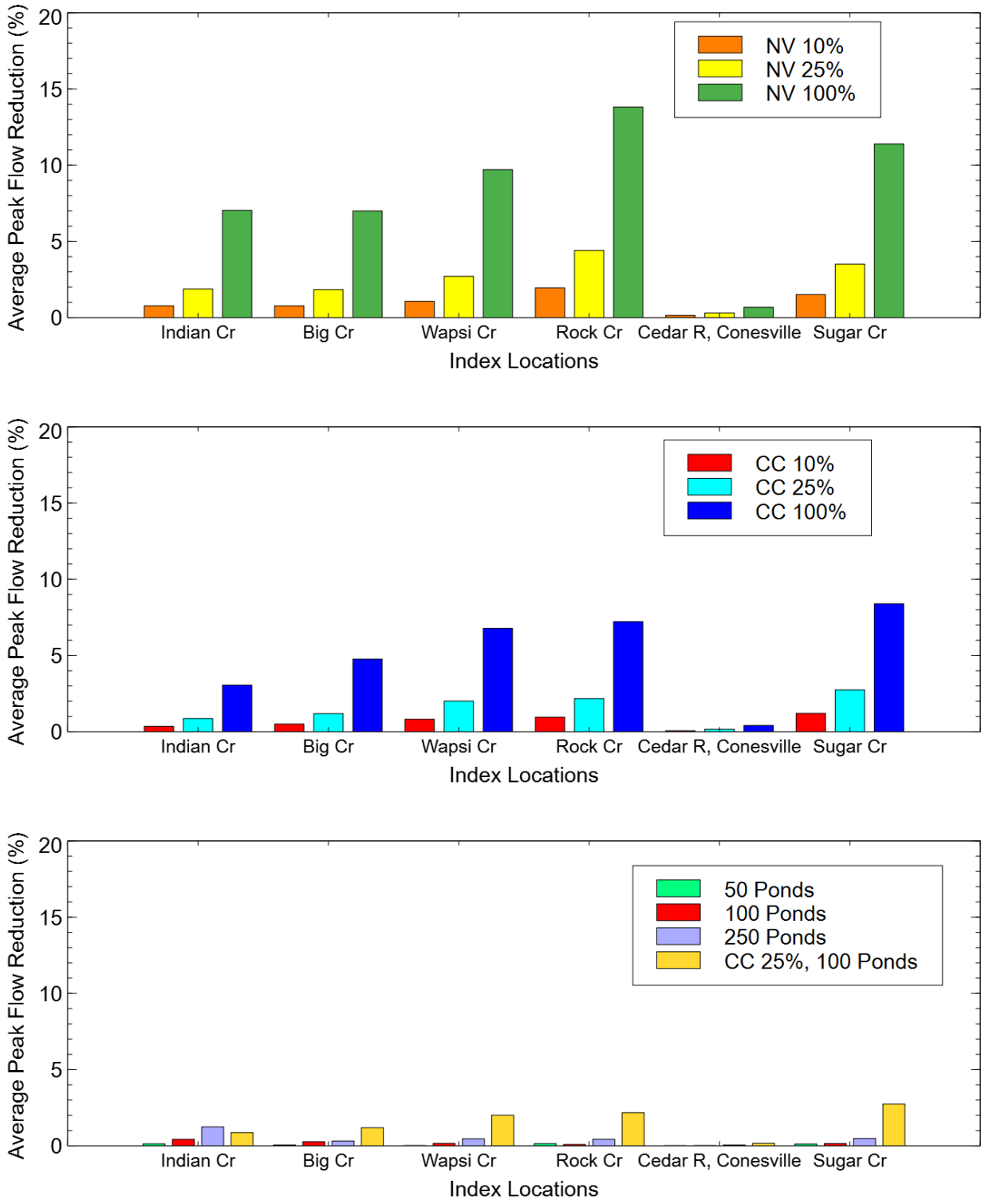

Figure 6-23. Average peak flow reductions for April – September 2008, native vegetation (top), cover crop/ improved soil health (middle), and distributed storage (bottom).

6.4.2 June – July 2014, Storm Event

Figure 6-24 shows the cumulative rainfall from June 29 – July 5, 2014. Much of the Lower Cedar River Watershed received 6-8 inches of cumulative rainfall for this particular event. Figure 6-25 shows simulated flow hydrographs at model index locations for the native vegetation scenarios. Figure 6-26 shows simulated flow hydrographs at model index locations for the cover crop / soil health improvement scenarios. Figure 6-27 shows simulated flow hydrographs at model index locations for the distributed pond scenarios. Average peak flow reductions for all scenarios for April – September 2014 are shown in Figure 6-28. As expected, broad scale changes in land cover result in large, broad-scale reductions in peak discharge.

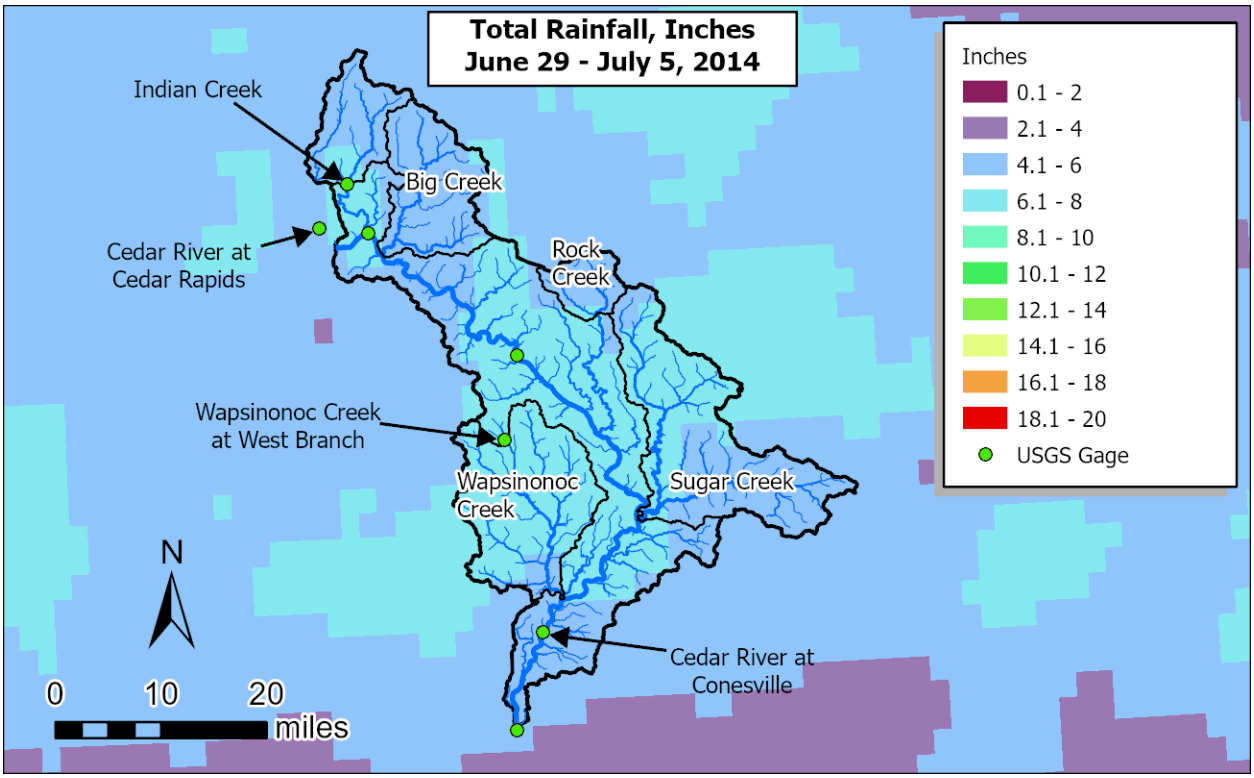

Figure 6-24. June 29 – July 5, 2014, cumulative rainfall used for simulating watershed scenarios.

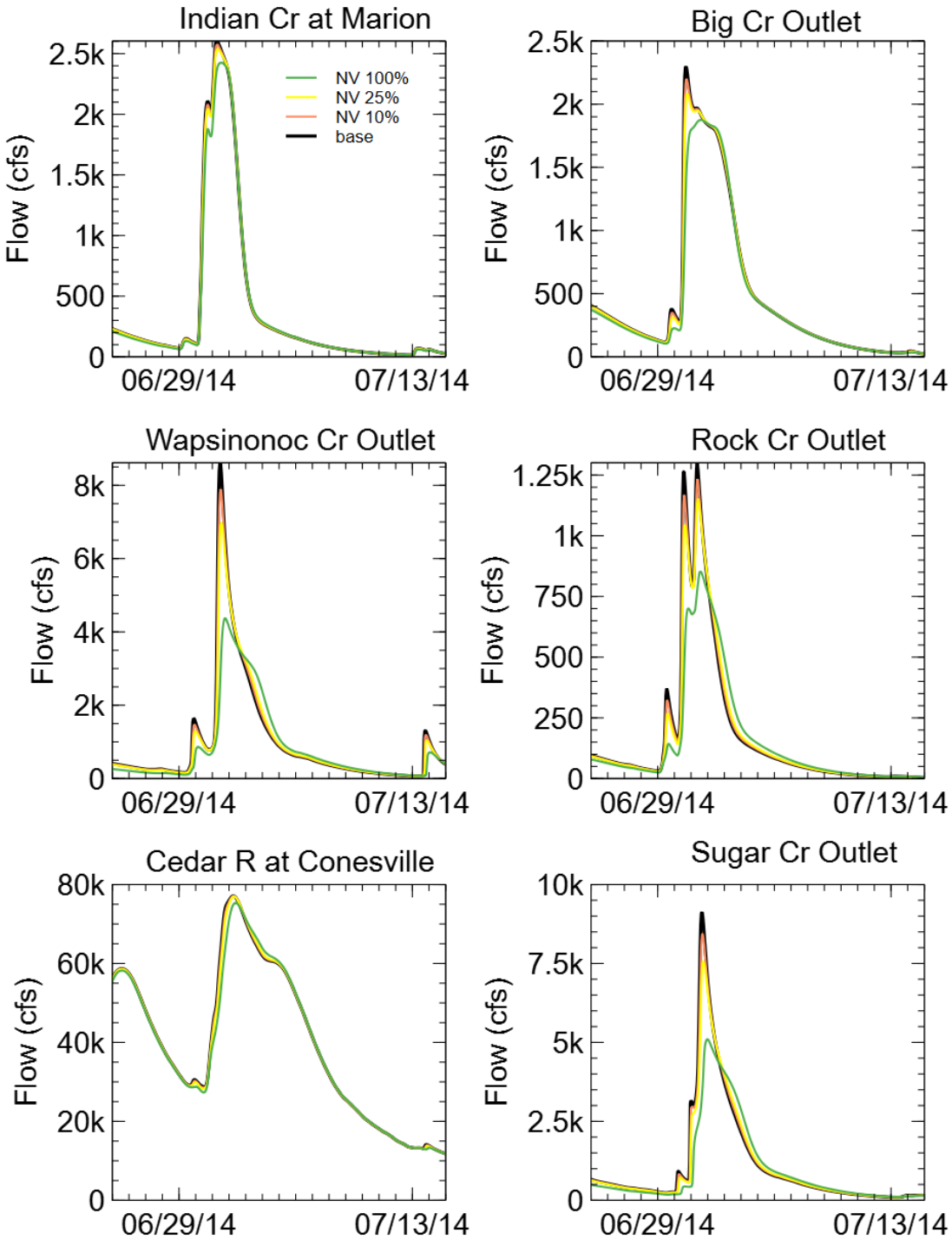

Figure 6-25. Simulated hydrographs at index locations for native vegetation scenario and June 29 – July 5, 2014, storm event.

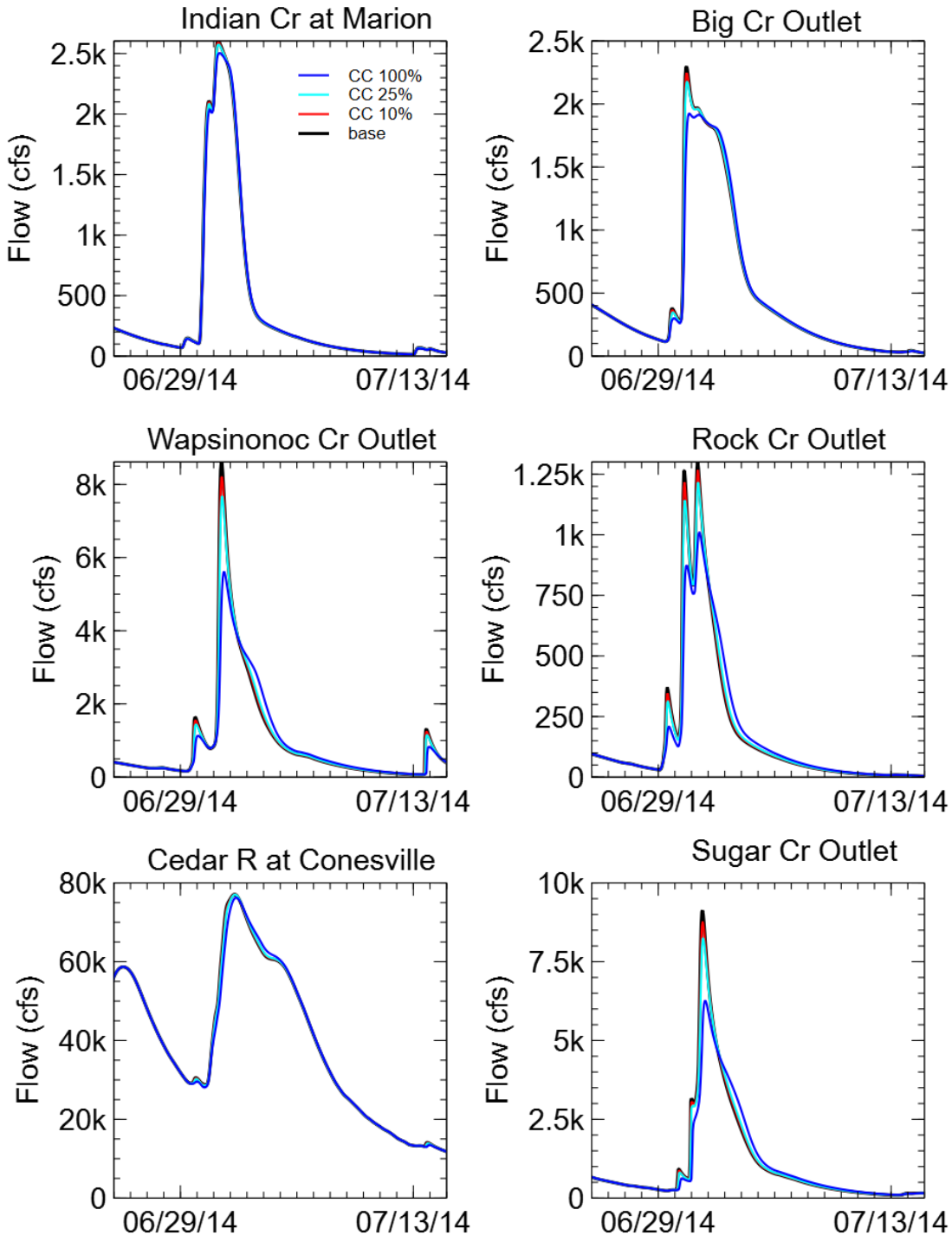

Figure 6-26. Simulated hydrographs at index locations for cover crops / soil health improvement scenario and June 29 – July 5, 2014, storm event.

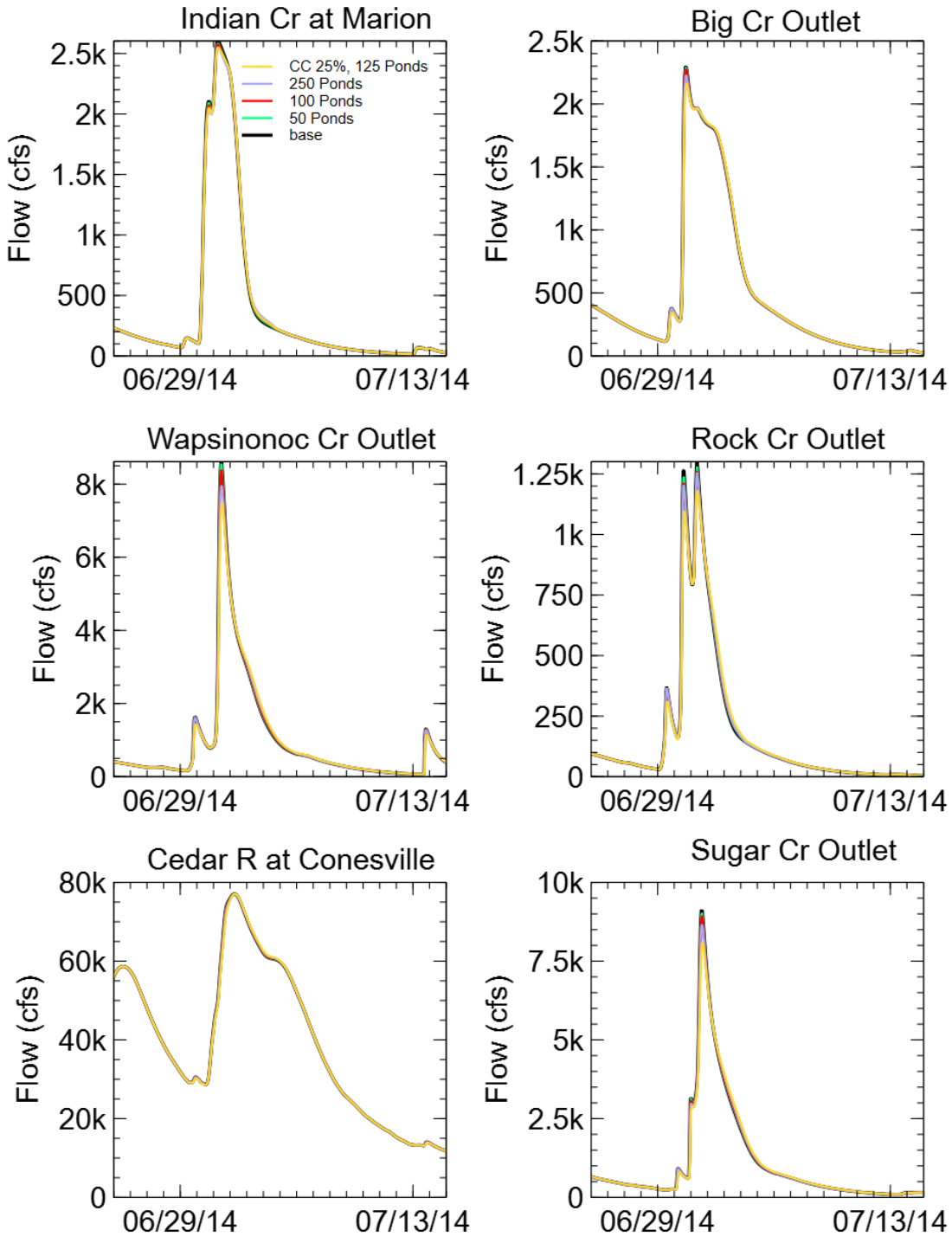

Figure 6-27. Simulated hydrographs at index locations for detention pond scenarios and June 29 – July 5, 2014, storm event.

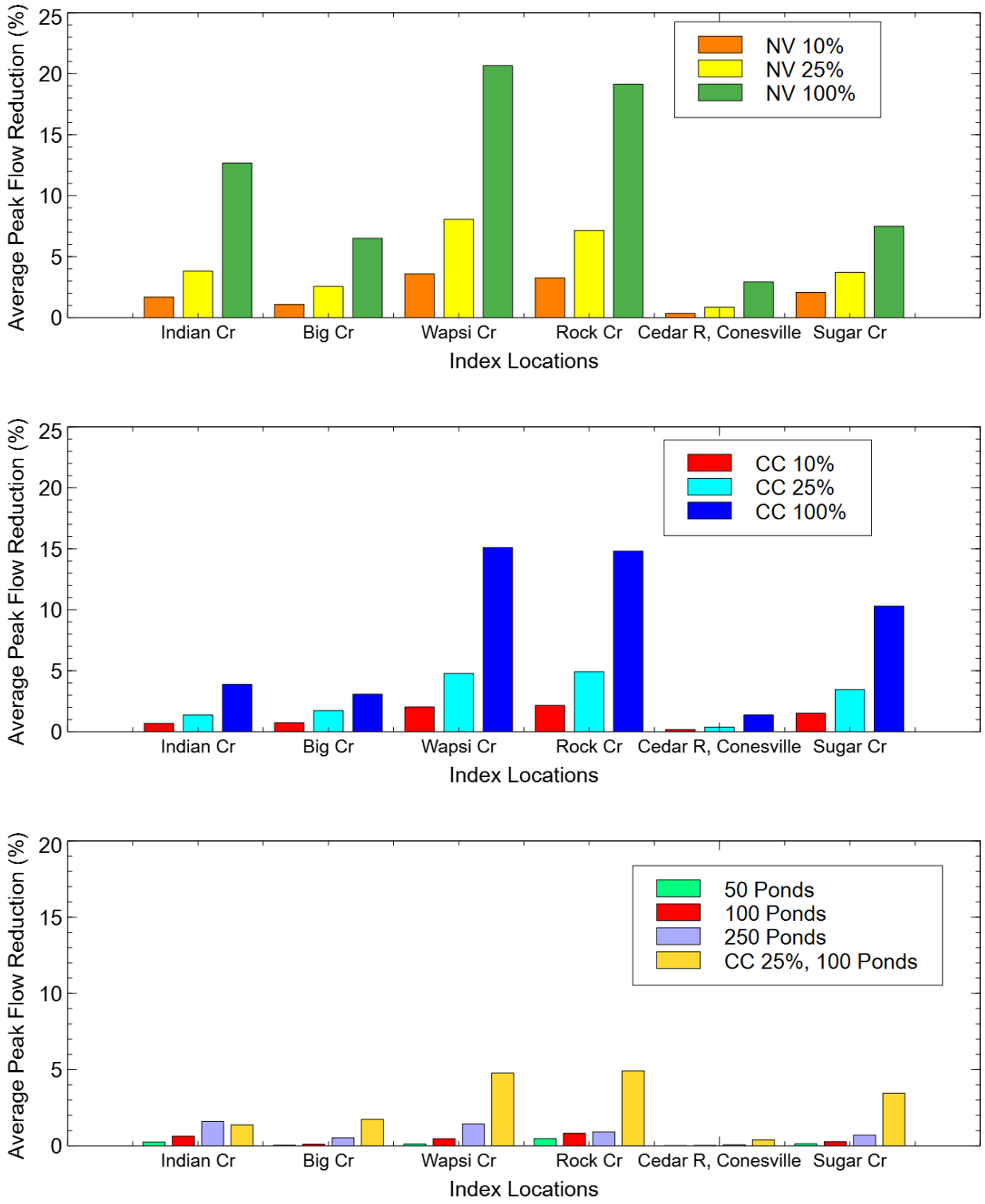

Figure 6-28. Average peak flow reductions for April - September 2014, native vegetation (top), cover crop/ improved soil health (middle), and distributed storage (bottom).

6.4.3 August 2016, Storm Event

Figure 6-29 shows the cumulative rainfall from August 10 – 17, 2016. The largest cumulative rainfall, 4-6 inches, occurred primarily over the far western and eastern corners of the watershed, with most areas receiving 2-4 inches over this period. There were other heavy rainfall events occurring at various times that affected various parts of the watershed. Figure 6-30 shows simulated flow hydrographs for the period of June 15 – August 20 at model index locations for the native vegetation scenarios. Figure 7 24 shows simulated flow hydrographs at model index locations for the cover crop / soil health improvement scenarios. Figure 7 25 shows simulated flow hydrographs at model index locations for the distributed pond scenarios. Average peak flow reductions for all scenarios for April – September 2016 are shown in Figure 7 26. As expected, broad scale changes in land cover result in large, broad-scale reductions in peak discharge. Reductions on the main stem of the Cedar River at Conesville are negligible due to the scenarios and heavy rainfall only being applied within the Lower Cedar River Watershed.

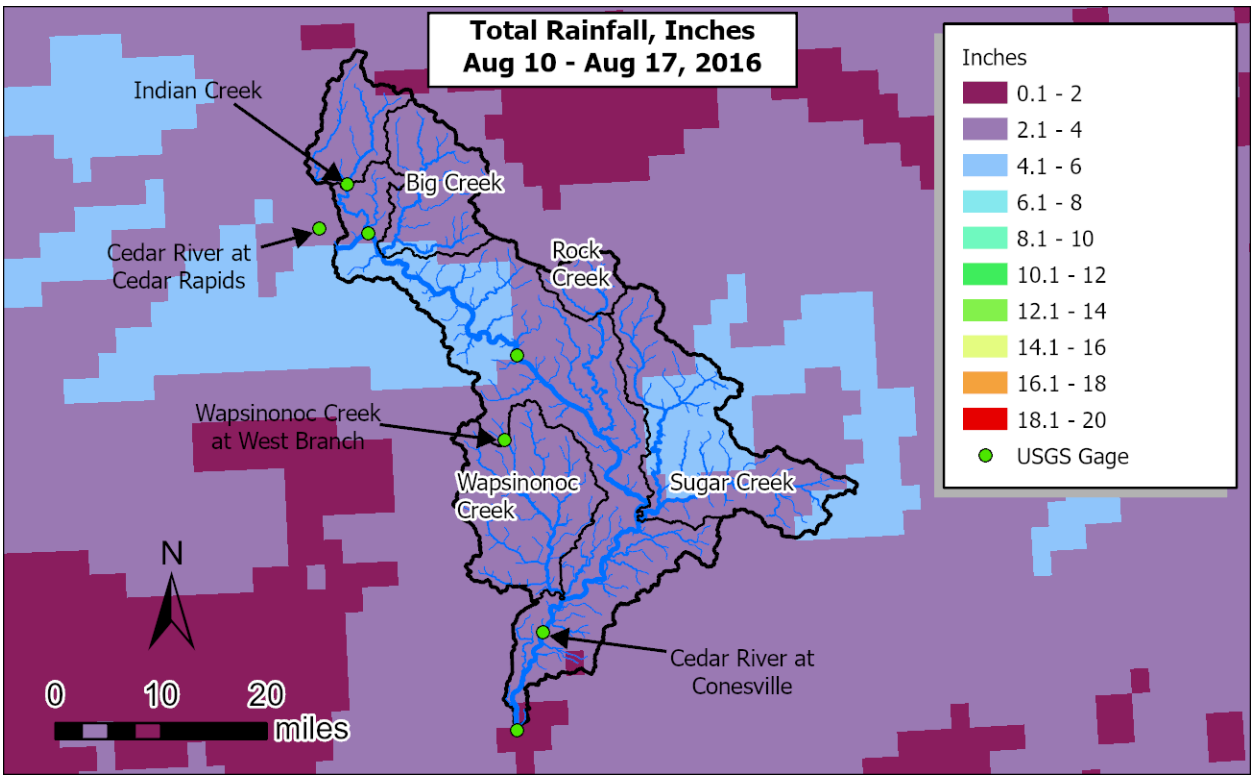

Figure 6-29. August 10-17, 2016, cumulative rainfall used for simulating watershed scenarios.

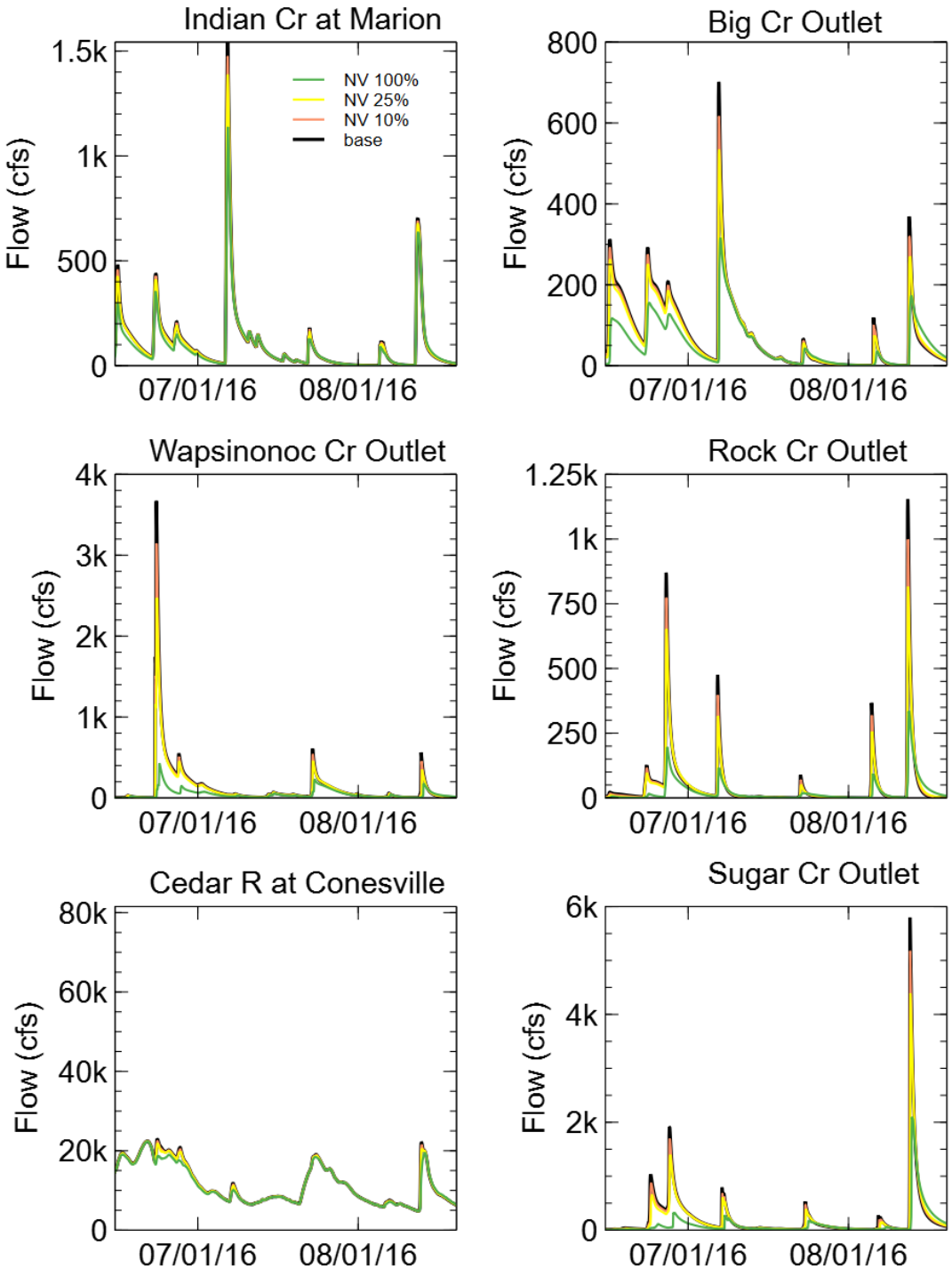

Figure 6-30. Simulated hydrographs at index locations for native vegetation scenario and June 15 – August 20, 2016 period.

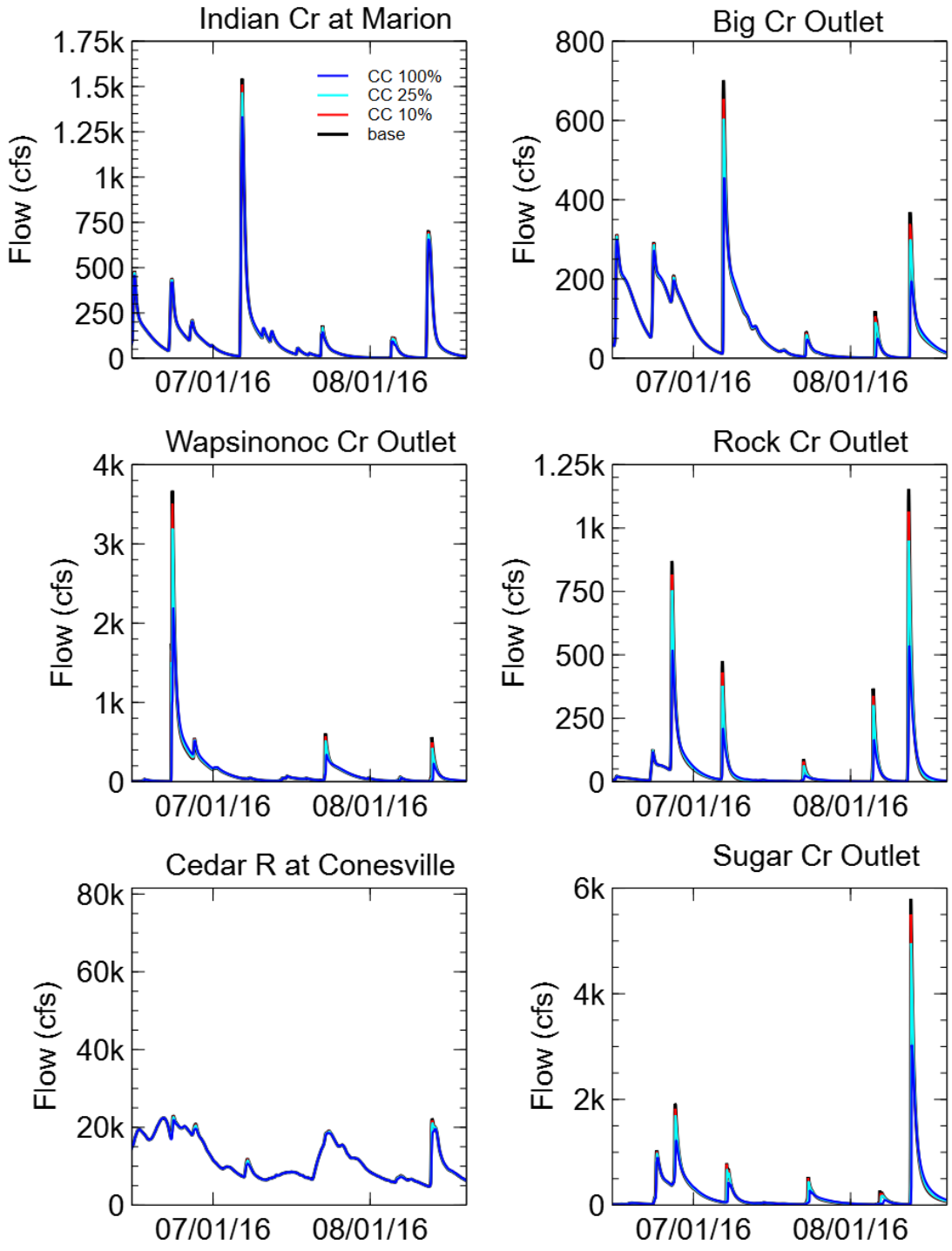

Figure 6-31. Simulated hydrographs at index locations for cover crops / soil health improvement scenario and June 15 – August 20, 2016 period.

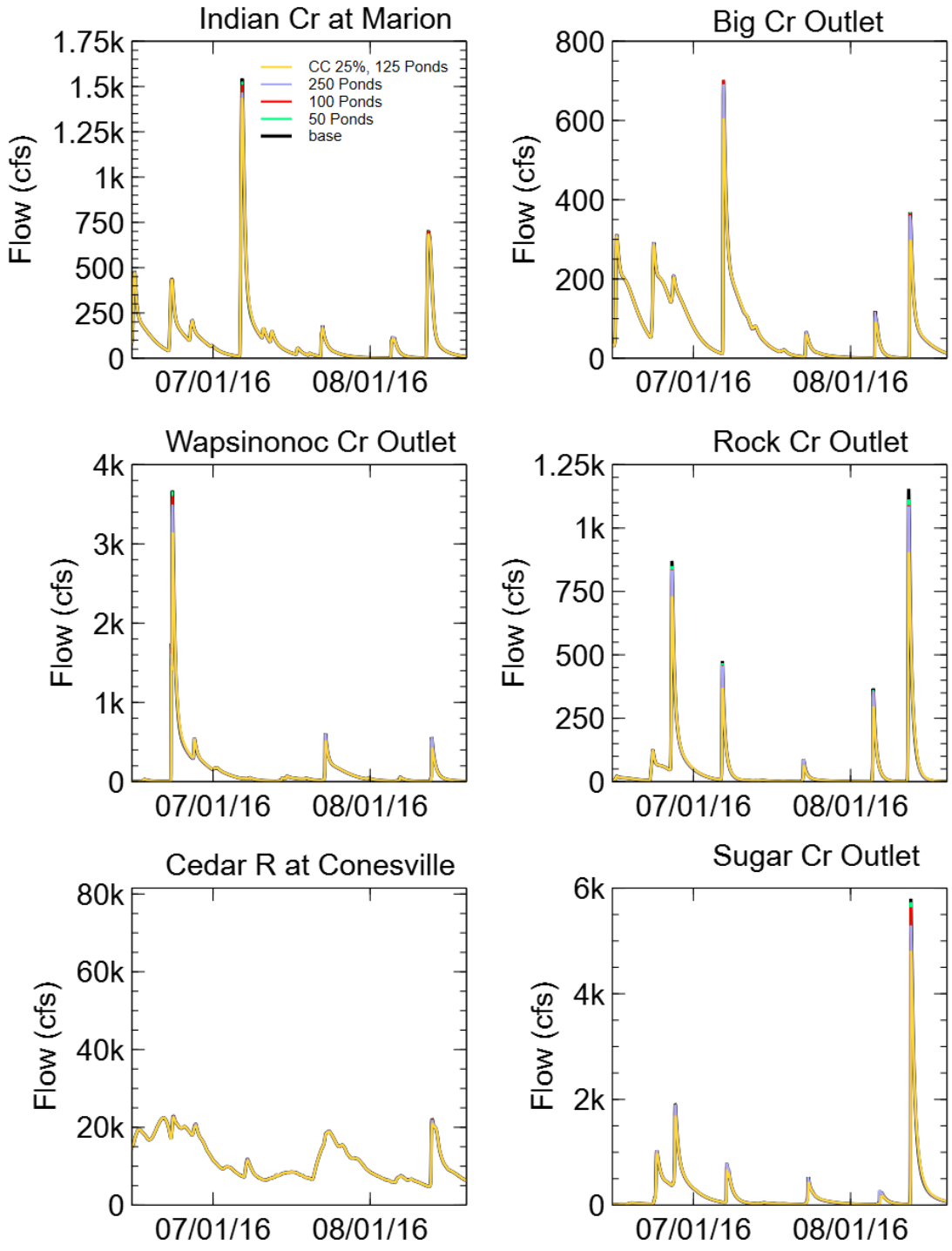

Figure 6-32. Simulated hydrographs at index locations for detention pond scenarios and June 15 – August 20, 2016 period.

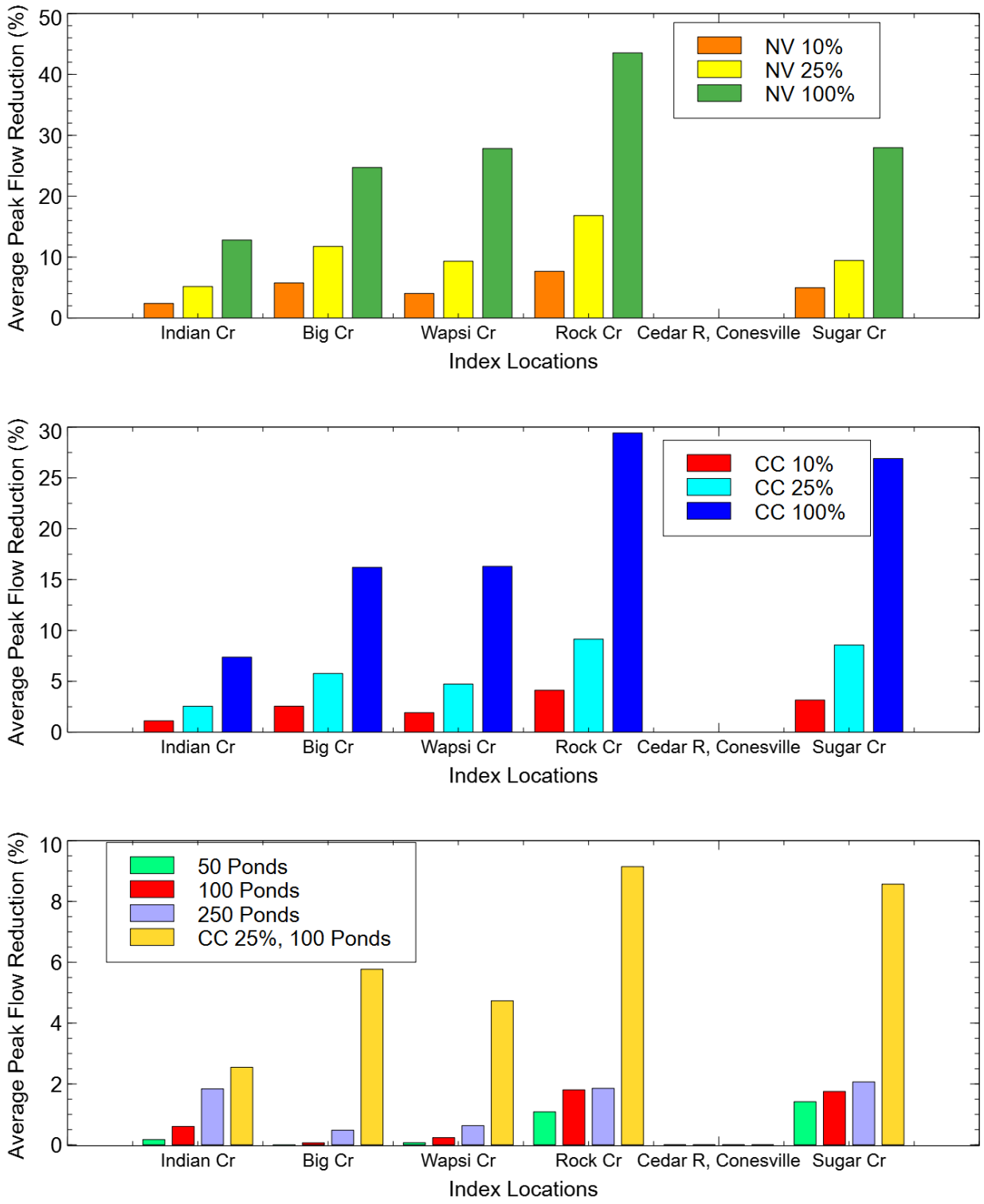

Figure 6-33. Average peak flow reductions for April – September 2016, native vegetation (top), cover crop/ improved soil health (middle), and distributed storage (bottom).

6.4.4 June 2024, Transposed Storm Event

A storm event that occurred June 19 – June 23, 2024, caused unprecedented flooding in many northwest Iowa and southeast South Dakota communities. Figure 6-34 shows the cumulative rainfall as it occurred during the event, with some areas receiving greater than 14 inches of rainfall. This rainfall event was transposed to the Lower Cedar River Watershed, as shown in Figure 6-35. The rainfall was transposed such that the largest cumulative rainfall was centered over the watershed. The observed 2024 Cedar Rapids flow at Cedar Rapids was used as an upstream boundary condition along with the transposed rainfall. Figure 6-36 shows simulated flow hydrographs at model index locations for the native vegetation scenarios. Figure 6-37 shows simulated flow hydrographs at model index locations for the cover crop / soil health improvement scenarios. Figure 6-38 shows simulated flow hydrographs at model index locations for the distributed pond scenarios. Average peak flow reductions for all scenarios are shown in Figure 6-39. As expected, broad scale changes in land cover result in large, broad-scale reductions in peak discharge.

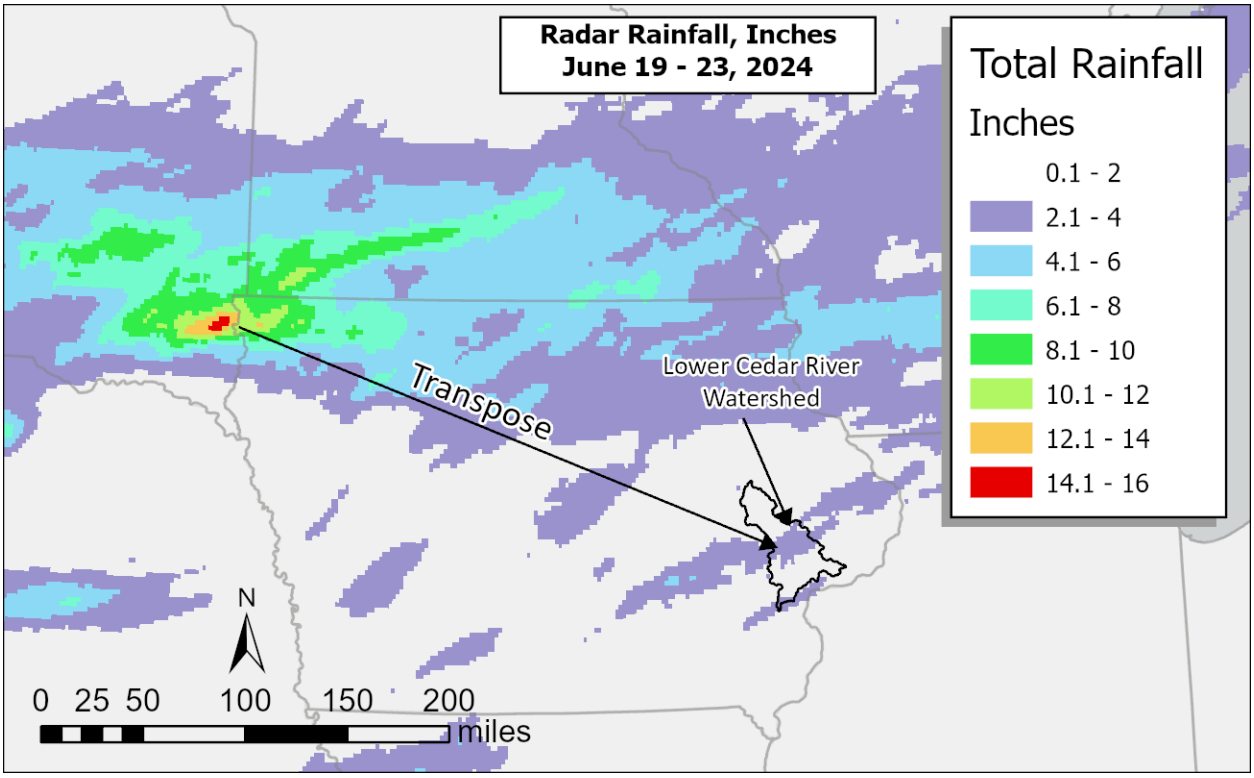

Figure 6-34. Cumulative rainfall from the June 19 – June 23, 2024 Flood event was transposed to the Lower Cedar River Watershed.

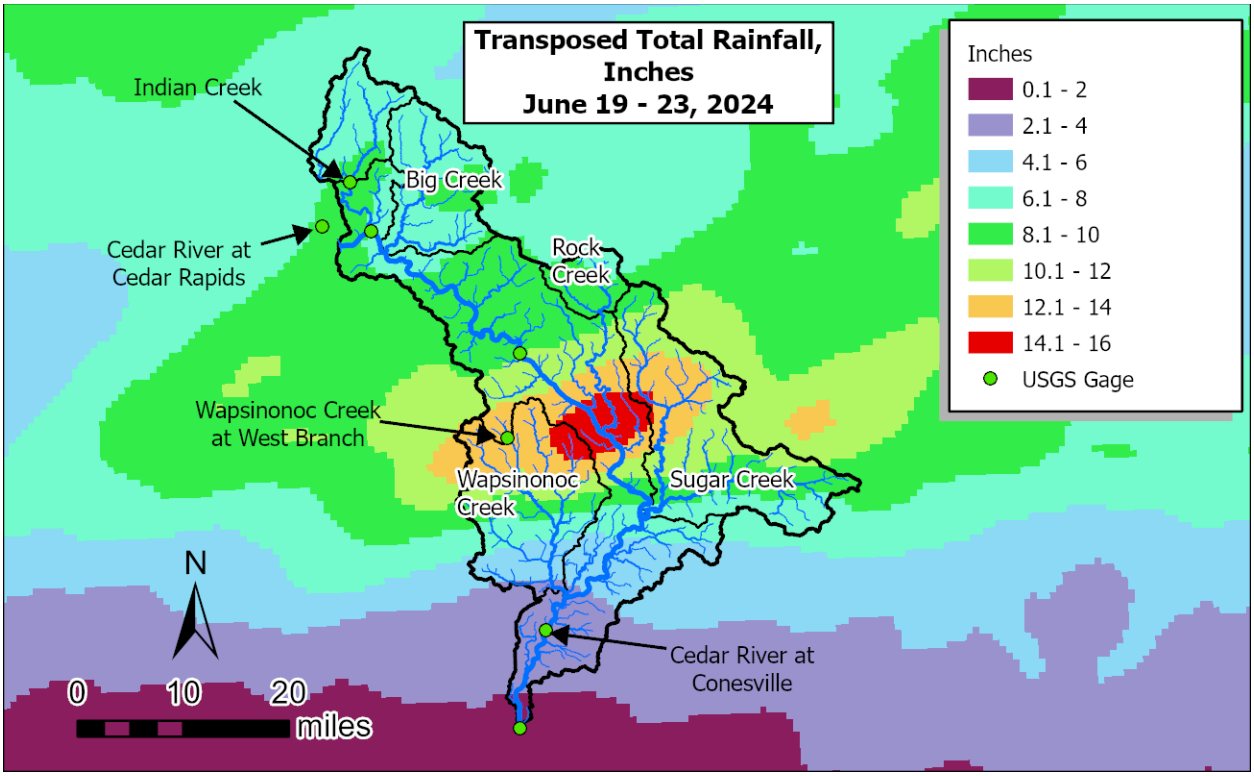

Figure 6-35. Transposed June 19 – June 23, 2024 cumulative rainfall from northwest Iowa used for simulating watershed scenarios.

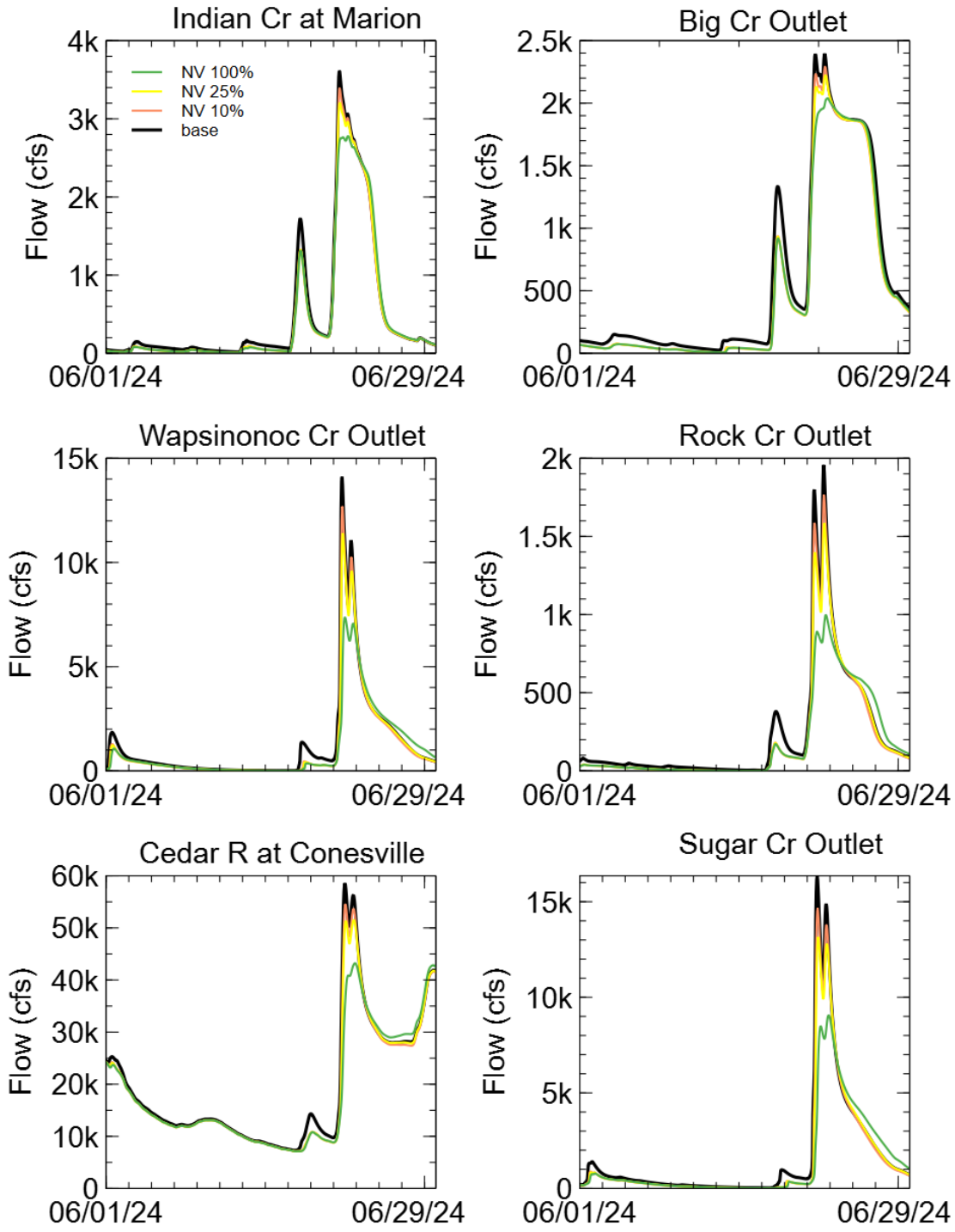

Figure 6-36. Simulated hydrographs at index locations for native vegetation scenario and June 19 – June 23, 2024 transposed storm event.

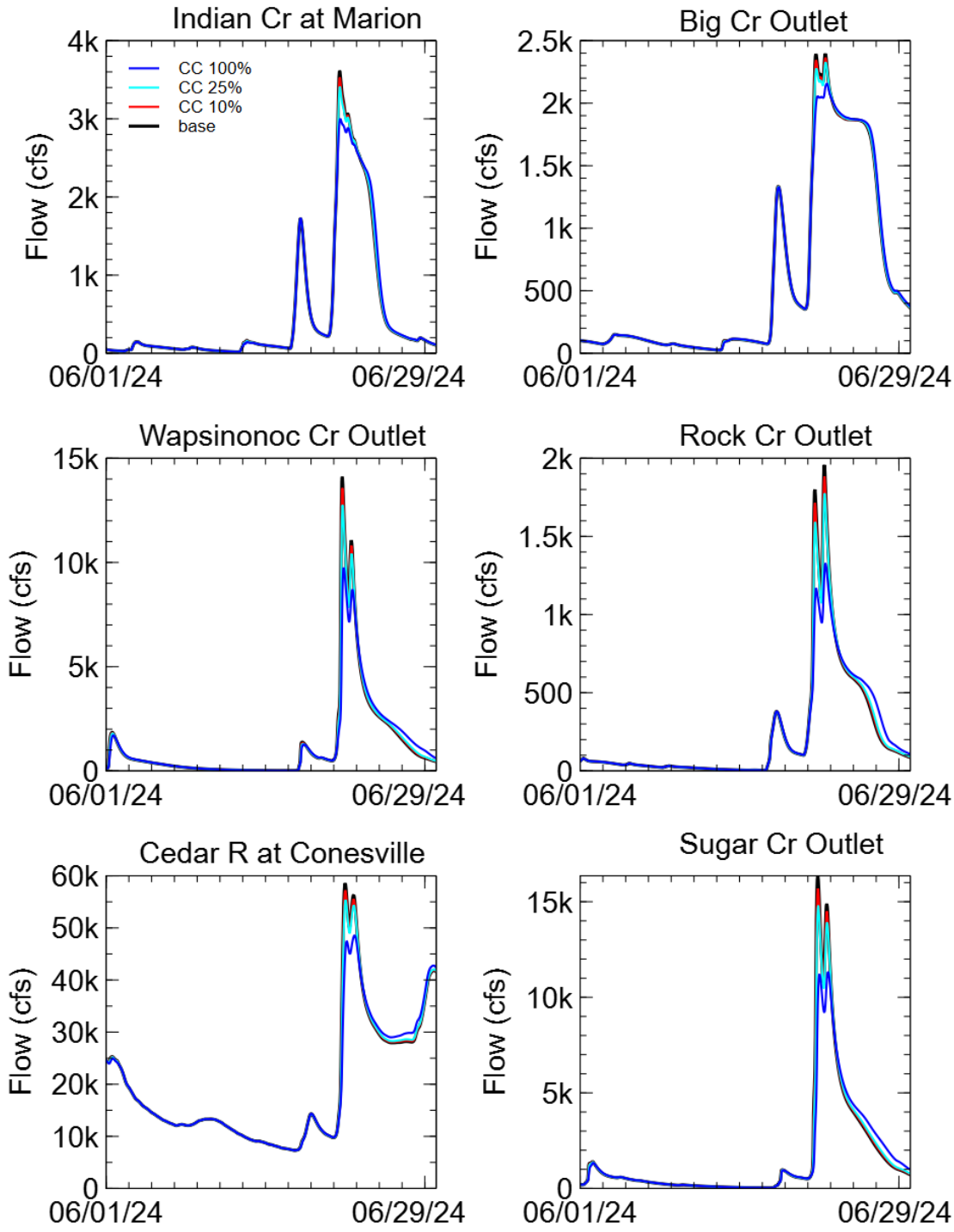

Figure 6-37. Simulated hydrographs at index locations for cover crops / soil health improvement scenario and June 19 – June 23, 2024 transposed storm event.

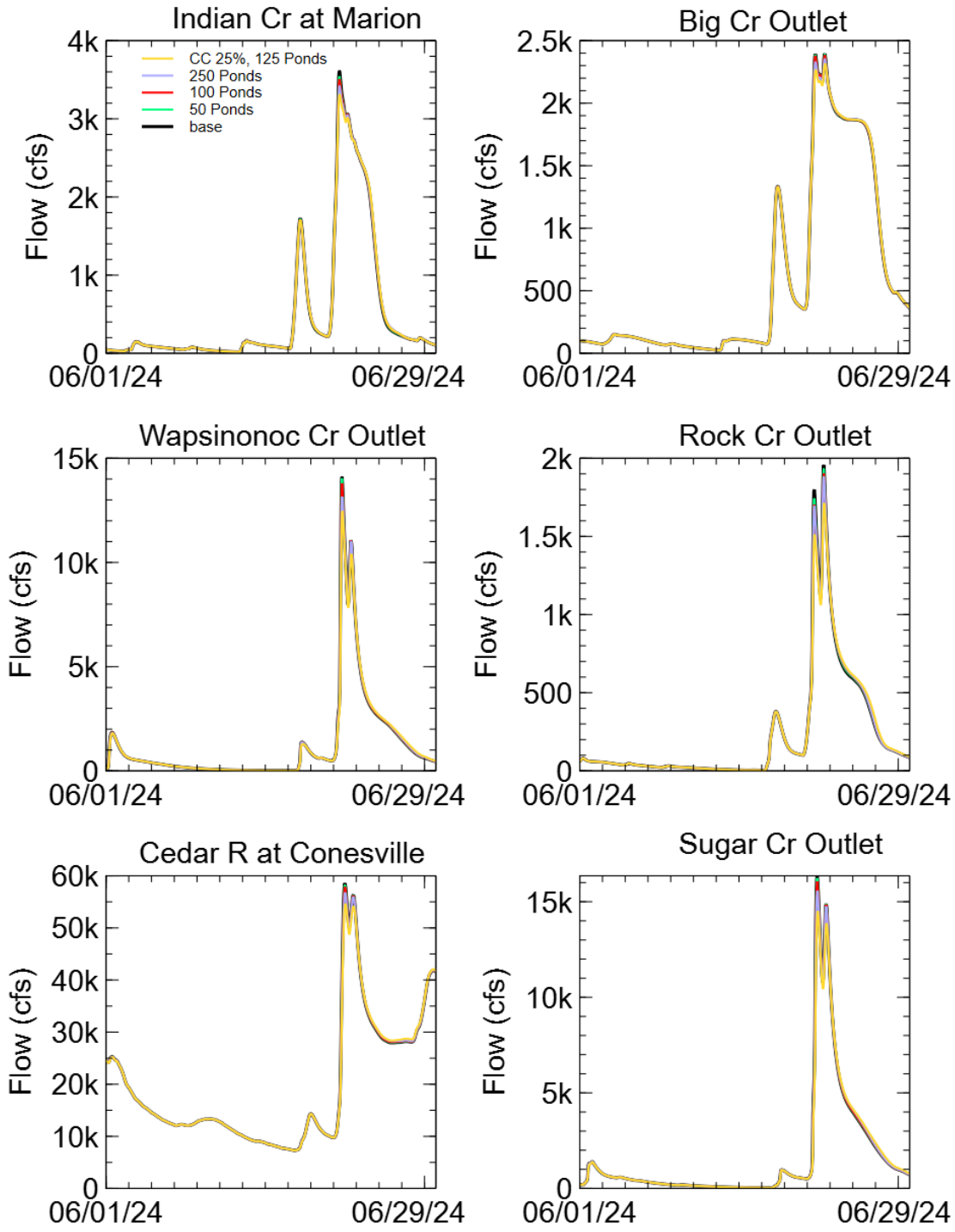

Figure 6-38. Simulated hydrographs at index locations for detention pond scenarios and June 19 – June 23, 2024 transposed storm event.

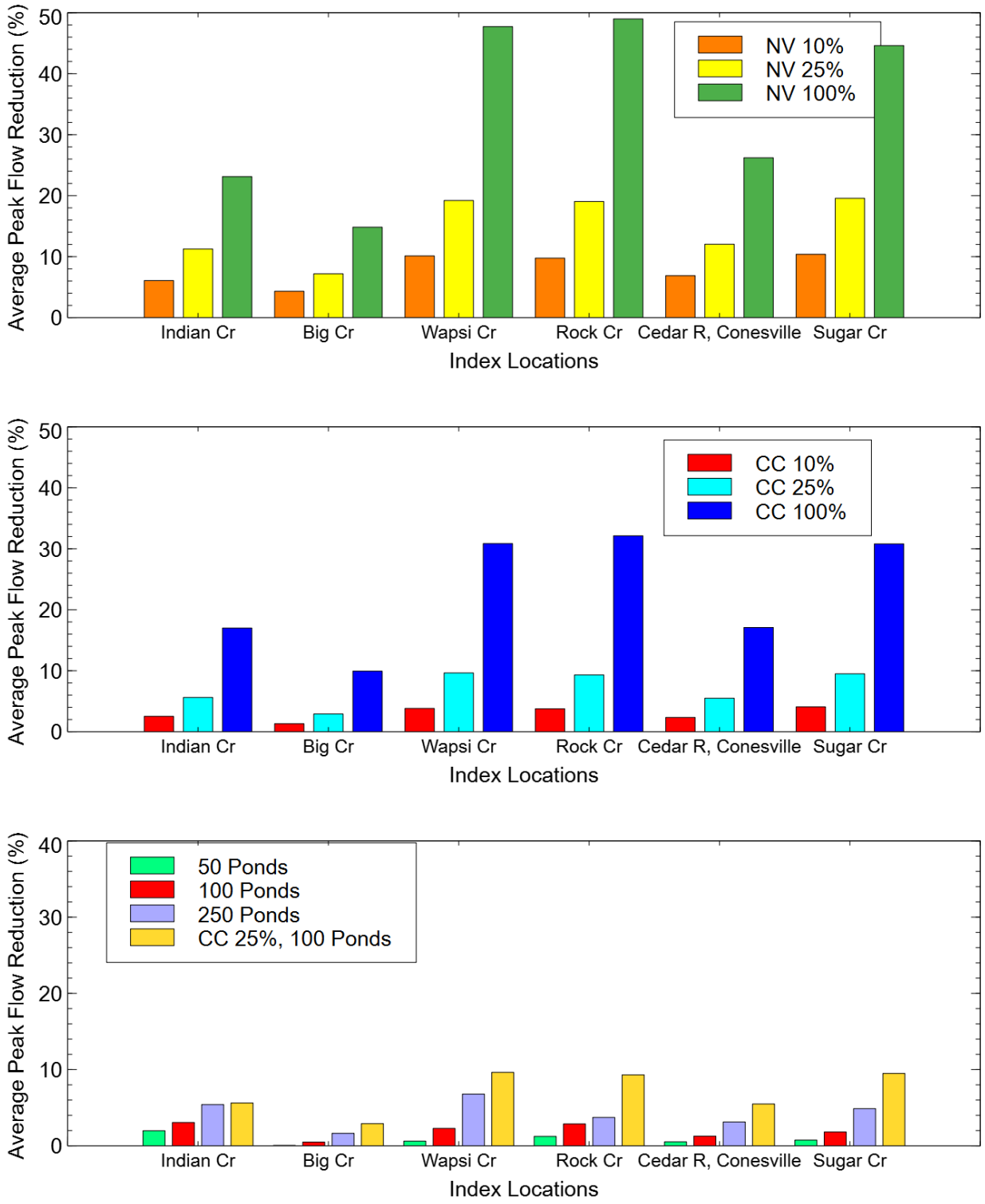

Figure 6-39. Average peak flow reductions for the June 19 – June 23, 2024 transposed storm event, and native vegetation (top), cover crop/ improved soil health (middle), and distributed storage (bottom).

A summary of the typical peak discharge reductions across all locations and historical events for each scenario are shown as box and whisker plots in Figure 6-40. Overall, the broad-scale infiltration practices like native vegetation and cover crop/ improved soil scenarios showed the largest peak flow reductions. The distributed storage scenarios showed the least peak flow reductions. As discussed previously, the individual detention storage projects provide large peak flow reductions just downstream, but that benefit is reduced as unregulated drainage area accumulates moving downstream.

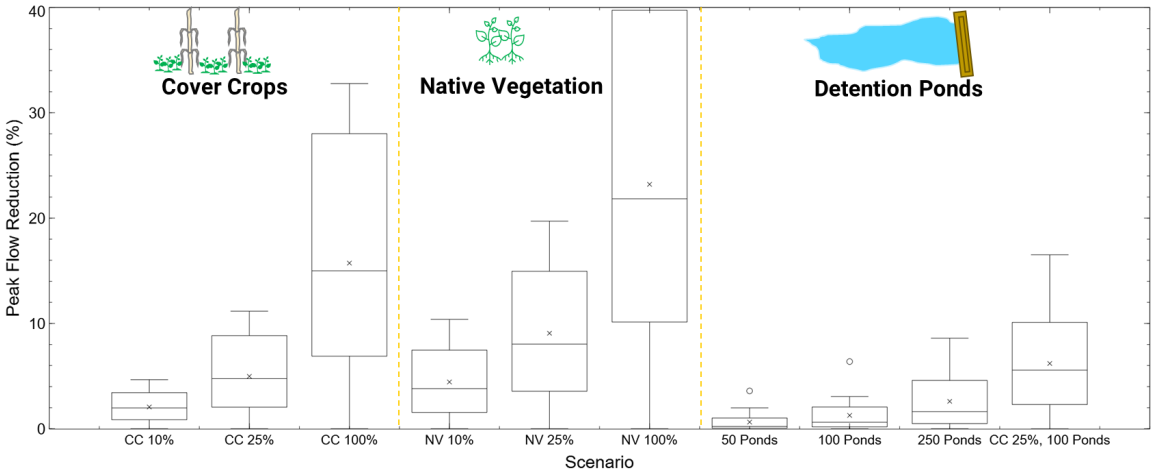

Figure 6-40. Summary of peak discharge reductions across all model index locations and historical events for each scenario.

6.5 Impact of Practices Implemented Throughout the Cedar River Watershed

Simulations in previous sections utilized the observed Cedar River flow at Cedar Rapids as upstream inflow into the HEC-HMS model. The what-if scenarios were only implemented in the Lower Cedar River Watershed which is only 14% of the total Cedar River Watershed drainage area. As a result, there were reasonable peak flow reductions along smaller tributaries but negligible flow reductions along the Cedar River. These negligible reductions occur whenever high flows originate from rainfall upstream of Cedar Rapids. This is particularly evident in simulations of the 2008 Flood event discussed in section 6.4.1. A parallel modeling effort investigating the effect of implementing practices in the upstream Cedar River Watershed was completed by IIHR graduate student Logan Mahoney for her master's degree research project (Mahoney, 2024). The entire Cedar River Watershed was modeled the same model and methodology, but with larger subbasins, which can be seen in Figure 6-41. This model was

calibrated to the 2008 and 2016 flood events and validated using several other events. The following summarizes the conclusions from her modeling efforts.

This Cedar River Watershed modeling effort also investigated increasing infiltration and soil capacity through broad changes in land use – converting all agricultural land to native prairie and long-term implementation of cover crops on all agricultural lands (Mahoney, 2024). The methodology to implement these changes were very similar to those discussed in section 6.2.1. These scenarios are not feasible to implement at this scale but demonstrate the required level of practice implementation to make meaningful peak flow reductions at the Cedar River Watershed scale. Average peak flow reductions at several locations within the Cedar River for the 2008 and 2016 water years are shown in Figure 6-42. Overall, the peak flow reductions are range from 20-40% and 10-25% for the native prairie scenario and cover crop scenario, respectively. These align closely with those discussed in previous sections. Generally, the largest reductions occur at the smaller drainage areas and decrease as drainage area increases moving downstream.

The Cedar River Watershed modeling effort also investigated adding distributed storage throughout the watershed (Mahoney, 2024). The storage ponds implemented were similar to the typical 20 acre-feet ponds implemented in the Lower Cedar River Watershed but were scaled to 480 acre-feet flood storage at the spillway height, commensurate with the larger subbasins. Only 10% of the subbasin drainage areas were routed through the storage ponds. There were three pond scenarios developed - one storage pond located within each of the 827 subbasins, one storage pond located within each of 414 subbasins, and one storage pond located within each of 207 subbasins. This results in additional total flood storage of 396,960 acre-feet, 198,720 acre-feet, and 99,360 acre-feet for the 827 ponds, 414 ponds, and 207 ponds scenarios, respectively. The 827 ponds scenario would add approximately the same flood storage to the watershed as the entire flood storage provided by the Coralville Reservoir located on the nearby Iowa River.

Average peak flow reductions at several locations within the Cedar River for the 2008 and 2016 water years are shown in Figure 6-43. Overall, the peak flow reductions range from 1-8% but are typically less than 2%. These reductions are much smaller than the broad-scale infiltration improvement scenarios. As discussed previously, while detention ponds provide significant flow reductions just downstream, they are only regulating a small percentage of the total drainage area. Unregulated drainage area accumulates significantly moving downstream from detention pond projects. Downstream locations with significant drainage area, like Conesville, experience

basically the same flow volumes with the detention ponds as without. While the pond projects may delay the arrival of the peak flows at downstream locations, they arrive at relatively the same time considering the long-time scale of events like the 2008 and 2016 Floods.

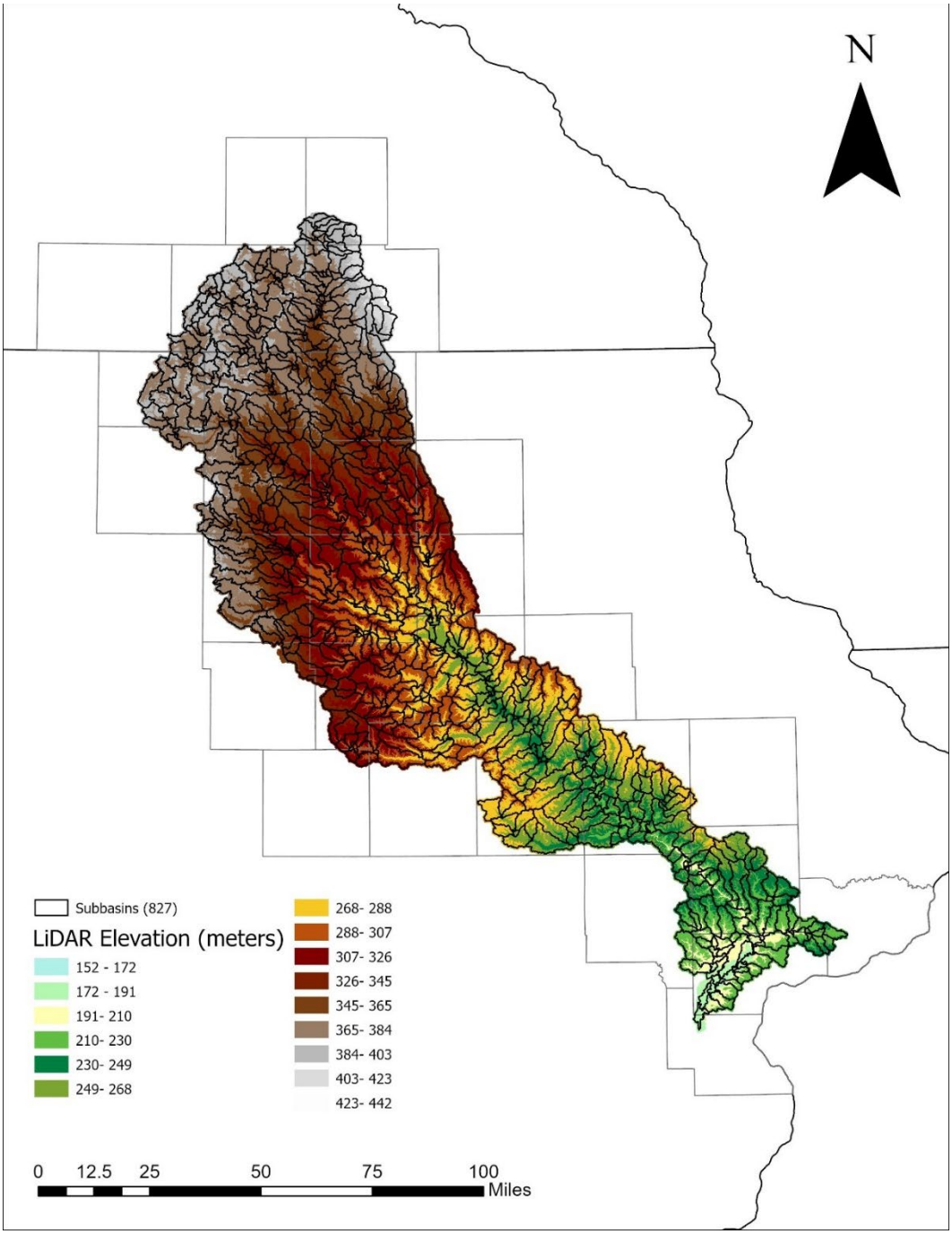

Figure 6-41. HEC-HMS subbasin delineation of the Cedar River Watershed (Mahoney, 2024).

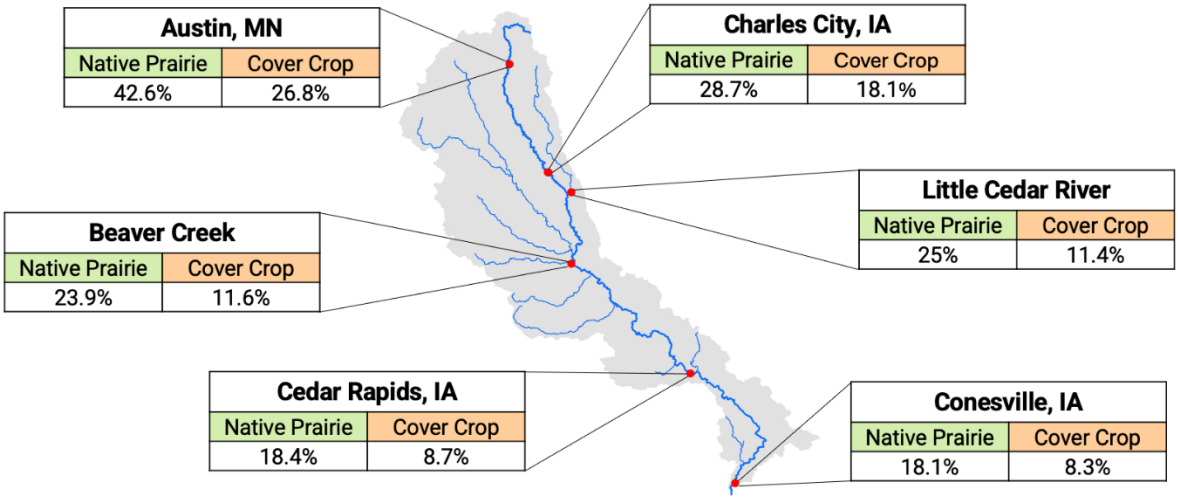

Figure 6-42. Average peak flow reduction percentages for the 100% conversion scenario to native prairie or cover crops at locations on the Cedar River (Austin, Charles City, Cedar Rapids, Conesville) and two tributaries (Beaver Creek, Little Cedar River) (Mahoney, 2024).

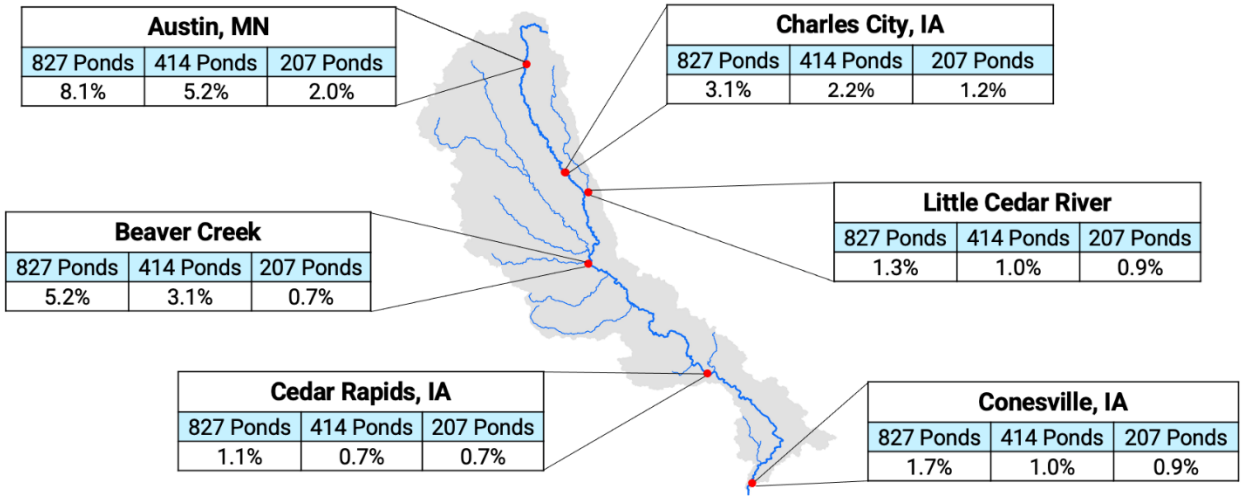

Figure 6-43. Average results for all 3 scenarios of distributed storage ponds at locations on the Cedar River (Austin, Charles City, Cedar Rapids, Conesville) and two tributaries (Beaver Creek, Little Cedar River) (Mahoney, 2024).

7. SUMMARY AND CONCLUSIONS

The purpose of this hydrologic assessment is to provide an understanding of the watershed hydrology in the Lower Cedar River Watershed and the potential of various hypothetical flood mitigation strategies that can be utilized to accomplish goals of the Lower Cedar River Watershed Management Authority.

7.1 Cedar River Water Cycle and Watershed Conditions

The water cycle of the Cedar River Watershed was examined using historical precipitation and streamflow records. The average annual precipitation for the Cedar River Watershed is 34 inches. Of this precipitation amount, 69% (23 inches) evaporates back into the atmosphere and the remaining 31% (11 inches) infiltrates or runs off the landscape into the streams and rivers. Most of the total streamflow volume is baseflow (73%, or 7.6 inches), and the rest is surface flow (27%, or 2.8 inches). Average monthly streamflow peaks in spring and early summer and decreases through the summer growing season. Flooding frequently occurs in March and April, associated with snowmelt and heavy spring rains. The largest floods, while less frequent than the early spring events, occur in June or July, associated with heavy spring/summer rains.

The water cycle has changed because of land use and climate changes. The largest change occurred in the late 1800s when the landscape was converted from low-runoff prairie and forest to higher-runoff farmland. Since the 1970s, Iowa precipitation has increased in quantity, while intense rain events have changed in timing and frequency. Streamflow records in Iowa (including those for the Cedar River) suggest that average flows, low flows, and perhaps high flows have all increased and become more variable since the late 1960s or 1970s; however, the relative contributions of land use and climate changes are difficult to sort out.

The majority of the Lower Cedar River Watershed is located within two distinct landform regions – the Iowan Surface and the Southern Iowa Drift Plain. A portion of the Cedar River floodplain is located within the Iowa-Cedar Lowland. Each landform region has a unique influence on the rainfall-runoff stream network characterization. The Iowan Surface is characterized gently rolling topography, common glacial ‘erratics’, and loess-mantled paha. The Southern Iowa Drift Plain is characterized by steeply rolling topography and well-developed drainage divides. Much of the watershed has soils with moderately high runoff potential. Typical land slopes are between 1.2% and 7.7% (25th and 75th percentiles), with the steepest areas occurring along the major river

and stream valleys. The land use is predominantly row crop agriculture, accounting for 70% of the area.

7.2 Lower Cedar River Hydrologic Model

The U.S. Army Corps of Engineers' (USACE) Hydrologic Engineering Center's Hydrologic Modeling System (HEC-HMS) was used to develop a hydrologic model for the Lower Cedar River Watershed. First, the watershed was divided into 670 smaller units, called subbasins, with an average area of 1.6 square miles. For model calibration and validation with actual (historical) rainfall events, radar rainfall estimates were used as the precipitation input for each simulation. For the analysis of watershed scenarios, a 24-hour duration SCS Design Storm with rainfall accumulations approximately equal to the 25-year return period was used to drive the watershed response. Several historical storm events and one transposed historic event were used to evaluate the relative difference between watershed scenario simulations.

The Soil Moisture Accounting (SMA) methodology was used to simulate hydrologic processes within each model subbasin in the Lower Cedar River Watershed HMS model. The SMA model simulates vertical movement and storage of water between the atmosphere, vegetative canopy, ground surface, soil, and groundwater, characterized by storage volumes and rate equations. The Clark Unit Hydrograph method was used to convert excess precipitation into a direct runoff hydrograph for each subbasin. This unit hydrograph method accounts for translation (delay) and attenuation (reduction) of the peak subbasin hydrograph discharge due to travel time of the excess precipitation to the subbasin outlet and temporary surface storage effects. Conveyance of runoff through the river network, or flood wave routing, was accomplished using kinematic wave routing methods.

Model calibration adjusts the initial set of model parameters, so the simulated results more closely match observed discharges at gaging stations more closely for historical events. The Lower Cedar River Watershed HEC-HMS model was calibrated and validated using historic events. The subbasins within Indian Creek watershed were calibrated using radar rainfall and USGS stream gage records for the May 2012 – August 2016 period. The rest of the subbasins were not altered due to a lack of localized streamflow observations. After calibration of model parameters, model validation assesses the predictive capability of the model to simulate discharge for the 2024 water

year. The model generated runoff volume, hydrograph shape, and peak flow timing very similar to the observed streamflow hydrographs during the validation period.

7.3 Watershed Scenarios for the Lower Cedar River Watershed

The HEC-HMS model was used to better understand the flood hydrology of the Lower Cedar River watershed and to evaluate potential flood mitigation strategies. The runoff potential throughout the watershed was first assessed using the HMS model's representation of storm runoff generated from a design storm. The highest runoff potential areas are located along the eastern and western edges of the watershed, areas largely dominated by agriculture use. The lowest runoff potential areas appear to follow the larger river corridors. From a hydrologic perspective, flood mitigation projects that can reduce runoff from these higher runoff areas should be a higher priority. It is worth noting that other land uses – particularly urban development – likely have the highest runoff potential. However, the footprint of these areas is small compared to the agricultural areas that dominate the watershed. In urban areas, local drainage issues could be improved by more effectively capturing and storing storm water (e.g., storm water detention and low-impact development practices).

The HEC-HMS model was used to quantify potential effects of flood mitigation strategies applied throughout the Lower Cedar River Watershed. Several flood mitigation strategies were considered — enhancing local infiltration through changes in land use (from agricultural to native prairie), enhancing local infiltration through improvements in soil quality through consistent use of cover crops, and storing floodwaters temporarily in distributed storage ponds to reduce downstream discharges. A blended scenario using cover crops and storage ponds was considered. The effects of these strategies were simulated for a 6-inch, 24-hour SCS Design Storm, occurring simultaneously over the entire watershed, and for several historical rainfall events. The results of these strategies to were compared to simulations of flows for the existing watershed condition. Although each scenario simulated is hypothetical and simplified, the results provide valuable insights on the relative performance of each strategy for flood mitigation planning.

There are many BMPs not investigated in this report that could potentially increase infiltration or runoff storage at the watershed scale. However, the analysis was limited by the resolution and capability of the HEC-HMS model to simulate effects of BMPs aggregated across subbasin areas of several square miles. Therefore, investigations were limited to distributed storage

provided by ponds, which are relatively large BMP structures, and broad-scale land cover changes. Simulation of other much smaller BMP structures like terracing or WASCOBS, while demonstrably effective in this watershed, would require considering many more individual structures to make any impact at the watershed scale, and a much higher degree of model resolution to reliably quantify impacts.

7.3.1 Increased Infiltration in the Watershed

Simulation results indicate that enhancements to local infiltration through broad changes in land use have the most significant impact on runoff. Converting current agricultural areas from row crop to native tall-grass prairie would reduce peak flows approximately 25 percent during large rainfall events. This hypothetical scenario illustrates the dramatic reductions in stream flow because of land use change. However, converting the entire agricultural landscape back to pre-settlement tall-grass prairie is not a practical or economically desirable strategy. This scenario provides support for targeted land use changes that could be an effective part of a watershed's flood mitigation efforts.

Agricultural management practices could increase the infiltration of precipitation without significantly decreasing agricultural production through the use of cover crops. Cover crop plantings during the dormant season can produce long-lasting improvements in soil quality. However, improvements in soil infiltration properties would take many years to be fully realized, and cover crops would need to be continuously implemented. From the simulation results, it is apparent that enhancement of local infiltration through soil quality improvement resulting from cover crops has a small but significant effect. The model predicts that adopting cover crop management practices would increase reduce peak flows by approximately 15% during large storm events, which is relatively less than a tall-grass prairie landscape, but significant, nonetheless. Reductions in peak discharge throughout the watershed ranged from 5–25%, depending on the storm event. Given the widespread agricultural land use in the Lower Cedar River Watershed and the growing interest in the use of cover crops as a part of Iowa's nutrient management strategy, cover crops could play an important role as a watershed-wide flood mitigation strategy.

7.3.2 Increased Storage on the Landscape

In some ways, using ponds to temporarily store floodwaters is an attempt to replace the loss of water that was once stored in soils (in the pre-agricultural landscape). Compared to the

extra water that was stored by infiltration in the previous simulated scenarios, the amount of storage replaced by ponds is quite small. As a result, the overall flood peak reduction with storage ponds is less than predicted for the other scenarios. Since there is no additional infiltration, the overall volume of runoff in the watershed is higher than the enhanced filtration scenarios. Still, compared to the other scenarios, the flood storage scenario is realistically more achievable. Ponds can effectively reduce flood peaks immediately downstream of their headwater sites. Reductions in peak discharge at watershed index points were generally less than 10%, depending on the storm event. The challenge to reducing flood peaks at the watershed scale is that downstream locations experience floodwaters originating from locations throughout the watershed arriving at different times; some areas have ponds, others do not. The result is that the storage effect from detention ponds is spread out over time, instead of being concentrated at the time of highest flows. Hence, at larger drainage areas downstream in the watershed, the flood peak reduction of storage ponds diminishes.

7.3.3 Increased Infiltration and Increased Storage

Future projects in the Lower Cedar River Watershed will likely use both enhanced infiltration practices and flood storage. A blended scenario was developed using cover crops / soil health improvement scenarios and detention ponds to evaluate the flood mitigation benefits of multiple mitigation strategies. The watershed scenario assumes 25% of agricultural lands would use cover crops to improve soil infiltration. The 100 flood storage ponds scenario were also incorporated. Reductions in peak discharge throughout the watershed generally ranged from 2–10%, depending on the storm event. Simulation results of the design storm and historical events indicate the use of cover crops would provide much broader benefits than ponds alone and further enhance the ability of ponds to store excess runoff. Improvements in soil infiltration properties would take many years to be fully realized, and cover crops would need to be continuously implemented.

7.3.4 Concluding Remarks

It is important to recognize that these modeling scenarios evaluate the hydrologic effectiveness of the flood mitigation strategies and not their effectiveness in other ways. For instance, while certain strategies are more effective in terms of hydrology, they may not be as effective economically. As part of the flood mitigation planning process, other factors should be

considered in addition to the hydrology, such as the cost and benefits of alternatives, landowner willingness to participate, and more.

REFERENCES

Archuleta, R. (2014, April). Cedar River Watershed Coalition Meeting - Cover Crops and Other Conservation Practices. (P. Interview, Interviewer)

Berendzen, P. B., Cruse, R. M., Jackson, L. L., Mulqueen, R., Mutel, C. F., Osterberg, D., . . . Thorne, P. S. (2011). *Climate Change Impacts on Iowa 2010.* Des Moines: Iowa Climate Change Impacts Committee.

Bharati, L., Lee, K. H., Isenhart, T. M., & Schultz, R. C. (2002). Soil-water infiltration under crops, pasture, and established riparian buffer in Midwestern USA. *Agroforest Systems*, 56(3), 249-257.

Brye, K. R., Norman, J. M., Bundy, L. G., & Gower, S. T. (2000). Water-budget evaluation of prairie and maize ecosystems. *Soil Science Society of America Journal*, 64(2) 715-724.

Dabney, S. M., Delgado, J. A., & Reeves, D. W. (2001). Using winter cover crops to improve soil and water quality. *Communications in Soil Science and Plant Analysis*, 1221-1250.

Fall, G., Kitzmiller, D., Pavlovic, S., Zhang, Z., Patrick, N., St. Laurent, M., . . . Miller, D. (2023). The Office of Water Prediction's Analysis of Record For Calibration, Version 1.1: Dataset Description and Precipitation Evaluation. *JAWRA Journal of the American Water Resources Association*, 1246-1272.

Gao, P., Li, P., Zhao, B., Xu, R., Zhao, G., Wenyi, S., & Xingmin, M. (2017). Use of double mass curves in hydrologic benefit evaluations. *Hydrological Processes*, 4639-4646.

Hernandez-Santana, V., Zhou, X., Helmers, M., Kolka, R., & Tomer, M. (2013). Native prairie filter strips reduce runoff from hillslopes under annual row crop systems in Iowa. *Journal of Hydrology*, 94-103.

Hydrologic Engineering Center. (2023). *HEC-HMS User's Manual Version 4.12.* USACE.

Hydrologic Engineering Center. (2024, September 15). *HEC-HMS Technical Reference Manual version 4.12.* Retrieved from Transform - Clark Unit Hydrograph Model: https://www.hec.usace.army.mil/confluence/hmsdocs/hmstrm/transform/clark-unit-hydrograph-model

Iowa DNR. (2024). *Soils Requiring Tile Drainage for Full Productivity that are Cropped.* Retrieved from Iowa Geospatial Data Clearinghouse: https://geodata.iowa.gov/documents/9a801c3e5b7246f99b40216dc2a330e0/about

Iowa State University. (2024, 01 01). *Iowa Environmental Mesonet*. Retrieved from ASOS Network: https://mesonet.agron.iastate.edu/request/download.phtml

Jackson, R. B., Canadell, J., Ehleringer, J. R., Mooney, H. A., Sala, O. E., & Schulze, E. D. (1996). A global analysis of root distributions for terrestrial biomes. *Oecologia*, 389-411.

Kling, H., Fuchs, M., & Paulin, M. (2012). Runoff conditions in the upper danube basin under an ensemble of climate change scenarios. *Journal of Hydrology*, 424, 264-277.

Mahoney, L. (2024). Evaluation of Flood Management Practices in the Cedar River Watershed. *Master of Science (MS), University of Iowa*.

McDaniel, L., Garton, J., Fiedler, W., King, W., & Schwanz, N. (2011). *Lake Delhi Dam Breach - Two Perspectives.* Washington D.C.: ASDSO Annual Conference.

Mutel, C. M. (2010). *A Watershed Year: Anatomy of the Iowa Floods of 2008.* Iowa City: University of Iowa Press.

Natural Resources Conservation Service, USDA. (1986). *TR-55 Urban Hydrology for Small Watersheds.* Washington D.C.: US Department of Agriculture.

Ontl, T. (2013, December). *Where do you hide 20,000 gallons of water?* Retrieved from Schulte Moore Lab, Iowa State University: https://faculty.sites.iastate.edu/lschulte/post/where-do-you-hide-20000-gallons-water

Perica, S., Martin, D., Pavlovic, S., Roy, I., St. Laurent, M., Trypaluk, C., . . . Bonnin, G. (2013). *NOAA Atlas 14 Volume 8 Version 2.* Retrieved from Precipitation-Frequency Atlas of the United States, Midwestern States. NOAA, National Weather Service: https://hdsc.nws.noaa.gov/pfds/

Prior, J. C., & Hutchinson, D. (2024). *Landforms of Iowa.* Retrieved from Iowa Geological Survey: https://iowageologicalsurvey.uiowa.edu/iowa-geology/landforms-iowa

PRISM Climate Group, Oregon State University. (2024, 01 01). *Recent Years (Jan 1981 - Apr 2024)*. Retrieved from Annual Values: https://prism.oregonstate.edu

Soil Survey Staff, NRCS, USDA. (2024). *Soil Survey Geographic Database (SSURGO).* Retrieved from Web Soil Survey: https://websoilsurvey.nrcs.usda.gov/

Stolze, J. H. (2024). *A Tale of Soap and Water: Soap Creek Leads the State in Flood Mitigation*. Retrieved from Iowa Watershed Approach: https://iowawatershedapproach.org/2018/02/a-tale-of-soap-and-water-soap-creek-leads-the-state-in-flood-mitigation/

The Urban Water Resources Research Council . (1992). *Design and Construction of Urban Stormwater Management Systems.* Reston: American Society of Civil Engineers.

U.S. Geological Survey (USGS). (2023). *Annual NLCD Collection 1 Science Products*. Retrieved from U.S. Geological Survey data release: https://doi.org/10.5066/P94UXNTS

U.S. Geological Survey. (2023). *Annual National Land Cover Database (NLCD) Collection 1 Land Cover.* Retrieved from Science Products: U.S. Geological Survey data release: https://doi.org/10.5066/P94UXNTS

USGS. (2024). *Iowa Regional Regressional Peak-Flow Statistics.* Retrieved from StreamStats: https://streamstats.usgs.gov/ss/

Wuertz, D., Lawrimore, J., & Korzeniewski, B. (2024, 01 01). *Cooperative Observer Program (COOP) Hourly Precipitation Data (HPD), Version 2.0.* Retrieved from NOAA National Centers for Environmental Information: doi:10.25921/p7j8-2170